Knowledge-Based Systems 296 (2024) 111880

Contents lists available at ScienceDirect

Knowledge-Based Systems

journal homepage: www.elsevier.com/locate/knosys

The Hiking Optimization Algorithm: A novel human-based metaheuristic approach

Sunday O. Oladejo [a,*], Stephen O. Ekwe [b], Seyedali Mirjalili [c,d]

[a] School for Data Science and Computational Thinking, Stellenbosch University, Stellenbosch, South Africa
[b] Department of Electrical, Electronic and Computer Engineering, Cape Peninsula University of Technology, Cape Town, South Africa
[c] Centre for Artificial Intelligence Research and Optimization, Torrens University Australia, Fortitude Valley, Brisbane, QLD 4006, Australia
[d] University Research and Innovation Center, Obuda University, 1034, Budapest

ARTICLE INFO

Keywords:
Optimization
Metaheuristics
Hiking
Tobler's Hiking function
Algorithm
Benchmark
Problem solving

ABSTRACT

In this paper, a novel metaheuristic called 'The Hiking Optimization Algorithm' (HOA) is proposed. HOA is inspired by hiking, a popular recreational activity, in recognition of the similarity between the search landscapes of optimization problems and the mountainous terrains traversed by hikers. HOA's mathematical model is premised on Tobler's Hiking Function (THF), which determines the walking velocity of hikers (i.e. agents) by considering the elevation of the terrain and the distance covered. THF is employed in determining hikers' positions in the course of solving an optimization problem. HOA's performance is demonstrated by benchmarking with 29 well-known test functions (including unimodal, multimodal, fixed-dimension multimodal, and composite functions), three engineering design problems (EDPs), (including I-beam, tension/compression spring, and gear train problems) and two N-P Hard problems (i.e. Traveling Salesman's and Knapsack Problems). Moreover, HOA's results are verified by comparison to 14 other metaheuristics, including Teaching Learning Based Optimization (TLBO), Genetic Algorithm (GA), Differential Evolution (DE), Particle Swarm Optimization, Grey Wolf Optimizer (GWO) as well as newly introduced algorithms such as Komodo Mlipir Algorithm (KMA), Quadratic Interpolation Optimization (QIO), and Coronavirus Optimization Algorithm (COVIDOA). In this study, we employ statistical tests such as the Wilcoxon rank sum, Friedman test, and Dunn's post hoc test for the performance evaluation. HOA's results are competitive and, in many instances, outperform the aforementioned well-known metaheuristics. The source codes of HOA and related metaheuristics can be accessed publicly via this link: https://github.com/DayoSun/The-Hiking-Optimization-Algorithm.

1. Introduction

Hiking is an outdoor recreational activity that entails walking in nature, over hills, mountains, or elsewhere in the countryside, as a group or alone [1–4]; a physical exercise in which hikers (i.e. people who engage in hiking) walk, on the average, between 7 km and 12 km for half a day and between 19 km and 30 km for a full day [5]. People engage in hiking for many reasons, including spirituality, physical fitness, health, adventure, socialization, and creativity [4,6,7], as per Fig. 1.

Hiking can be arduous depending on the terrain in question, which may include upward slopes, forests, overgrown wilderness, parks, flat grounds, and farmlands [8–10]. Hiking terrains are random, with stochastic topography. In this, they are similar to the search spaces of optimization tools and, in particular, metaheuristics. Metaheuristics are characteristically stochastic and have been widely employed in solving optimization problems. They have gained interest in several fields owing to their ease of implementation, simple structure, fast convergence time, reduced computational resource usage, flexibility and robustness, and local optima avoidance ability [11–14]. Fig. 2 highlights the applications of metaheuristics in several fields of endeavor, such as wireless networks [15–22] and machine learning [23].

Unlike metaheuristics, classical optimization approaches, such as sequential quadratic, quasi-Newton conjugate gradient, and fast-steepest methods, find it difficult to solve many real-world problems. This is due to the characteristics peculiar to real-world problems. Real-world problems often require huge computational resources, such as time, space, and cost, which are computationally expensive for classical methods. Metaheuristics, however, are capable of handling real-world problems due to their intelligence.

* Corresponding author.
E-mail addresses: sunday@sun.ac.za (S.O. Oladejo), ekwes@cput.ac.za (S.O. Ekwe), ali.mirjalili@torrens.edu.au (S. Mirjalili).

https://doi.org/10.1016/j.knosys.2024.111880
Received 26 October 2023; Received in revised form 25 April 2024; Accepted 28 April 2024
Available online 3 May 2024

Fig. 1. Some reasons why people engage in hiking.

Fig. 2. Some areas of application of metaheuristic algorithms.

In the literature, optimization techniques are generally either deterministic or stochastic [24]. Deterministic techniques generate the same results or outcomes for all simulation runs, whereas stochastic models or techniques such as metaheuristics run the risk of generating different results or outcomes for all simulation runs. Metaheuristics can be broadly categorized by the [14,25–28]: (i) size of the solutions or population, (ii) inspiration of the metaheuristics, and (iii) search experience of the agents. An illustration of the classification and respective examples is presented in Fig. 3.

Metaheuristics are categorized by the size of the solution into (i) single-solution-based metaheuristics, and (ii) population-based metaheuristics. Single-solution-based metaheuristics, otherwise known as trajectory methods [28], are iterative procedures and operate in two (2) phases [14,29,30]. In the first phase, i.e. the generation stage, a set of solutions is generated from the current solution. This is done by the transformation of the current solution, after which the second phase begins. In the second phase, i.e. the replacement phase, a new solution is chosen from the set of generated solutions to replace the current solution. The iteration continues until the maximum iteration threshold is reached or a stopping condition is met. Examples of single-solution based metaheuristics include the Tabu Search (TS) [29,31], Simulated Annealing (SA) [32], Greedy Randomized Adaptive Search Procedures (GRASP) [33], and Iterative Local Search (ILS) [34,35].

In population-based metaheuristics, a set of candidate solutions, otherwise referred to as the ‘population’, is generated. These initially generated solutions are replaced with another, better set of solutions. Unlike the single-solution-based candidates, the new candidate solutions are not a single solution but a set of solutions. They can include Grey Wolf Optimization (GWO) [11], Particle Swarm Optimization (PSO) [36], Ant Colony Optimization (ACO) [37], Genetic Algorithm (GA) [38,39], Differential Evolution (DE) [40], Whale Optimization Algorithm (WOA) [12], Artificial Bee Colony (ABC) [41,42], and Harris Hawk Optimization (HHO) [43]. Population-based solution are mostly inspired by nature [25,44].

Metaheuristics are also categorized by their source of inspiration: (i) swarm-inspired, (ii) evolution-inspired, (iii) physics-inspired, and (iv) human-inspired techniques. These evolution-inspired metaheuristics rely more on biological evolution in nature. In natural evolution, the characteristics of species change over several generations. Species pass on favorable attributes that improve their survival skills to future generations. This strategy has been employed in metaheuristics by improving the candidate solutions over numerous simulation runs (i.e. generations, in this case). Examples include GA [38,39], the Biogeography-Based Optimizer (BBO) [45], Covariance Matrix Adaption Evolution Strategy (CMAES) [46], DE [40], Evolution Strategy [47], Genetic Programming (GP) [48], Evolutionary Programming (EP) [49], and Quantum-Inspired Algorithm [50].

In recent times, swarms have inspired the development of metaheuristics such as the Grasshopper Optimization Algorithm (GOA) [51], Cuckoo Search (CS) [52], Ant Lion Optimization (ALO) [53], Firefly Algorithm (FFA) [54], Salp Swarm Algorithm (SSA) [13], Bat Algorithm (BA) [55], Dolphin Echolocation (DEL) [56], GWO, ACO, and ABC. Swarm-inspired metaheuristics have exploited the collective gain of swarm emergence, which entails the cooperation of swarms in directional navigation and food foraging [57,58]. Swarms of animals such as spiders, bees, birds, termites, fish, and termites have inspired the development of several metaheuristics.

The universe’s physical laws have also inspired the development of metaheuristics. The operation and fundamentals of laws such as relativity, gravity, Brownian motion, and explosions have been exploited in the development of physics-inspired metaheuristics such as the Solar System Algorithm (SoSA) [59], Sine Cosine Algorithm (CSA) [60], Central Force Optimization (CFO) [61], Big-Bang Big-Crunch (BBBC) [62], Gravitational Search Algorithm (GSA) [63] and SA.

Human-inspired metaheuristics are inspired by the social behavior, lifestyle, or beliefs of humans and animals. Metaheuristics such as the Firework Algorithm (FA) [64], Harmony Search (HS) [65], Teaching Learning Based Optimization (TLBO) [66], Group Search Optimizer (GSO) [67], Social Network Search (SNS) for Global Optimization [68], Deep Sleep Optimizer (DSO) [69], and TS were inspired by human and animal behavioral characteristics.

Lastly, metaheuristics can be categorized by their search experience. Metaheuristics’ search experience is premised on memory usage [25–27]. To this end, metaheuristics are categorized into: (i) memory-less methods, and (ii) memory-usage. In memory-less-based metaheuristics, past search experience does not influence future experience. LS, SA, and GRASP are examples of memory-less metaheuristics. However, for memory-usage-based metaheuristics, future search experiences are greatly influenced by current search experience. This is premised on the usage of memory to update new search experiences and store candidate solutions of past search experiences. Examples of memory-usage-based metaheuristics are ACO, TS, PSO, GWO, BA, GA, ABC, and FFA.

The No Free Lunch theorem (NFL) [70] for optimization, devised by David H. Wolpert and William Macready, justifies the development of new metaheuristics and modification of existing metaheuristics. NFL states that no one existing metaheuristic can solve all types of optimization problems perfectly and therefore, they all have their strengths and weaknesses. Consequently, no existing metaheuristic is better than the rest. For this reason, we propose a novel metaheuristic, the Hiking Optimization Algorithm (HOA), which is premised on the concept of hiking.

This present paper addresses the development of a novel metaheuristic that can be employed in solving large dimensionality problems for diverse problems, such as engineering design problems and NP-hard problems. To test the proposed metaheuristic, we subjected it to several benchmark tests and statistical analyses. The contributions to this work are as follows:

- A novel metaheuristic called the Hiking Optimization Algorithm (HOA) is proposed. The HOA simulates the idiosyncrasies involved in a hiking expedition with the ultimate goal of summiting a peak. The hiking environment is rugged terrain with several local peaks, topography, and many times a global peak, and this terrain is synonymous with the characteristics of an optimization search landscape.
- The mathematical foundations of HOA are thoroughly explained in order to provide a solid framework for simulating the algorithm. In addition, the computational complexity of HOA is explained succinctly.
- To show the robustness and efficacy of HOA, the algorithm was subjected to rigorous benchmark functions, tests, and applications. In this regard, 29 traditional benchmark functions (i.e., unimodal, multimodal, fixed multimodal, and composite) were employed to test the exploratory and exploitative capabilities and the ability to withstand the harsh search landscape of composite functions. Additionally, HOA was tested in solving three engineering design problems, six widely known traveling salesman problems (TSPs), and two types of knapsack problems (KPs) with varying dimensions. The TSPs and KPs are to show the HOA's suitability for solving NP-hard problems.
- The performance of HOA is compared with 10 widely known metaheuristics in the literature and four state-of-the-art, recently developed metaheuristics. To ensure the accuracy of the comparison, extensive and rigorous Monte Carlo simulations were carried out.
- Statistical tests like the Friedman test, the Wilcoxon Rank Sum test, and Dunn's post-hoc analysis were used in this work to show the accuracy of the simulation results.

The outline of this paper is as follows: In Section 2, a review of some recently developed metaheuristics is discussed. Section 3 presents a brief background of HOA. Section 4 describes HOA and its mathematical foundation. We present a detailed description of the performance evaluation of HOA and comparisons to other metaheuristics in Section 5. Section 6 examines the application of HOA to some engineering case studies. In Section 7, the HOA's performance is evaluated and compared with dynamic programming in solving N-P Hard problems. We conclude this paper in Section 8.

2. Literature review on recent metaheuristics

This section provides an overview of newly developed metaheuristics designed to solve optimization challenges. We focus solely on examining modern algorithms due to the comprehensive evaluations conducted on popular metaheuristics, including GA, PSO, TLBO, GWO, DE, and ACO, which have been extensively employed in academic research.

In 2021, the authors in [71–73] proposed a bio-inspired metaheuristic that imitates: (i) Komodo dragons peculiar to East Nusa Tenggara, Indonesia. Komodo dragons averagely weigh 135 kg with a length of 3 metres, and (ii) a popular Javanese sidewalk termed mlipir. The agents are grouped into three: (i) big strong male dragons for high-exploitation, low-exploration movement of agents; (ii) female dragons who engage in exploratory movements and also mate with the strong male dragons to reproduce better agents or solutions. (iii) The last group is a set of low-quality male dragons that engage in the mlipir movement, with the sole aim of trailing the strong male dragons. One of the major limitations of KMA is that it only has two parameters (i.e., the number of big males and the mlipir rate), which do not guarantee global optima for optimization problems with a flat, wide search landscape. Additionally, KMA was only subjected to 23 benchmarks, as it was not tested with NP-hard and engineering design problems. Finally, unlike HOA, KMA relies on an initial solution guess or an exact solution to discover its optimal value, potentially leading to accurate results for benchmark testing. However, this reliance on upfront information may render KMA impractical for solving real-world problems where prior knowledge of solutions is unavailable.

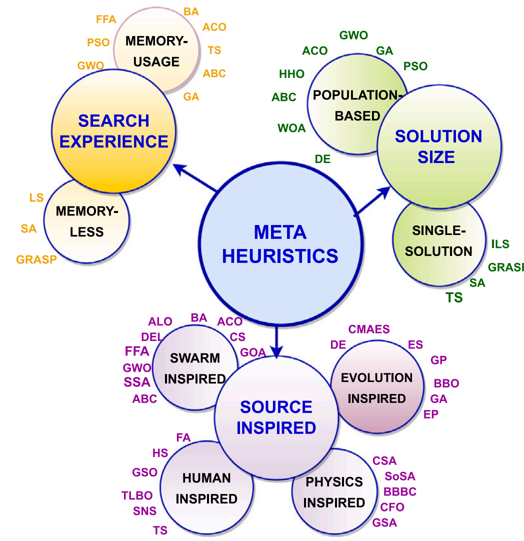

Fig. 3. Classification of metaheuristic algorithms.

The Golden Search Optimization (GSA) Algorithm [74] is a population-based metaheuristic. GSA attempts to strike a delicate balance between exploration and exploitation while utilizing the benefits of PSO and the Sine Cosine Optimization Algorithm (SCA) in the random generation of its agents. Furthermore, the only tuning parameters for GSA are the quantity of agents and the number of evaluation/iteration points.

The Golden eagle optimizer (GEO) [75] is a swarm-based metaheuristics which is inspired by the prey searching and attacking styles of a golden eagle, a family of birds of prey such as hawks and eagles. To this end, GEO [75] incorporates two distinctive tuning parameters: attack propensities and cruise propensities. In contrast to what was done in [71–74], 33 benchmark functions from the literature were utilized to assess the performance of GEO. Nevertheless, the evaluation of GEO's performance was limited to six metaheuristics (i.e. GWO, GA, CSA, PSO, HS, and DA).

The authors in [76,77] proposed an evolutionary-based metaheuristic called Coronavirus Optimization Algorithm (COVIDOA). COVIDOA mimics the viral replication process, more precisely that of coronavirus [78–80]. The replication process involves the subsequent steps of entry, uncoating, replication, assembly, and release of virion. COVIDOA has three peculiar parameters (i.e., number of proteins, frameshifting number, and mutation rate) other than the general parameters associated with all metaheuristics (i.e., upper and lower bounds of solutions, dimensionality, number of agents, and maximum iterations). The authors evaluated the performance of COVIDOA using 20 classical benchmark functions and six real-life problems, and numerical results were compared with eight metaheuristic algorithms.

The Quadratic Interpolation Optimization Algorithm (QIO) [81] offers a sophisticated approach to optimization problems. It employs quadratic interpolation to efficiently estimate the minimum of a univariate function. QIO exhibits rapid convergence, often outperforming traditional optimization methods in terms of speed and accuracy. Its ability to dynamically adjust step sizes enhances adaptability to various problem landscapes. However, QIO's effectiveness may vary depending on the characteristics of the objective function, warranting careful consideration of its applicability to specific scenarios.

A novel population-based metaheuristic that is inspired by the survival capability of gazelles, which are consistently preyed on, is proposed in [82]. This metaheuristic, named Gazelle Optimization Algorithm (GOA), mimics the fast or high-speed characteristics of the gazelle, found in sub-Saharan and Sahel Africa, the Arabian Peninsula, and China. The initialization of the agent. The GOA experiences the exploration phases when a gazelle sees a predator and switches to exploitation when a predator identifies a prey. Similar to our work, the GOA is benchmarked against four EDPs and other classical functions in the literature.

In [83], the authors developed a novel population-based metaheuristic that mimics a Coatis, a diurnal mammal that is found in the Southwestern United States of America. The mathematical foundation of the Coartis Optimization Algorithm (COA) is premised on her predatory tendencies towards iguanas and also her own escape strategy from her own predators.

A swarm-based metaheuristic that mimics the summer vacation, foraging, and competitive behavior of the crayfish was proposed in [84] as the Crayfish Optimization Algorithm. The above-named behavioral characteristics of the crayfish are similar to exploration and exploitation of the metaheuristic agents and are influenced by the temperature of either the pond, cave, or holes the crayfish lives in. In [84], this temperature is modeled as a normal distribution. With temperatures greater than 30 °C, the crayfish will go on vacation to a cool place, while the feeding range of the crayfish lies between 15 °C and 30 °C.

In their study, [85], the authors introduced a swarm-based metaheuristic method called the Archerfish Hunting Optimizer (AHO). This approach draws inspiration from the hunting behaviors of archerfish, specifically their shooting and jumping techniques used to capture aerial insects like dragonflies. Archerfish are commonly found in the mangrove waters of the Indo-Pacific region. The AHO algorithm is characterized by three key parameters: the perceiving/swapping angle, swarm size, and the attractiveness rate between an archerfish and its prey. The efficacy of AHO was demonstrated through benchmarking against 10 test functions and five engineering design problems. In contrast, this current study evaluates the performance of HOA across 29 benchmark functions, three engineering design problems, and two types of NP-Hard problems.

In this study, we evaluate the performance of HOA by comparing it with both established metaheuristics from the literature and three newly developed ones: KMA, COVIDOA, and QIO. Through this comparative analysis, we aim to assess HOA's effectiveness within the context of contemporary metaheuristic optimization techniques.

3. Background

The hiker's objective is to cross a varying amount of distance on foot, sometimes traveling over hills, mountains, and other geographic obstacles [86]. However, due to various factors, including the weather, the terrain, externally imposed time limits, and the hiker's level of fitness and preparedness, this goal may not be met. Fig. 4 illustrates a typical hiking terrain, with several peaks and a rugged landscape.

A careful inspection of mountainous terrain shows that there are many local peaks and only one global peak [87]. Hikers reach a local peak and then descend, ending the hike. However, global peaks are sometimes difficult to summit. The rugged terrains of mountainous landscapes, often containing rocky, rough, steep, and exposed trails [86,88], are similar to the land search spaces of optimization problems. Just as mountains and hills differ in their terrains [89], so too do the land search spaces of optimization problems.

Hikers summit mountains as a group to encourage and support one another and make the best use of individual hikers' knowledge of the trail. In other words, in 'conquering' the highest peak (i.e. the global optima) of a mountain, there is a cooperative effort by all hikers.

Fig. 4. Illustration of a hiking landscape similar to the optimization landscape.

In a hiking expedition, hikers follow the lead of the 'trail leader' or 'trail hiker'. These roles are swapped in the course of a hike depending on the fitness of the hikers and who has the most knowledge of a particular section of the trail or of the entire trail. The trail leader must be able to pass information across the group in such a manner that all the hikers arrive safely at the summit, either at the same time or at different times. Additionally, hikers gather information about the trails' peaks from encounters with other hikers on the trail.

4. Hiking optimization algorithm

In this section, HOA's inspiration and mathematical background are discussed. Furthermore, we describe HOA's algorithm and its computational complexity. The main notations employed in this section are listed in Table 1.

4.1. Inspiration for HOA

The inspiration for HOA stems from the experiences of hikers attempting to summit the peaks of mountains, hills, or rocks, as the case may be.

In the course of hiking, hikers knowingly or subconsciously take into consideration the terrain's steepness. They avoid highly steep terrains and trails in order to maintain their hiking or walking speed. In other words, highly steep terrains and trails slow down hikers and ultimately lengthen the hike.

Armed with awareness of the terrain's geography, hikers can determine or roughly estimate the time it will take them to get to the peak. This is similar to agents trying to find the local optima or global optima of an optimization problem. The landscape or search space of the optimization is similar to the mountainous terrains crossed by the hikers to reach a summit. Additionally, in finding the global optima, agents become bogged down in certain search space positions owing to the complexity of the optimization problem, and this may prolong the time taken to locate the global optima, which is also similar to what hikers experience in the course of hiking.

The work is premised on emulating the experience of hiking in solving optimization problems.

4.2. Mathematical background

The mathematical foundation of HOA is based on the widely known Tobler's Hiking Function [90,91] formulated by an American-Swiss geographer and cartographer, Waldo Tobler. The Tobler's Hiking Function is an exponential function that determines a hiker's speed, taking into consideration the steepness or slope of the terrain or trail.

Table 1
List of Notations.

Symbol	Description
i, $\mathcal{I}$	An individual hiker, and total number of hikers
$\mathcal{T}$	Number of maximum function evaluations
t	An iteration or time
$\mathcal{W}_{i,t}$	Hiker i velocity in km/h
$\mathcal{S}_{i,t}$	Slope of the trail
$\theta_{i,t}$	Angle of inclination of the trail experienced at t by hiker t
$\gamma_{i,t}$	Uniformly distributed random variable [0,1]
$\alpha_{i,t}$	Sweep Factor (SF) of the hiker i lies in [1, 3]
$\beta_{i,t}$	Current position of hiker i at time t
β_{best}	Position of the lead hiker
$\beta_{i,t+1}$	Updated position of the lead hiker
δ_j	Uniformly distributed random variable [0,1]
ϕ_j^1	Lower bound of the decision variables
ϕ_j^2	Upper bound of the decision variables

The Tobler's Hiking Function (THF) is given by [90,91]

$$\mathcal{W}_{i,t} = 6e^{-3.5\left|\mathcal{S}_{i,t}\ +\ 0.05\right|}, \tag{1}$$

where $\mathcal{W}_{i,t}$ is the hiker i velocity (i.e. in km/h) at iteration or time t, and $\mathcal{S}_{i,t}$ is the slope of the trail or terrain. Additionally, the slope $\mathcal{S}_{i,t}$ is given by

$$\mathcal{S}_{i,t} = \frac{\mathrm{d}h}{\mathrm{d}x} = \tan\theta_{i,t}, \tag{2}$$

where dh and dx indicate the difference in elevation and the distance covered by the hiker, respectively. Additionally, $\theta_{i,t}$, is the angle of inclination of the trail or terrain and it lies within $[0, 50°]$.

HOA exploits the benefits of the social thinking of the hikers as a group and the personal cognitive abilities of individual hikers. The updated or actual velocity of a hiker is a function of the initial velocity determined by THF, the position of the lead hiker, the actual position of the hiker, and the sweep factor. Hence, the current velocity of the hiker i given by

$$\mathcal{W}_{i,t} = \mathcal{W}_{i,t-1} + \gamma_{i,t}(\beta_{best} - \alpha_{i,t}\beta_{i,t})\ , \tag{3}$$

where $\gamma_{i,t}$ is a uniformly distributed number within the range [0, 1]; $\mathcal{W}_{i,t}$ and $\mathcal{W}_{i,t-1}$ denote the current and initial velocity of the hiker i, respectively. β_{best} is the position of the lead hiker and $\alpha_{i,t}$ is the sweep factor (SF) of the hiker i and lies in [1, 3]. The SF ensures the hiker does not stray too far away from the lead hiker, so they can see where the lead hiker is headed and also receive signals from the lead hiker.

By considering the velocity of the hiker in (1), the updated position $\beta_{i,t+1}$ of hiker i is given by:

$$\beta_{i,t+1} = \beta_{i,t} + W_{i,t}\ . \tag{4}$$

In various metaheuristic algorithms, including the HOA, the initial setup of agents is a crucial aspect that significantly affects the attainability of feasible solutions and the speed at which convergence is achieved. In this particular study, the HOA implements the random initialization technique [92–94] for initializing the positions of its agents, although alternative approaches like heuristic-based or problem-specific initialization methods also exist.

The initialization of hiker positions $\beta_{i,t}$ is determined by the upper bound ϕ_j^2 and lower bound ϕ_j^1 of the solutions, represented by the equation:

$$\beta_{i,t} = \phi_j^1\ +\ \delta_j(\phi_j^2 - \phi_j^1), \tag{5}$$

where δ_j is a uniformly distribution number within the range [0, 1]. Additionally, ϕ_j^1 and ϕ_j^2 represent the lower and upper bounds of the jth dimension of the decision variables about the optimization problem. The exploratory and exploitative tendencies of the HOA are influenced by a parameter termed the sweep factor (SF). This factor greatly impacts the distance between the trail leader and other hikers, as illustrated in Eq. (3). Furthermore, the slope of the trail, influencing hiker velocity as indicated in Eqs. (1) and (2), also plays a significant role in shaping the exploratory and exploitative behaviors of the HOA.

When the SF range is increased, the HOA tends to lean more towards an exploitation phase. Conversely, decreasing the SF range tends to encourage an exploratory phase within the HOA. Moreover, reducing the range of the angle of inclination of the trail tends to steer the HOA towards the exploitation phase. These factors collectively contribute to shaping the behavior and performance of the HOA in solving optimization problems.

4.3. HOA

HOA is a global optimization algorithm that exploits the search space of the optimization problem while leveraging the experience of hikers in the traversing of trails and mountains. Alg. 1 shows the implementation of HOA.

At the beginning of the hike, the initial positions of the hikers are determined, and with the help of Tobler's Hiking Function, the new positions of the hikers are estimated after a given time. The fitness of all the hikers is evaluated and the fittest hiker becomes the lead hiker. The lead hiker position is re-examined every iteration to ensure the fittest hiker at each instance becomes the lead hiker.

4.4. Computational complexity

The computational complexity of HOA is premised on the big Omicron (big-$\mathcal{O}$). By employing the big-$\mathcal{O}$ characterization, the theoretical worst-case growth rate of the computational memory or execution time of an algorithm is described; HOA, in this case. From a careful inspection of Alg. 1, the big-$\mathcal{O}$ notation of HOA is given as $\mathcal{O}(T * I)$, where T is the maximum number of iterations or time involved in the hiking process and I denotes the total number of hikers.

Algorithm 1 : HOA.

```
Input: UB, LB, T, I, d

F ← Preallocate fitness vector ℝ^{I×1}
F_best ← Preallocate best fitness vector ℝ^{(T+1)×1}
β ← Initialize the hikers' position randomly ℝ^{I×d}
for i ← 1 to I  do
    F_i ← Evaluate a hiker's fitness
end for
F_best,1 ← Initial best fitness of the hikers
for t ← 1 to T  do
    F_best, t ← Determine the best fitness hiker
    β_best ← Extract position of best fitness F_best, t
    for i ← 1 to I  do
        β_i, t ← Extract initial position of hiker i
        θ_i,t ← Determine trail/terrain angle of elevation
        S_i,t ← Compute the slope using (2)
        W_i,t−1 ←Compute the initial hiking velocity using (1)
        W_i,t ← Determine the actual velocity of hiker i using (3)
        β_i,t+1 ←Update the hiker's position using (4)
        β_i,t ← Bound β_i,t+1 within LB and UB
        if F_n ≤ F(n) then
            γ(n, :) ← H⃗
            F(n) ← F_n
        end if
    end for
    F_sol(i + 1) ← min (F)
end for
F*_sol ← argmin (F_sol)
return
```

Table 2
Unimodal benchmark functions.

Function	Var.	Range	f_{min}
$F_1(\mathcal{X}) = \sum_{i=1}^{n} \mathcal{X}_i^2$	30	[−100,100]	0
$F_2(\mathcal{X}) = \sum_{i=1}^{n} \lvert\mathcal{X}_i\rvert + \prod_{i=1}^{n} \lvert\mathcal{X}_i\rvert$	30	[−10,10]	0
$F_3(\mathcal{X}) = \sum_{i=1}^{n} \left(\sum_{j=1}^{i} \mathcal{X}_j\right)^2$	30	[−100,100]	0
$F_4(\mathcal{X}) = \max_i\{\lvert\mathcal{X}_i\rvert,\ 1 \le i \le n\}$	30	[−100,100]	0
$F_5(\mathcal{X}) = \sum_{i=1}^{n-1} \left[100(\mathcal{X}_{i+1} - \mathcal{X}_i^2)^2 + (\mathcal{X}_i - 1)^2\right]$	30	[−30,30]	0
$F_6(\mathcal{X}) = \sum_{i=1}^{n} (\mathcal{X}_i + 0.5)^2$	30	[−100,100]	0
$F_7(\mathcal{X}) = \sum_{i=1}^{n} i\mathcal{X}_i^4 + random[0,1)$	30	[−1.28,1.28]	0

Table 3
Multimodal benchmark functions.

Function	Var.	Range	f_{min}
$F_8(\mathcal{X}) = \sum_{i=1}^{n} -\mathcal{X}_i \sin\left(\lvert\mathcal{X}_i\rvert^{0.5}\right)$	30	$[-500, 500]$	−418.9829
$F_9(\mathcal{X}) = \sum_{i=1}^{n} [\mathcal{X}_i^2 - 10\cos\left(2\pi\mathcal{X}_i\right) + 10]$	30	$[-5.12, 5.12]$	0
$F_{10}(\mathcal{X}) = -20e^{\left[-0.2\left(1/n \sum_{i=1}^{n} \mathcal{X}_i^2\right)^{0.5}\right]} - e^{\left[1/n \sum_{i=1}^{n} \cos(2\pi\mathcal{X}_i)\right]} + 20 + e$	30	$[-32, 32]$	0
$F_{11}(\mathcal{X}) = \frac{1}{4000} \sum_{i=1}^{n} \mathcal{X}_i^2 - \prod_{i=1}^{n} \cos\left(\frac{\mathcal{X}_i}{\sqrt{i}}\right) + 1$	30	$[-600, 600]$	0
$F_{12}(\mathcal{X}) = \frac{\pi}{n}\left[10\sin\left(\pi y_1\right) + \sum_{i=1}^{n-1} (y_i - 1)^2[1 + 10\sin^2(\pi y_{i+1})] + (y_i - 1)^2\right] + \sum_{i=1}^{n} u(\mathcal{X}_i, 10, 100, 4)$	30	[−50,50]	0
$y_i = 1 + \frac{\mathcal{X}_i + 1}{4}, \quad u(\mathcal{X}_i, a, k, m) = \begin{cases} k(\mathcal{X}_i - a)^m, & \mathcal{X}_i > a \\ 0, & -a < \mathcal{X}_i < a \\ k(-\mathcal{X}_i - a)^m, & \mathcal{X}_i < -a \end{cases}$			
$F_{13}(\mathcal{X}) = 0.1\left[\sin^2(3\pi\mathcal{X}_1) + \sum_{i=1}^{n} (\mathcal{X}_i - 1)^2\left[1 + \sin^2(3\pi\mathcal{X}_i + 1)\right] + (\mathcal{X}_n - 1)^2\left[1 + \sin^2(2\pi\mathcal{X}_n)\right]\right] + \sum_{i=1}^{n} u(\mathcal{X}_i, 5, 100, 4)$	30	[−50,50]	0

Table 4
Fixed-dimension multimodal benchmark functions.

Function	Var.	Range	f_{min}
$F_{14}(x) = \left(\frac{1}{500} \sum_{j=1}^{25} \frac{1}{j + \sum_{i=1}^{2} (x_i - a_{ij})^6}\right)^{-1}$	2	$[-65, 65]$	1
$F_{15}(x) = \sum_{i=1}^{11} \left[a_i - \frac{x_1(b_i^2 + b_i x_2)}{b_i^2 + b_i x_3 + x_4}\right]^2$	4	$[-5, 5]$	0.00030
$F_{16}(x) = 4x_1^2 - 2.1x_1^4 + \frac{1}{3}x_1^6 + x_1x_2 - 4x_2^2 + 4x_2^4$	2	$[-5, 5]$	−1.0316
$F_{17}(x) = (x_2 - \frac{5.1}{4\pi^2}x_1^2 + \frac{5}{\pi}x_1 - 6)^2 + 10(1 - \frac{1}{8\pi})\cos x_1 + 10$	2	$[-5, 5]$	0.398
$F_{18}(x) = [1 + (x_1 + x_2 + 1)^2(19 - 14x_1 + 3x_1^2 - 14x_2 + 6x_1x_2 + 3x_2^2)]$ $\times [30 + (2x_1 - 3x_2)^2 \times (18 - 32x_1 + 12x_1^2 + 48x_2 - 36x_1x_2 + 27x_2^2)]$	2	[−2,2]	3
$F_{19}(x) = -\sum_{i=1}^{4} C_i e^{\left(-\sum_{j=1}^{3} a_{ij}(x_j - P_{ij})^2\right)}$	3	$[1, 3]$	−3.86
$F_{20}(x) = -\sum_{i=1}^{4} C_i e^{\left(-\sum_{j=1}^{6} a_{ij}(x_j - P_{ij})^2\right)}$	6	$[0, 1]$	−3.32
$F_{21}(x) = -\sum_{i=1}^{5} [(x - a_i)(x - a_i)^T + C_i]^{-1}$	4	$[0, 10]$	−10.1532
$F_{22}(x) = -\sum_{i=1}^{7} [(x - a_i)(x - a_i)^T + C_i]^{-1}$	4	$[0, 10]$	−10.4028
$F_{23}(x) = -\sum_{i=1}^{10} [(x - a_i)(x - a_i)^T + C_i]^{-1}$	4	$[0, 10]$	−10.5363

5. Results and discussions

In this section, HOA is benchmarked on 29 functions and engineering problems. The benchmark functions are divided into two: (i) traditional benchmark functions, and (ii) composite benchmark functions. The first 23 benchmark functions (i.e. F1-F23) are the traditional or classical functions for evaluating the performance of metaheuristics. In Tables 2, 3, and 4, we describe the classical benchmark functions which can be further grouped into (i) unimodal, (ii) multimodal, and (iii) fixed-dimensional multimodal optimization benchmark functions.

Simply put, unimodal functions are characterized by a single global solution. This set of benchmark functions evaluates the exploitative capabilities of metaheuristics. Moreover, multimodal functions are synonymous with a harsh search landscape with multiple local optima and a single global solution. The fixed-dimensional multimodal functions have numerous local optima and single global optima. Similar to multimodal functions, however, they have a fixed dimension. The exploratory capabilities of metaheuristics are tested using the multimodal and fixed-dimension multimodal benchmark functions. A detailed description of these functions is presented in [95–98].

In this work, six composite benchmark test functions, F24-F29, are employed. We briefly describe the composite functions employed in Table 5. The composite functions examine the metaheuristics' ability to find a balance between exploitation and exploration in the search for a global optimum in the landscape. Composite functions are similar to multimodal functions in that they have multiple local optima. Consequently, the search landscape is harsh and challenging for the hikers or agents to navigate. Furthermore, composite functions are structurally recursive and are critical local optima avoidance test beds for the performance of metaheuristics. To this end, composite functions test metaheuristics' exploration and exploitation capabilities [96].

HOA is implemented and evaluated in a MATLAB [99] environment using an Intel(R) Xeon CPU E5-2630 v2 with a dual processor of 2.6 GHz and an installed RAM of 64.0 GB. To ensure fairness, each metaheuristic runs recursively for 30 individual runs and terminates at 500 iterations per run. Subsequently, we examine HOA's performance with regard to the traditional benchmark functions. Furthermore, the control parameters of HOA and the 14 metaheuristics employed in the performance evaluation simulation are presented in Table 6.

Table 5
Composite benchmark functions.

Function	Var.	Range	f_{min}
F_{24}: Hybrid Func. f_1, f_2 = Rastrigin Function f_3, f_4 = Weierstras's Function f_5, f_6 = Griewank's Function f_7, f_8 = Ackley's Function f_9, f_{10} = Sphere Function $[\sigma_1, \sigma_2, \sigma_3, \ldots, \sigma_{10}] = [1, 1, 1, \ldots, 1]$ $[\lambda_1, \lambda_2, \lambda_3, \ldots, \lambda_{10}] = \left[1,\ 1,\ 10,\ 10,\ \frac{5}{60},\ \frac{5}{60},\ \frac{5}{32},\ \frac{5}{32},\ \frac{5}{100},\ \frac{5}{100}\right]$	10	[−5,5]	0
F_{25}: Rotated Hybrid Func. f_1, f_2 = Rastrigin Function f_3, f_4 = Weierstras's Function f_5, f_6 = Griewank's Function f_7, f_8 = Ackley's Function f_9, f_{10} = Sphere Function $[\sigma_1, \sigma_2, \sigma_3, \ldots, \sigma_{10}] = [1, 1, 1, \ldots, 1]$ $[\lambda_1, \lambda_2, \lambda_3, \ldots, \lambda_{10}] = \left[1,\ 1,\ 10,\ 10,\ \frac{5}{60},\ \frac{5}{60},\ \frac{5}{32},\ \frac{5}{32},\ \frac{5}{100},\ \frac{5}{100}\right]$	10	[−5,5]	0
F_{26}: Rotated Hybrid Func. 1 with noise $F_{26} = F25 * (1 + 0.2\ \lvert\mathcal{N}(0,1)\rvert) + 120$	10	[−5,5]	0
F_{27}: Rotated Hybrid Func. 2 f_1, f_2 = Ackley's Function f_3, f_4 = Rastrigin Function f_5, f_6 = Sphere Function f_7, f_8 = Weierstras's Function f_9, f_{10} = Griewank's Function $[\sigma_1, \sigma_2, \ldots, \sigma_{10}] = [1,\ 2,\ 1.5,\ 1.5,\ 1, 1, 1.5, 1.5, 2, 2]$ $[\lambda_1, \lambda_2, \ldots, \lambda_{10}] = \left[\frac{2*5}{32},\ \frac{5}{32},\ 2*1,\ 1,\ \frac{2*5}{100},\ \frac{5}{100},\ 2*10,\ 10,\ \frac{2*5}{60},\ \frac{5}{60}\right]$	10	[−5,5]	0
F_{28}: Rotated Hybrid Func. 2 with a narrow basin for global optimum f_1, f_2 = Ackley's Function f_3, f_4 = Rastrigin Function f_5, f_6 = Sphere Function f_7, f_8 = Weierstras's Function f_9, f_{10} = Griewank's Function $[\sigma_1, \sigma_2, \ldots, \sigma_{10}] = [0.1,\ 2,\ 1.5,\ 1.5,\ 1, 1, 1.5, 1.5, 2, 2]$ $[\lambda_1, \lambda_2, \ldots, \lambda_{10}] = \left[\frac{0.1*5}{32},\ \frac{5}{32},\ 2*1,\ 1,\ \frac{2*5}{100},\ \frac{5}{100},\ 2*10,\ 10,\ \frac{2*5}{60},\ \frac{5}{60}\right]$	10	[−5,5]	0
F_{29}: Rotated Hybrid Func. 2 with the global optimum on the bounds f_1, f_2 = Ackley's Function f_3, f_4 = Rastrigin Function f_5, f_6 =Sphere Function f_7, f_8 = Weierstras's Function f_9, f_{10} = Griewank's Function $[\sigma_1, \sigma_2, \ldots, \sigma_{10}] = [1,\ 2,\ 1.5,\ 1.5,\ 1, 1, 1.5, 1.5, 2, 2]$ $[\lambda_1, \lambda_2, \ldots, \lambda_{10}] = \left[\frac{2*5}{32},\ \frac{5}{32},\ 2*1,\ 1,\ \frac{2*5}{100},\ \frac{5}{100},\ 2*10,\ 10,\ \frac{2*5}{60},\ \frac{5}{60}\right]$	10	[−5,5]	0

5.1. Traditional benchmark functions

In this subsection, we delve into the examination of HOA's performance concerning test accuracy, search and convergence dynamics, search trajectory, computational time, as well as statistical analyses including the Wilcoxon rank sum test, Friedman test, and Dunn's post hoc test.

5.1.1. Accuracy test benchmark

We examine HOA's accuracy in Tables 7–10 with unimodal, multimodal, fixed-dimension multimodal functions (i.e. those described in Tables 2–4).

In Tables 7–10, the average accuracy of HOA is compared to 14 widely known metaheuristics in literature, namely: TLBO, GA, DE, PSO, ABC, GWO, SCA, BBO, ACO, RCSA, HS, COVIDOA, KMA, and QIO. A brief description and related literature of these metaheuristics is highlighted in Sections 1 and 2. By comparing the "f_{min}" column in Tables 2–4, with the performance results in Tables 7–10, we observe that HOA performed well outperforming several metaheuristics across functions and varying dimensions. Our analysis reveals that across all functions assessed in Tables 7–10, HOA consistently maintains its position among the top-performing metaheuristics, consistently ranking within the top four along with KMA, QIO, and TLBO. Notably, HOA exhibits a remarkable level of performance superiority when compared to various well-established metaheuristics documented in the existing literature, GA and Particle Swarm Optimization PSO. This observation underscores the effectiveness and competitiveness of HOA in optimizing diverse problem domains, showcasing its potential as a robust optimization technique capable of outperforming traditional approaches.

5.1.2. Search and convergence analysis

Herein, we examine the search space, search history, convergence, and average fitness. The search space (i.e. parameter space) describes the 3D view of the respective benchmark functions. The search history or trail history plot shows the hikers' trail in the course of the hike; that is, during iterations. Moreover, the convergence plot presents the stochastic characteristic of the lead hiker's fitness in a hiking expedition. The average fitness describes the mean fitness of all the hikers in the course of the expedition or, rather, the optimization process.

Figs. 9(a) –9(x) illustrate the search space, search history, convergence, and average fitness of some unimodal, multimodal, and fixed-dimension multimodal functions. In Figs. 9(a) –9(x), we observe that

Table 6
The control parameters of the respective metaheuristics.

Metaheuristic	Control Param.	Values
HOA	Angle of inclination of the trail	$[0, 50°]$
	Sweep Factor (SF) of the hiker	[1, 3]
TLBO	Teaching factor,	1,2
GA	Distribution index for crossover	20
	Distribution index for mutation	20
	Probability of crossover	0.8
	Probability of mutation	0.2
DE	Crossover probability	0.8
	Scaling factor	0.45
PSO	Inertia weight	0.45
	Personal learning coef.	1
	Global learning coef.	1
ABC	Percentage onlooker bee	50% of the colony
	Number of scout	1
GWO	Convergence parameter	Linear reduction 2 to 0
SCA	Convergence parameter	Linear reduction 2 to 0
BBO	Probability of modifying a habitat	1
ACO	Deviation-distance ratio	1
	Intensification Factor	0.5
	Sample size	40
RCSA	Initial Temp.	0.1
	Temp. reduction rate	0.99
	Mutation rate	0.5
	Mutation range	0.1(UB-LB)
	Max. no of sub-iterations	20
	Neighbors per individual	5
HS	No. of new harmonies	20
	Harmony memory consideration rate	0.9
	Pitch adjustment rate	0.1
	Fret width damp ratio	0.995
COVIDOA	Mutation rate	0.1
	Shifting Number	1
	Number of Subproteins	2
KMA	Mlipir Rate	0.5
	Female mutation rate	0.5
	Female mutation radius	0.5
QIO	Number of agents	30
	Number of iterations	500

Table 7
Results of accuracy test with unimodal and multimodal benchmark functions having 30 dimensions.

Alg.	Metric	F1	F2	F3	F4	F5	F6	F7	F8	F9	F10	F11	F12	F13
HOA	AVG	9.1653E−21	2.2209E−10	1.9428E−15	1.2798E−10	1.1600E+01	5.2535E+00	1.0134E−03	−4.2489E+03	1.3265E+01	5.6914E−11	0.0000E+00	6.0213E−01	1.0443E−01
	STD	9.6958E−21	1.3790E−10	5.6679E−15	9.0956E−11	6.9391E+00	4.6524E−01	6.3138E−04	6.4578E+02	3.5191E+01	3.9900E−11	0.0000E+00	1.5231E−01	3.4934E−02
TLBO	AVG	2.1995E−48	1.0043E−24	5.5615E−09	3.8345E−20	2.5397E+01	3.1362E−03	1.8596E−03	−6.9957E+03	1.6436E+01	4.2810E−15	0.0000E+00	2.3680E−05	6.7763E−02
	STD	2.9217E−48	7.4359E−25	2.6864E−08	2.8977E−20	6.7594E−01	2.4226E−02	7.6582E−04	1.2430E+03	8.0625E+00	9.6868E−16	0.0000E+00	9.7154E−05	7.5437E−02
GA	AVG	5.5213E+04	7.4870E+08	1.0382E+05	8.0180E+01	1.8062E+08	5.6141E+04	3.2072E+01	−3.9017E+03	3.4466E+02	2.0007E+01	5.1027E+02	1.3533E+01	2.1882E+01
	STD	7.8202E+03	4.8338E+09	3.2386E+04	3.6524E+00	3.7456E+07	7.1110E+03	8.0330E+00	4.6843E+02	2.5460E+01	2.6198E−01	5.5318E+01	2.1945E+00	2.5030E+00
DE	AVG	1.9989E+00	8.9437E−02	6.0698E+03	1.9366E+01	3.9621E+03	2.4142E+00	5.4937E−02	−5.3445E+03	1.9214E+02	2.5341E−01	2.7111E−01	1.0082E−03	2.8127E−03
	STD	9.7511E+00	3.9400E−02	2.1251E+03	6.5288E+00	1.2360E+04	1.6296E+01	2.5133E−02	5.1559E+02	1.3639E+01	3.1011E−01	2.1810E−01	7.8408E−03	8.4937E−03
PSO	AVG	2.7012E+02	2.8163E+01	7.9370E+03	2.8064E+01	1.2105E+04	1.6923E+02	1.1786E+00	−6.8245E+03	1.0171E+02	1.2583E+01	3.4924E+00	8.2831E−01	2.2055E+00
	STD	9.9951E+02	1.0539E+01	3.7020E+03	4.8605E+00	2.4063E+04	2.0805E+02	5.9934E−01	7.4716E+02	2.8104E+01	1.8900E+00	9.1635E+00	5.0426E−01	1.2357E+00
ABC	AVG	3.8481E+03	1.6878E+01	3.8372E+04	6.9690E+01	1.2844E+06	3.8999E+03	3.4811E+00	−7.4208E+03	1.4172E+02	1.5001E+01	3.4662E+01	1.5409E+00	1.9639E+00
	STD	1.9606E+03	3.6586E+00	5.6007E+03	5.0468E+00	1.2581E+06	1.6796E+03	1.1873E+00	3.4595E+02	2.0110E+01	1.3372E+00	1.5664E+01	6.1359E−01	8.1805E−01
GWO	AVG	6.5626E+00	2.5226E−01	4.5528E+03	1.6501E+01	6.2700E+02	1.2050E+01	5.2236E−01	−5.2826E+03	1.8294E+02	2.1311E+01	9.2565E−01	3.3330E+00	8.5256E−01
	STD	6.7896E+00	2.4447E−01	2.7863E+03	8.1193E+00	1.0175E+03	5.7042E+00	2.9314E−01	6.6497E+02	3.6617E+01	1.6481E−01	2.3149E−01	1.6629E+00	2.4088E−01
SCA	AVG	1.3087E+02	3.2033E−01	1.4276E+04	4.9000E+01	1.0640E+06	1.8601E+02	1.6989E−01	−3.6330E+03	6.3221E+01	1.4046E+01	2.6562E+00	9.6703E−01	2.5759E+00
	STD	1.8672E+02	3.8025E−01	7.3179E+03	1.1467E+01	2.7177E+06	2.5771E+02	1.4029E−01	2.8266E+02	4.0326E+01	8.0812E+00	2.5954E+00	4.4850E−01	2.7810E−01
BBO	AVG	4.5196E+00	6.8084E−01	1.8171E+03	3.6743E+00	3.3753E+02	4.5128E+00	3.0624E−02	−8.1986E+03	5.3237E+01	8.5630E−01	1.0414E+00	3.5683E−02	1.4450E−03
	STD	1.1029E+00	9.0243E−02	6.7453E+02	1.8037E+00	4.2191E+02	9.5987E−01	9.7892E−03	6.4947E+02	1.4833E+01	1.3868E−01	1.1927E−02	7.1035E−02	3.9726E−04
ACO	AVG	1.4896E+03	2.8917E+01	6.2302E+04	8.5858E+01	3.1211E+06	1.4676E+03	8.4214E−01	−4.1703E+03	2.8896E+02	1.9354E+01	1.4870E+01	2.9938E+00	7.0734E−01
	STD	4.8400E+02	1.1065E+01	8.8864E+03	5.2580E+00	1.7134E+06	4.6077E+02	3.4605E−01	2.5589E+02	1.8431E+01	2.7281E+00	4.5674E+00	1.0381E+00	1.9879E−01
RCSA	AVG	2.3799E−02	6.4432E−02	1.0006E−01	6.8650E−02	4.1978E+01	2.3885E−02	6.0046E−03	−1.1710E+04	3.7247E+01	4.0817E−02	5.3459E−02	2.0754E−03	6.7959E−06
	STD	3.4715E−03	5.9357E−03	2.1804E−02	5.4714E−03	4.3402E+01	3.5655E−03	2.0870E−03	2.7011E+02	8.5659E+00	3.8631E−03	1.2974E−02	1.4587E−02	1.3458E−06
HS	AVG	7.7942E+02	5.6504E+00	2.8210E+04	2.9162E+01	1.3853E+05	7.6622E+02	2.2672E−01	−1.2142E+04	3.2486E+01	6.9608E+00	7.8622E+00	6.1488E−02	3.0919E−01
	STD	2.0020E+02	9.1753E−01	6.1253E+03	2.9115E+00	5.0772E+04	1.7390E+02	6.5392E−02	1.4395E+02	4.4358E+00	5.8399E−01	1.5054E+00	3.5520E−02	7.7478E−02
COVIDOA	AVG	1.5294E+03	1.3157E+01	1.1900E+04	2.1694E+01	2.6259E+05	1.4985E+03	1.2488E−01	−7.1456E+03	1.5034E+02	9.0474E+00	1.4857E+01	5.2815E−01	5.8655E−01
	STD	3.8501E+02	1.7633E+00	4.3293E+03	3.5484E+00	1.7913E+05	4.2117E+02	4.4486E−02	8.5690E+02	1.8700E+01	8.1872E−01	3.6185E+00	2.0493E−01	1.6287E−01
KMA	AVG	0.0000E+00	0.0000E+00	0.0000E+00	1.1148E−310	2.8847E+01	3.8814E+00	5.1695E−04	−5.2281E+03	0.0000E+00	4.4409E−16	0.0000E+00	1.5269E−01	7.1545E−01
	STD	0.0000E+00	0.0000E+00	0.0000E+00	0.0000E+00	8.1899E−02	9.2606E−01	4.4552E−04	1.1767E+03	0.0000E+00	0.0000E+00	0.0000E+00	1.2123E−01	2.7921E−01
QIO	AVG	0.0000E+00	3.1677E−173	3.1235E−170	5.1966E−158	1.1277E+00	2.8075E−08	1.2330E−03	−1.2569E+04	0.0000E+00	4.4409E−16	0.0000E+00	3.7561E−09	1.2452E−08
	STD	0.0000E+00	0.0000E+00	0.0000E+00	5.1929E−157	5.2063E+00	8.0977E−09	8.7638E−04	1.3302E−07	0.0000E+00	0.0000E+00	0.0000E+00	1.1586E−09	4.3620E−09

Table 8
Results of accuracy test with unimodal and multimodal benchmark functions having 100 dimensions.

Alg.	Metric	F1	F2	F3	F4	F5	F6	F7	F8	F9	F10	F11	F12	F13
HOA	AVG	1.8522E−19	1.3502E−09	4.1630E−12	6.1640E−10	4.7372E+01	2.2390E+01	1.2457E−03	−8.3363E+03	8.2017E+01	1.2690E−10	0.0000E+00	9.6350E−01	5.3158E−01
	STD	2.6280E−19	7.9614E−10	1.2774E−11	3.7091E−10	2.5169E+01	6.5707E−01	8.4266E−04	1.1935E+03	1.9437E+02	8.0440E−11	0.0000E+00	8.5512E−02	1.4757E−01
TLBO	AVG	7.8910E−44	1.6026E−22	2.9567E−02	3.6370E−18	9.6965E+01	4.2937E+00	2.4912E−03	−1.4192E+04	1.2439E+01	1.3329E−01	0.0000E+00	4.8875E−02	5.6734E+00
	STD	9.0264E−44	9.5581E−23	4.8667E−02	1.7244E−18	7.4020E−01	7.1253E−01	8.1693E−04	3.5931E+03	5.1515E+01	9.3802E−01	0.0000E+00	1.5302E−02	8.3825E−01
GA	AVG	2.5612E+05	5.5031E+42	1.1815E+06	9.3367E+01	1.0498E+09	2.5504E+05	6.2054E+02	−7.4157E+03	1.4622E+03	2.0668E+01	2.2962E+03	2.2887E+01	1.0148E+02
	STD	1.3318E+04	3.8753E+43	3.7627E+05	1.6536E+00	8.8337E+07	1.3198E+04	6.9640E+01	9.8543E+02	5.3286E+01	8.1945E−02	1.3245E+02	1.6664E+00	6.2592E+00
DE	AVG	4.1764E+03	3.5309E+01	2.9570E+05	9.5955E+01	3.5387E+06	4.0071E+03	3.0426E+00	−9.6733E+03	9.1387E+02	8.9379E+00	3.8500E+01	3.9590E−01	2.4170E+00
	STD	1.4288E+03	6.8318E+00	5.0110E+04	1.2927E+00	1.6689E+06	1.4130E+03	1.0118E+00	1.0159E+03	3.9350E+01	9.5762E−01	1.2747E+01	1.3908E−01	8.8640E−01
PSO	AVG	2.9201E+04	2.7391E+02	1.2375E+05	4.9466E+01	1.6578E+07	2.8785E+04	4.6313E+01	−1.8705E+04	5.8094E+02	1.8040E+01	2.5621E+02	3.5016E+00	3.3448E+01
	STD	8.7410E+03	4.1214E+01	3.1915E+04	4.0771E+00	1.8971E+07	8.9960E+03	1.6211E+01	1.5556E+03	6.1977E+01	4.7271E−01	7.9594E+01	7.9398E−01	5.5665E+00
ABC	AVG	1.1051E+05	2.2905E+03	4.1870E+05	9.2571E+01	3.2581E+08	1.0535E+05	2.8284E+02	−1.6927E+04	9.8646E+02	1.9691E+01	9.7477E+02	1.0101E+01	4.5401E+01
	STD	1.7137E+04	2.1119E+04	5.2513E+04	1.2624E+00	9.9898E+07	1.9481E+04	4.7004E+01	1.1555E+03	7.1973E+01	2.8360E−01	1.6272E+02	1.8282E+00	6.7841E+00
GWO	AVG	1.7776E+03	3.5755E+00	2.4460E+05	9.2045E+01	2.2874E+06	1.9248E+03	2.1348E+00	−9.4109E+03	8.6169E+02	2.1333E+01	1.8376E+01	4.8705E+00	5.7020E+00
	STD	9.9266E+02	1.5855E+00	5.2343E+04	5.5551E+00	2.4222E+06	1.1237E+03	1.0548E+00	1.0671E+03	1.0591E+02	9.2555E−02	8.0334E+00	1.8164E+00	1.2757E+00
SCA	AVG	1.8189E+04	1.5557E+01	3.0177E+05	9.1648E+01	1.8981E+08	1.9100E+04	8.9360E+01	−6.6587E+03	3.1417E+02	1.8682E+01	1.9056E+02	4.3175E+00	1.5699E+01
	STD	1.1304E+04	9.6292E+00	7.3795E+04	2.4322E+00	7.8999E+07	1.1794E+04	3.7147E+01	5.2755E+02	1.4949E+02	4.0594E+00	1.1081E+02	1.6711E+00	2.9895E+00
BBO	AVG	2.7798E+02	1.2691E+01	7.4452E+04	3.0028E+01	8.1004E+03	2.7476E+02	2.2358E−01	−2.2517E+04	3.2198E+02	3.6627E+00	3.4512E+00	3.0841E−01	1.0798E−01
	STD	2.8246E+01	1.6814E+00	1.4044E+04	2.9831E+00	1.7137E+03	2.5929E+01	4.2326E−02	1.1783E+03	3.6224E+01	1.1548E−01	2.7431E−01	2.0872E−01	1.7066E−02
ACO	AVG	2.2660E+05	5.8950E+37	7.2911E+05	9.6155E+01	1.1995E+09	2.2546E+05	6.9892E+02	−7.8097E+03	1.5177E+03	2.0714E+01	2.0284E+03	2.6751E+01	6.9986E+01
	STD	1.2208E+04	3.6012E+38	9.7341E+04	1.3294E+00	8.7438E+07	1.1427E+04	6.2670E+01	5.1648E+02	3.3649E+01	3.3463E−02	1.1113E+02	1.5191E+00	3.2526E+00
RCSA	AVG	4.9182E−01	2.6740E+00	1.9059E+01	2.7046E−01	1.4394E+02	4.9339E−01	7.0660E−02	−3.2716E+04	2.2286E+02	1.1788E−01	3.2323E−01	6.8561E−03	2.0341E−03
	STD	4.9577E−02	1.6091E+01	2.1966E+00	1.8042E−02	9.8349E+01	4.4985E−02	1.6990E−02	1.0598E+03	2.7516E+01	6.9073E−03	2.5483E−02	1.8004E−02	4.1959E−03
HS	AVG	3.7624E+04	9.7662E+01	4.7496E+05	7.1530E+01	7.0277E+07	3.7456E+04	3.6797E+01	−3.1557E+04	4.5311E+02	1.5902E+01	3.3955E+02	3.2249E+00	1.4799E+01
	STD	3.4351E+03	6.6169E+00	6.1073E+04	1.7553E+00	8.0095E+06	3.3857E+03	3.8575E+00	7.2971E+02	2.6193E+01	3.1526E−01	3.1361E+01	3.8800E−01	1.1941E+00
COVIDOA	AVG	4.1677E+04	1.5373E+02	4.2805E+05	9.2039E+01	6.3002E+07	4.1207E+04	3.1168E+01	−1.1671E+04	9.5900E+02	1.6414E+01	3.8395E+02	5.3179E+00	1.6481E+01
	STD	5.2759E+03	1.2992E+01	5.8011E+04	7.3159E+00	1.4200E+07	5.0490E+03	6.3090E+00	9.9598E+02	3.5752E+01	3.7314E−01	4.4115E+01	6.7145E−01	2.1925E+00
KMA	AVG	0.0000E+00	0.0000E+00	0.0000E+00	1.5711E−321	9.8746E+01	1.6700E+01	4.9848E−04	−1.7603E+04	0.0000E+00	4.4409E−16	0.0000E+00	1.8016E−01	2.5887E+00
	STD	0.0000E+00	0.0000E+00	0.0000E+00	0.0000E+00	1.3196E−01	3.6159E+00	3.7792E−04	4.6369E+03	0.0000E+00	0.0000E+00	0.0000E+00	9.2647E−02	9.3055E−01
QIO	AVG	0.0000E+00	2.2305E−161	4.9558E−18	3.7506E−148	1.0615E−05	9.8227E−08	1.5476E−03	−4.1898E+04	0.0000E+00	4.4409E−16	0.0000E+00	6.3917E−09	3.9836E−08
	STD	0.0000E+00	2.2305E−160	4.9558E−17	3.7456E−147	6.3722E−05	3.2662E−08	1.0570E−03	6.7432E−07	0.0000E+00	0.0000E+00	0.0000E+00	1.8000E−09	1.0830E−08

Table 9
Results of accuracy test with unimodal and multimodal benchmark functions having 250 dimensions.

Alg.	Metric	F1	F2	F3	F4	F5	F6	F7	F8	F9	F10	F11	F12	F13
HOA	AVG	8.3998E−19	3.9635E−09	3.1103E−10	1.8102E−09	1.3486E+02	5.9627E+01	1.2239E−03	−1.3845E+04	2.5595E+02	1.6041E−10	0.0000E+00	1.0800E+00	1.6259E+00
	STD	9.3717E−19	2.5305E−09	1.4241E−09	1.8220E−09	7.0543E+01	6.8081E−01	7.0935E−04	1.9804E+03	5.5157E+02	1.0141E−10	0.0000E+00	4.2740E−02	4.4945E−01
TLBO	AVG	2.4600E−42	1.1833E−21	6.2834E+00	2.1158E−17	2.4747E+02	3.0662E+01	2.8216E−03	−2.3546E+04	0.0000E+00	8.7182E−01	0.0000E+00	2.4631E−01	2.3828E+01
	STD	2.6430E−42	5.2388E−22	8.7207E+00	9.0722E−18	4.4924E−01	1.4624E+00	9.1102E−04	6.8148E+03	0.0000E+00	2.5178E+00	0.0000E+00	3.2740E−02	1.0860E+00
GA	AVG	7.1785E+05	2.8753E+122	7.0363E+06	9.7910E+01	3.1935E+09	7.0998E+05	4.6945E+03	−1.1751E+04	3.9990E+03	2.0887E+01	6.4293E+03	2.8501E+01	2.8910E+02
	STD	2.0564E+04	2.6335E+123	2.1944E+06	6.5881E−01	1.4049E+08	2.5602E+04	2.8558E+02	1.3087E+03	7.4782E+01	4.6206E−02	1.7860E+02	1.3374E+00	9.8840E+00
DE	AVG	7.1490E+04	3.2774E+02	2.0373E+06	9.8455E+01	9.7049E+07	7.0961E+04	1.1384E+02	−1.5352E+04	2.6193E+03	1.5365E+01	6.3797E+02	2.7740E+00	3.8160E+01
	STD	8.4825E+03	3.2224E+01	2.9734E+05	4.5959E−01	2.2570E+07	8.9983E+03	2.4808E+01	1.7320E+03	8.8001E+01	5.1975E−01	8.5167E+01	5.2516E−01	4.9657E+00
PSO	AVG	1.8463E+05	1.4610E+10	7.4214E+05	5.8633E+01	3.0494E+08	1.8634E+05	5.7934E+02	−3.3656E+04	2.0747E+03	1.9111E+01	1.6458E+03	6.8110E+00	1.2041E+02
	STD	2.6239E+04	1.4445E+11	1.8889E+05	3.6300E+00	1.0667E+08	2.8993E+04	1.7090E+02	2.8517E+03	1.5287E+02	3.5941E−01	2.7212E+02	1.2453E+00	1.2703E+01
ABC	AVG	5.0208E+05	2.5419E+79	2.4831E+06	9.7361E+01	2.0405E+09	4.9854E+05	3.3459E+03	−3.0039E+04	3.2786E+03	2.0468E+01	4.4451E+03	1.9532E+01	2.0186E+02
	STD	3.8428E+04	2.5419E+80	3.2163E+05	4.6542E−01	2.3978E+08	3.9683E+04	3.4417E+02	3.1951E+03	1.5141E+02	9.0582E−02	4.1641E+02	1.9356E+00	1.4377E+01
GWO	AVG	2.1505E+04	1.7694E+01	2.4029E+06	9.9090E+01	8.9792E+07	2.4827E+04	1.1472E+02	−1.5313E+04	2.3856E+03	2.1346E+01	2.1571E+02	6.9116E+00	1.8052E+01
	STD	6.9976E+03	4.5073E+00	5.4000E+05	6.9498E−01	5.9418E+07	8.1549E+03	7.1290E+01	1.5279E+03	2.0694E+02	6.4607E−02	7.4220E+01	1.7947E+00	2.8412E+00
SCA	AVG	1.0578E+05	6.1965E+01	2.0101E+06	9.8040E+01	1.0157E+09	9.7058E+04	1.4012E+03	−1.0648E+04	7.4713E+02	1.9683E+01	9.4495E+02	6.6806E+00	4.8986E+01
	STD	4.6164E+04	2.6647E+01	4.1971E+05	6.7138E−01	2.5813E+08	3.9059E+04	3.7912E+02	9.2171E+02	3.1371E+02	2.9549E+00	3.8209E+02	2.1563E+00	9.9238E+00
BBO	AVG	2.2513E+03	9.2118E+01	4.9044E+05	4.6701E+01	2.0941E+05	2.2504E+03	1.4161E+00	−4.9305E+04	1.2802E+03	5.4528E+00	2.1269E+01	1.1543E+00	4.5756E+00
	STD	1.9273E+02	8.8800E+00	7.0040E+04	2.4637E+00	3.8851E+04	1.8574E+02	1.7174E−01	2.3376E+03	7.1632E+01	1.8955E−01	1.5752E+00	1.8280E−01	2.0426E+00
ACO	AVG	7.3732E+05	1.2058E+126	4.5384E+06	9.8433E+01	3.3894E+09	7.3664E+05	5.0903E+03	−1.2476E+04	4.2870E+03	2.0884E+01	6.6267E+03	3.3958E+01	2.9018E+02
	STD	2.1243E+04	8.4529E+126	5.7197E+05	4.9069E−01	1.2874E+08	2.1932E+04	2.4231E+02	9.5371E+02	6.1697E+01	1.6467E−02	1.9960E+02	1.2836E+00	7.5714E+00
RCSA	AVG	4.8592E+00	1.0861E+19	2.6342E+04	1.6628E+00	3.9688E+02	4.8918E+00	3.7776E−01	−7.1274E+04	8.6048E+02	2.9456E−01	9.0091E−01	6.4894E−03	4.5648E−03
	STD	2.7462E−01	1.0861E+20	3.1993E+03	6.1741E−01	2.0038E+02	3.1989E−01	5.3292E−02	1.7347E+03	6.2164E+01	1.0342E−02	2.4449E−02	1.2433E−02	5.1621E−03
HS	AVG	2.2855E+05	5.0070E+02	3.1637E+06	8.7794E+01	6.4330E+08	2.2801E+05	8.7235E+02	−5.4887E+04	2.0785E+03	1.8805E+01	2.0600E+03	9.4913E+00	9.1525E+01
	STD	8.3135E+03	1.6282E+01	3.9008E+05	7.1621E−01	4.2426E+07	1.0384E+04	6.3773E+01	1.0905E+03	5.9340E+01	1.3504E−01	8.5800E+01	5.5902E−01	4.1818E+00
COVIDOA	AVG	2.6194E+05	1.0854E+36	3.2682E+06	9.8385E+01	7.9841E+08	2.6297E+05	1.0095E+03	−1.7391E+04	3.0212E+03	1.9227E+01	2.3614E+03	1.2718E+01	1.0200E+02
	STD	1.2358E+04	8.7890E+36	3.6729E+05	5.3475E−01	8.4603E+07	1.5689E+04	1.1016E+02	1.2477E+03	6.8806E+01	1.5585E−01	1.2830E+02	7.8932E−01	6.2967E+00
KMA	AVG	0.0000E+00	0.0000E+00	0.0000E+00	4.9407E−324	2.4852E+02	4.4767E+01	5.5131E−04	−4.6088E+04	0.0000E+00	4.7962E−16	0.0000E+00	1.8184E−01	6.7229E+00
	STD	0.0000E+00	0.0000E+00	0.0000E+00	0.0000E+00	2.8276E−01	7.9271E+00	5.1459E−04	1.2217E+04	0.0000E+00	3.5527E−16	0.0000E+00	8.5467E−02	2.7128E+00
QIO	AVG	1.8324E−318	7.1579E−163	8.9323E−13	1.8450E−119	4.7394E−05	2.4471E−07	1.8945E−03	−1.0475E+05	0.0000E+00	4.4409E−16	0.0000E+00	9.8090E−09	8.9549E−08
	STD	0.0000E+00	4.4455E−162	6.1873E−12	1.8450E−118	2.3305E−04	8.5753E−08	1.4864E−03	3.7655E−05	0.0000E+00	0.0000E+00	0.0000E+00	3.1320E−09	2.2559E−08

HOA follows a similar pattern to hikers exploring divergent spaces and then exploiting the landscape that shows the favorable location. The exploitation process involves focusing on the neighborhoods with favorable or ideal locations. HOA's exploration and exploitation capabilities help it avoid being stuck in a local optimum.

Furthermore, in Figs. 9(a)–9(x), we see that as the iteration increases, HOA tends towards convergence. This is similar to a hiking expedition; as the hikers proceed in the hike, the more the hikers tend towards the peak of a mountain.

We observe that, in a similar trend to the convergence analysis, the hikers' average fitness in finding the best solution improves as the iterations increase.

5.1.3. Computational time test benchmark

In Tables 11–14, we present the results of the computational time benchmark tests of HOA with the respective unimodal, multimodal, and fixed-dimension multimodal functions for varying dimension sizes of 30, 100, and 250.

In Table 11, we observe that HOA outperformed all the other metaheuristics except for PSO and GWO. Furthermore, HOA outperformed all the other metaheuristics except for PSO and GWO for a dimension size of 100 in Table 12. Similarly, in Table 13, which presents the computational time benchmark test for a dimension size of 250, HOA outperformed all the other metaheuristics with no exception. Moreover, for fixed-dimension multimodal functions presented in Table 14, HOA

Table 10
Results of accuracy test with fixed-dimension multimodal benchmark functions.

Alg.	Metric	F14	F15	F16	F17	F18	F19	F20	F21	F22	F23
HOA	AVG	6.3882E+00	4.0143E−04	−1.0312E+00	3.9796E−01	9.2462E+00	−3.0048E−01	−3.2106E+00	−9.1618E+00	−8.2984E+00	−8.9006E+00
	STD	2.5939E+00	1.4962E−04	1.3210E−03	3.5458E−04	1.3784E+01	1.6737E−16	1.1513E−01	1.1222E+00	2.1171E+00	1.8186E+00
TLBO	AVG	9.9800E−01	4.5990E−04	−1.0316E+00	3.9789E−01	3.0000E+00	−3.0048E−01	−3.3035E+00	−7.4032E+00	−8.5512E+00	−9.4398E+00
	STD	3.8653E−17	2.4916E−04	6.5254E−16	0.0000E+00	6.2962E−16	1.6737E−16	4.1784E−02	2.4892E+00	2.5097E+00	2.2169E+00
GA	AVG	2.1379E+00	5.9223E−02	−1.0148E+00	9.6243E−01	1.3539E+01	−3.0048E−01	−2.4489E+00	−1.2188E+00	−1.1003E+00	−1.0974E+00
	STD	2.1293E+00	1.3687E−01	2.8033E−02	9.1232E−01	1.3635E+01	1.6737E−16	4.5070E−01	1.0512E+00	9.9972E−01	9.6225E−01
DE	AVG	1.2258E+00	1.1902E−03	−1.0316E+00	3.9789E−01	3.0000E+00	−3.0020E−01	−3.2435E+00	−8.9807E+00	−9.2953E+00	−9.9487E+00
	STD	7.7983E−01	2.8381E−03	6.5824E−16	0.0000E+00	9.3835E−16	2.7410E−03	5.6505E−02	2.1562E+00	2.2803E+00	1.7966E+00
PSO	AVG	5.3019E+00	3.5977E−03	−1.0316E+00	3.9789E−01	3.8100E+00	−3.0048E−01	−3.2485E+00	−6.3807E+00	−5.7049E+00	−5.8608E+00
	STD	3.8992E+00	6.7421E−03	6.2923E−16	0.0000E+00	8.1000E+00	1.6737E−16	9.8395E−02	2.2474E+00	2.2048E+00	2.4131E+00
ABC	AVG	9.9800E−01	1.1462E−03	−1.0316E+00	3.9789E−01	3.0023E+00	−3.0048E−01	−3.3208E+00	−6.6656E+00	−7.6180E+00	−9.3174E+00
	STD	1.8778E−09	3.0538E−04	5.4135E−09	1.1405E−07	3.6428E−03	1.6737E−16	8.1538E−04	1.3395E+00	1.5958E+00	1.0885E+00
GWO	AVG	1.5332E+01	6.7029E−04	−1.0266E+00	4.0181E−01	2.9650E+01	−3.0047E−01	−3.2514E+00	−9.1245E+00	−6.6676E+00	−6.8618E+00
	STD	5.5692E+00	8.6377E−05	1.1405E−02	4.7553E−03	3.6240E+01	6.2994E−05	6.0375E−02	5.3531E−01	2.9158E+00	2.9375E+00
SCA	AVG	2.0423E+00	1.0932E−03	−1.0316E+00	4.0042E−01	3.0002E+00	−3.0048E−01	−2.8417E+00	−4.4618E+00	−4.6149E+00	−4.8548E+00
	STD	1.5804E+00	3.5229E−04	6.1379E−05	2.6306E−03	3.1437E−04	1.6737E−16	3.7013E−01	1.0805E+00	1.2553E+00	1.3873E+00
BBO	AVG	6.2957E+00	3.5328E−03	−1.0316E+00	3.9789E−01	6.5230E+00	−3.0048E−01	−3.2828E+00	−5.8709E+00	−6.6522E+00	−7.3481E+00
	STD	4.6108E+00	5.7338E−03	2.3074E−11	1.4401E−09	1.1380E+01	1.6737E−16	5.6187E−02	1.8784E+00	2.6167E+00	2.7383E+00
ACO	AVG	1.1254E+00	2.7724E−03	−1.0316E+00	3.9789E−01	3.0000E+00	−3.0048E−01	−3.2649E+00	−9.2356E+00	−6.9027E+00	−8.2751E+00
	STD	9.9828E−01	5.7102E−03	6.6949E−16	0.0000E+00	7.6007E−16	1.6737E−16	5.9698E−02	1.9685E+00	3.2091E+00	3.0684E+00
RCSA	AVG	9.9800E−01	5.9046E−04	−1.0316E+00	3.9789E−01	3.0000E+00	−3.0048E−01	−3.2677E+00	−8.2160E+00	−8.2579E+00	−8.9113E+00
	STD	4.2165E−16	2.0145E−03	1.5551E−14	3.5131E−13	7.4261E−12	1.6737E−16	5.4182E−02	2.4870E+00	2.1234E+00	1.9069E+00
HS	AVG	9.9800E−01	4.7374E−03	−1.0316E+00	3.9789E−01	4.9251E+00	−3.0048E−01	−3.2958E+00	−6.3296E+00	−7.8897E+00	−8.5361E+00
	STD	1.1305E−10	7.4681E−03	6.8308E−08	2.3194E−06	6.9197E+00	1.6737E−16	4.9499E−02	2.2186E+00	2.7519E+00	2.6925E+00
COVIDOA	AVG	9.9994E−01	2.4493E−03	−1.0309E+00	4.0222E−01	3.2641E+00	−3.0048E−01	−2.9800E+00	−8.3257E+00	−9.3079E+00	−9.5036E+00
	STD	5.4742E−03	1.0474E−03	6.9440E−04	4.8867E−03	2.4590E−01	1.6737E−16	9.5629E−02	1.6750E+00	9.3738E−01	9.5630E−01
KMA	AVG	4.3981E+00	1.6098E−02	−1.0313E+00	3.9859E−01	3.6153E+00	−3.0048E−01	−2.2886E+00	−7.6776E+00	−6.5649E+00	−5.8292E+00
	STD	3.9700E+00	1.2557E−02	1.9465E−03	5.9248E−03	3.8078E+00	1.6737E−16	7.8199E−01	1.9432E+00	2.3312E+00	2.1446E+00
QIO	AVG	9.9800E−01	3.1678E−04	−1.0316E+00	3.9789E−01	3.0000E+00	−3.0047E−01	−3.2958E+00	−1.0153E+01	−1.0403E+01	−1.0536E+01
	STD	8.7787E−13	9.1561E−05	1.5457E−10	2.1627E−10	1.1981E−09	2.0509E−06	4.9499E−02	1.5614E−08	1.3476E−08	1.3827E−08

Table 11
Results of computational time test in seconds (s) with unimodal and multimodal benchmark functions having 30 dimensions.

Alg.	Metric	F1	F2	F3	F4	F5	F6	F7	F8	F9	F10	F11	F12	F13
HOA	AVG	2.8900E−02	2.8100E−02	6.3100E−02	2.7500E−02	3.1700E−02	3.0200E−02	4.5900E−02	3.4700E−02	3.2600E−02	3.0600E−02	3.5600E−02	1.0400E−01	1.0700E−01
	STD	8.6600E−03	5.1500E−03	1.0200E−02	5.7300E−03	7.5700E−03	1.1600E−02	9.9200E−03	8.2100E−03	7.1300E−03	5.4900E−03	8.4600E−03	1.6500E−02	1.9000E−02
TLBO	AVG	2.4400E−02	2.4100E−02	6.6500E−02	2.2900E−02	2.9600E−02	2.4600E−02	5.3700E−02	3.1700E−02	3.0900E−02	2.7400E−02	3.3900E−02	1.1300E−01	1.1500E−01
	STD	5.9400E−03	4.7300E−03	8.2100E−03	3.7100E−03	4.5600E−03	7.4600E−03	8.4800E−03	6.1500E−03	8.2200E−03	4.6900E−03	6.5000E−03	1.6700E−02	2.0600E−02
GA	AVG	1.9500E−02	1.9100E−02	4.0000E−02	1.8600E−02	2.1800E−02	1.9700E−02	3.2900E−02	2.2400E−02	2.3600E−02	2.2500E−02	2.5000E−02	6.1600E−02	6.2100E−02
	STD	5.3600E−03	3.1500E−03	6.6300E−03	2.5000E−03	3.3100E−03	4.7000E−03	5.9600E−03	4.2600E−03	6.2800E−03	3.8800E−03	4.3100E−03	1.0800E−02	1.2100E−02
DE	AVG	2.0700E−02	2.0000E−02	4.0900E−02	2.0000E−02	2.2900E−02	2.1800E−02	3.3800E−02	2.4200E−02	2.4500E−02	2.4500E−02	2.6000E−02	6.0800E−02	6.3900E−02
	STD	5.1400E−03	4.3200E−03	6.6000E−03	3.9200E−03	4.4200E−03	7.1800E−03	4.9000E−03	6.4100E−03	5.1000E−03	7.5100E−03	6.0400E−03	8.9200E−03	1.5600E−02
PSO	AVG	5.0400E−03	5.1600E−03	2.6500E−02	4.9400E−03	7.7100E−03	4.9800E−03	1.8400E−02	8.3700E−03	7.3500E−03	8.1200E−03	1.0000E−02	4.5300E−02	4.6900E−02
	STD	1.7400E−03	1.3200E−03	5.4000E−03	1.4700E−03	1.6900E−03	1.7500E−03	1.9400E−03	2.2500E−03	1.9200E−03	2.4000E−03	3.1400E−03	6.6400E−03	9.5400E−03
ABC	AVG	1.5900E−02	1.6700E−02	5.9500E−02	1.4700E−02	2.2500E−02	1.7000E−02	4.5800E−02	2.4500E−02	2.1900E−02	2.2500E−02	2.8500E−02	1.0100E−01	1.0500E−01
	STD	4.9600E−03	4.1800E−03	1.1400E−02	3.3700E−03	5.1500E−03	7.9700E−03	8.7500E−03	7.6200E−03	4.7900E−03	5.7000E−03	6.3700E−03	1.5000E−02	1.9300E−02
GWO	AVG	8.1500E−03	8.0600E−03	2.8400E−02	7.7500E−03	1.0300E−02	8.5400E−03	1.6400E−02	1.1300E−02	1.0400E−02	1.0300E−02	1.2600E−02	4.0900E−02	4.2700E−02
	STD	3.2900E−03	2.1900E−03	5.1200E−03	2.2800E−03	2.8800E−03	5.5500E−03	3.5100E−03	3.9100E−03	2.9600E−03	3.1300E−03	3.0200E−03	6.4300E−03	1.1900E−02
SCA	AVG	1.4900E−02	1.4600E−02	3.6000E−02	1.4800E−02	1.8000E−02	1.7000E−02	2.7700E−02	1.8600E−02	1.7900E−02	1.8000E−02	2.1200E−02	5.2900E−02	5.4000E−02
	STD	4.2300E−03	2.6200E−03	7.4600E−03	3.2800E−03	4.5200E−03	1.2500E−02	5.1800E−03	4.0800E−03	3.4400E−03	3.2200E−03	5.7300E−03	8.0700E−03	9.4000E−03
BBO	AVG	1.7200E−01	1.6900E−01	1.9700E−01	1.7300E−01	1.7700E−01	1.8700E−01	1.8900E−01	1.8200E−01	1.9100E−01	1.7800E−01	1.8800E−01	2.2300E−01	2.3300E−01
	STD	3.1200E−02	2.6900E−02	4.2800E−02	3.6100E−02	3.0500E−02	5.2000E−02	3.2700E−02	3.6800E−02	3.8900E−02	2.5200E−02	3.2500E−02	3.8000E−02	4.5600E−02
ACO	AVG	2.0800E−01	2.0600E−01	2.4400E−01	2.1000E−01	2.2200E−01	2.3300E−01	2.3200E−01	2.2400E−01	2.3800E−01	2.2100E−01	2.3100E−01	2.7600E−01	2.8500E−01
	STD	3.1100E−02	2.9100E−02	4.2300E−02	3.2500E−02	3.6600E−02	9.4500E−02	3.5500E−02	4.5100E−02	4.8300E−02	3.0600E−02	3.8300E−02	4.0200E−02	4.8100E−02
RCSA	AVG	2.1600E+00	2.2900E+00	4.4100E+00	2.2600E+00	2.5300E+00	2.4300E+00	3.7400E+00	2.8600E+00	2.8100E+00	2.6800E+00	3.0800E+00	6.7200E+00	7.1400E+00
	STD	1.1600E−01	1.6100E−01	2.4100E−01	1.6800E−01	1.7300E−01	4.9100E−01	2.5600E−01	2.2600E−01	4.0100E−01	1.5600E−01	1.8200E−01	6.7600E−01	9.9500E−01
HS	AVG	7.8100E−02	7.9800E−02	9.6800E−02	8.1700E−02	8.1700E−02	8.5200E−02	9.0700E−02	8.4300E−02	8.9700E−02	8.8700E−02	8.7500E−02	1.1400E−01	1.2300E−01
	STD	1.1900E−02	1.2900E−02	1.2100E−02	1.7600E−02	9.4100E−03	2.4700E−02	1.5900E−02	1.2700E−02	1.6100E−02	1.7700E−02	1.1700E−02	1.9800E−02	2.6200E−02
COVIDOA	AVG	2.3600E−01	2.3900E−01	2.9000E−01	2.3700E−01	2.4600E−01	2.5500E−01	2.7500E−01	2.6300E−01	2.7600E−01	2.6000E−01	2.6600E−01	3.3400E−01	3.5500E−01
	STD	3.3300E−02	3.1900E−02	4.5300E−02	2.9200E−02	2.9400E−02	5.1200E−02	3.2500E−02	3.3400E−02	3.9500E−02	3.5500E−02	3.0400E−02	4.5600E−02	6.5200E−02
KMA	AVG	7.7200E−01	1.4200E+00	1.0000E+00	1.5900E+00	1.6400E+00	1.7100E+00	2.3000E−01	3.2900E−03	5.4800E−02	1.6500E+00	6.0700E−02	2.1600E+00	2.2800E+00
	STD	8.0000E−02	1.0100E−01	9.1400E−02	1.1800E−01	1.2400E−01	4.0300E−01	2.8300E−01	1.3500E−03	1.5600E−02	1.2400E−01	1.1700E−02	1.7100E−01	3.6900E−01
QIO	AVG	1.3800E−01	1.3400E−01	1.6300E−01	1.3600E−01	1.4400E−01	1.4600E−01	1.5400E−01	1.5200E−01	1.5700E−01	1.4500E−01	1.4900E−01	2.0000E−01	2.0000E−01
	STD	2.1400E−02	1.5900E−02	2.3000E−02	2.1800E−02	2.6300E−02	4.3600E−02	2.4200E−02	2.2800E−02	2.8900E−02	2.1600E−02	2.3000E−02	3.3600E−02	3.9500E−02

outperforms KMA, COVIDOA, QIO, TLBO, ABC, BBO, ACO, RCSA, and HS. To be specific, HOA exhibits a lightweight nature while maintaining a commendable level of accuracy across all traditional functions, regardless of dimension size. In terms of computational efficiency, HOA surpasses the three recently developed metaheuristics (namely, KMA, COVIDOA, and QIO) that we investigated.

Table 12
Results of computational time test in seconds (s) with unimodal and multimodal benchmark functions having 100 dimensions.

Alg.	Metric	F1	F2	F3	F4	F5	F6	F7	F8	F9	F10	F11	F12	F13
HOA	AVG	3.4100E−02	3.8800E−02	1.7900E−01	3.7500E−02	3.3400E−02	3.5000E−02	7.9000E−02	4.8800E−02	4.1000E−02	3.7200E−02	4.2500E−02	1.9300E−01	1.8800E−01
	STD	6.4900E−03	1.1500E−02	6.2700E−02	1.6000E−02	3.1500E−03	1.2600E−02	4.8300E−03	8.2200E−03	1.2400E−02	4.2900E−03	8.9200E−03	1.5600E−02	6.5900E−03
TLBO	AVG	3.3900E−02	3.6900E−02	2.1600E−01	3.7800E−02	3.8900E−02	3.6000E−02	1.2000E−01	5.1100E−02	4.4700E−02	4.0000E−02	4.8800E−02	2.4500E−01	2.4900E−01
	STD	4.3500E−03	6.9500E−03	7.7200E−02	1.0500E−02	2.9700E−03	1.4200E−02	6.8500E−03	7.2000E−03	1.0300E−02	5.5700E−03	8.8100E−03	1.2500E−02	1.8800E−02
GA	AVG	4.4400E−02	4.7800E−02	1.3500E−01	4.8300E−02	4.4800E−02	4.4400E−02	8.1900E−02	5.1600E−02	5.5400E−02	5.1000E−02	5.3400E−02	1.4300E−01	1.4300E−01
	STD	5.3100E−03	7.9100E−03	3.2400E−02	1.0300E−02	3.3800E−03	7.4900E−03	9.3800E−03	7.0100E−03	2.2500E−02	4.2400E−03	5.1600E−03	1.6900E−02	8.9500E−03
DE	AVG	3.0800E−02	3.5800E−02	1.3600E−01	3.4400E−02	3.2200E−02	3.2300E−02	6.9900E−02	3.8900E−02	4.2500E−02	3.9000E−02	4.1800E−02	1.3100E−01	1.3500E−01
	STD	5.7200E−03	1.4400E−02	7.2300E−02	1.1000E−02	6.5000E−03	1.1900E−02	1.1000E−02	8.2000E−03	1.8500E−02	7.5700E−03	8.9500E−03	1.3000E−02	1.9700E−02
PSO	AVG	1.0300E−02	1.2500E−02	1.0900E−01	1.0800E−02	1.2400E−02	1.0700E−02	5.1100E−02	1.7500E−02	1.8100E−02	1.7600E−02	2.0700E−02	1.1100E−01	1.1500E−01
	STD	1.8800E−03	9.1300E−03	6.4500E−02	2.7700E−03	1.7100E−03	2.9300E−03	6.7000E−03	3.6700E−03	5.0900E−03	2.0800E−03	3.0600E−03	1.0300E−02	1.3400E−02
ABC	AVG	1.8300E−02	2.2600E−02	2.0000E−01	1.8000E−02	2.3500E−02	1.9000E−02	1.0200E−01	3.5500E−02	3.6700E−02	3.4000E−02	4.5000E−02	2.2900E−01	2.2800E−01
	STD	6.6700E−03	6.7500E−03	8.3400E−02	4.1600E−03	3.3900E−03	7.3700E−03	1.0700E−02	7.1700E−03	1.1100E−02	4.6000E−03	1.3300E−02	1.8100E−02	1.6200E−02
GWO	AVG	2.4100E−02	2.7300E−02	1.1700E−01	2.5900E−02	2.5600E−02	2.5700E−02	4.7200E−02	3.2000E−02	3.5400E−02	3.0100E−02	3.5700E−02	1.0600E−01	1.0400E−01
	STD	3.9300E−03	8.7400E−03	6.1900E−02	9.6500E−03	6.8800E−03	1.1200E−02	1.2700E−02	1.1500E−02	1.8000E−02	1.0100E−02	1.2000E−02	1.6700E−02	1.5300E−02
SCA	AVG	4.1700E−02	4.5300E−02	1.3400E−01	4.4100E−02	4.4500E−02	4.5400E−02	7.6000E−02	5.1900E−02	5.2400E−02	5.1400E−02	5.5700E−02	1.3700E−01	1.3800E−01
	STD	6.5400E−03	1.1700E−02	6.5600E−02	1.0300E−02	1.0200E−02	1.5500E−02	1.3000E−02	1.1100E−02	1.6000E−02	9.4600E−03	1.5800E−02	1.8200E−02	1.8900E−02
BBO	AVG	5.3200E−01	5.6300E−01	6.9300E−01	5.5900E−01	5.3200E−01	5.6000E−01	5.4100E−01	5.2500E−01	5.6500E−01	5.5500E−01	5.4500E−01	6.0700E−01	6.2400E−01
	STD	5.1200E−02	1.1000E−01	2.5900E−01	1.3100E−01	8.8000E−02	1.2900E−01	8.8100E−02	8.6100E−02	1.4700E−01	9.3900E−02	9.0000E−02	4.8600E−02	6.6500E−02
ACO	AVG	6.2700E−01	6.3700E−01	7.8400E−01	6.5000E−01	6.4500E−01	6.1300E−01	6.2900E−01	6.0700E−01	6.3700E−01	6.1800E−01	6.4100E−01	7.2900E−01	7.3300E−01
	STD	6.2000E−02	5.9400E−02	2.0100E−01	8.4600E−02	6.9300E−02	8.1000E−02	4.3200E−02	4.2700E−02	1.0900E−01	4.2700E−02	6.0400E−02	6.7000E−02	7.6200E−02
RCSA	AVG	3.0000E+00	3.1000E+00	1.1200E+01	3.1800E+00	3.2800E+00	2.9300E+00	7.1100E+00	3.8400E+00	3.6700E+00	3.8900E+00	4.2500E+00	1.3500E+01	1.3500E+01
	STD	1.5900E−01	2.8000E−01	1.3500E+00	4.6100E−01	2.2700E−01	2.8000E−01	4.5600E−01	1.8200E−01	1.8400E−01	3.3700E−01	2.0900E−01	2.4300E−01	2.2400E−01
HS	AVG	2.2000E−01	2.2700E−01	3.0800E−01	2.1800E−01	2.1000E−01	2.1000E−01	2.4500E−01	2.1600E−01	2.1500E−01	2.1800E−01	2.2400E−01	2.8700E−01	2.8600E−01
	STD	2.3700E−02	3.1300E−02	1.3800E−01	1.9400E−02	1.8600E−02	2.3400E−02	3.4700E−02	1.7800E−02	1.9900E−02	2.3900E−02	2.5800E−02	2.1600E−02	1.7600E−02
COVIDOA	AVG	2.7500E−01	2.8600E−01	3.8800E−01	2.8100E−01	2.8800E−01	2.9900E−01	3.3000E−01	3.0300E−01	3.1300E−01	3.0100E−01	3.0800E−01	4.0500E−01	4.2400E−01
	STD	7.3500E−02	8.6800E−02	1.9500E−01	7.8400E−02	7.6800E−02	8.0800E−02	9.8400E−02	8.3200E−02	6.9100E−02	8.3000E−02	7.6300E−02	1.1600E−01	1.1400E−01
KMA	AVG	1.1800E+00	2.2400E+00	1.6200E+00	2.5000E+00	2.4400E+00	2.6200E+00	3.2800E−01	4.1500E−03	8.0000E−02	2.4600E+00	8.6700E−02	3.1200E+00	3.2300E+00
	STD	6.4000E−01	1.2600E+00	1.1200E+00	1.4000E+00	1.2700E+00	1.4500E+00	4.9900E−01	2.0400E−03	4.0100E−02	1.2800E+00	4.4600E−02	1.4700E+00	1.4100E+00
QIO	AVG	2.2300E−01	2.3600E−01	2.8300E−01	2.2500E−01	2.2100E−01	2.3700E−01	2.3800E−01	2.4000E−01	2.4500E−01	2.2800E−01	2.2900E−01	2.9300E−01	2.9800E−01
	STD	1.3400E−01	1.7300E−01	1.9800E−01	1.4600E−01	1.2600E−01	1.5500E−01	1.3400E−01	1.4500E−01	1.3700E−01	1.3100E−01	1.2800E−01	1.5400E−01	1.5300E−01

Table 13
Results of computational time test in seconds (s) with unimodal and multimodal benchmark functions having 250 dimensions.

Alg.	Metric	F1	F2	F3	F4	F5	F6	F7	F8	F9	F10	F11	F12	F13
HOA	AVG	4.1411E−02	4.8041E−02	3.0210E−01	5.4695E−02	4.5885E−02	5.5553E−02	1.6828E−01	9.5100E−02	8.0970E−02	7.5489E−02	8.4009E−02	4.4651E−01	3.8074E−01
	STD	6.8671E−03	9.3941E−03	1.4475E−02	9.6456E−03	4.5528E−03	8.5550E−03	2.2352E−02	1.4853E−02	8.3184E−03	6.8730E−03	6.4812E−03	2.4878E−01	1.3768E−02
TLBO	AVG	4.9808E−02	5.6906E−02	4.6834E−01	6.2332E−02	6.0112E−02	6.3038E−02	3.2023E−01	1.1359E−01	8.8479E−02	9.1376E−02	1.0516E−01	7.3293E−01	6.2067E−01
	STD	4.7424E−03	9.3647E−03	2.8024E−02	1.0723E−02	1.4573E−02	7.0424E−03	4.4419E−02	1.8048E−02	1.3342E−02	1.3209E−02	1.2384E−02	4.5138E−01	3.6348E−02
GA	AVG	9.4117E−02	9.5467E−02	2.9969E−01	1.1104E−01	9.4985E−02	1.1436E−01	2.3365E−01	1.3261E−01	1.3581E−01	1.3783E−01	1.4269E−01	4.3319E−01	3.8714E−01
	STD	1.1038E−02	8.7457E−03	2.0737E−02	1.2695E−02	5.5745E−03	1.7199E−02	3.5015E−02	1.2235E−02	1.0827E−02	1.3161E−02	1.1385E−02	2.3788E−01	1.7188E−02
DE	AVG	4.9481E−02	5.2126E−02	2.6192E−01	5.9124E−02	5.4216E−02	6.4945E−02	1.8278E−01	8.9229E−02	9.0972E−02	9.3314E−02	9.9813E−02	3.8096E−01	3.4417E−01
	STD	9.8772E−03	1.4320E−02	3.8194E−02	1.1593E−02	1.3307E−02	1.5975E−02	2.7978E−02	1.8235E−02	1.6807E−02	1.7373E−02	1.8349E−02	1.8815E−01	2.7454E−02
PSO	AVG	2.0593E−02	2.1672E−02	2.2460E−01	2.4813E−02	2.4518E−02	2.7819E−02	1.5068E−01	5.1681E−02	5.0365E−02	5.1557E−02	5.9194E−02	3.3751E−01	3.1021E−01
	STD	3.0165E−03	3.5580E−03	1.4490E−02	5.7183E−03	3.7214E−03	5.9908E−03	2.0271E−02	9.4177E−03	6.6729E−03	8.9713E−03	8.2136E−03	1.5590E−01	1.3060E−02
ABC	AVG	2.1841E−02	2.6428E−02	4.3955E−01	2.6190E−02	2.8874E−02	2.8491E−02	2.7929E−01	7.8659E−02	7.8390E−02	8.3426E−02	9.9837E−02	6.6622E−01	6.0895E−01
	STD	4.5175E−03	6.5927E−03	4.7853E−02	6.1025E−03	6.1091E−03	7.3358E−03	3.3290E−02	1.4794E−02	1.0971E−02	1.1481E−02	1.4360E−02	3.0742E−01	2.9618E−02
GWO	AVG	5.8181E−02	6.1007E−02	2.6381E−01	6.9284E−02	6.3464E−02	7.6802E−02	1.4467E−01	9.7145E−02	9.6705E−02	9.4666E−02	1.0641E−01	3.2896E−01	2.9426E−01
	STD	1.3828E−02	1.6662E−02	3.5594E−02	1.8826E−02	2.2092E−02	2.2598E−02	2.3796E−02	2.2791E−02	2.1563E−02	2.2832E−02	2.3158E−02	1.5296E−01	2.1567E−02
SCA	AVG	1.0125E−01	1.0423E−01	3.1749E−01	1.1716E−01	1.0498E−01	1.2619E−01	2.2773E−01	1.5014E−01	1.4554E−01	1.5612E−01	1.6480E−01	4.2351E−01	3.8593E−01
	STD	1.7380E−02	2.3190E−02	4.7595E−02	2.5751E−02	2.4762E−02	2.4531E−02	3.4718E−02	2.4998E−02	2.6267E−02	2.6306E−02	2.5709E−02	1.7084E−01	2.1285E−02
BBO	AVG	1.2681E+00	1.3079E+00	1.5957E+00	1.5362E+00	1.2765E+00	1.7437E+00	1.8300E+00	1.7119E+00	1.6996E+00	1.7332E+00	1.7649E+00	2.1096E+00	1.9545E+00
	STD	1.1106E−01	1.2087E−01	1.5181E−01	1.8121E−01	8.1654E−02	2.2696E−01	2.0175E−01	1.8883E−01	9.8890E−02	1.4557E−01	1.3616E−01	6.3869E−01	1.3663E−01
ACO	AVG	1.4606E+00	1.4966E+00	1.8501E+00	1.7316E+00	1.5604E+00	1.9618E+00	2.0485E+00	1.9660E+00	1.9677E+00	1.9665E+00	2.0322E+00	2.3742E+00	2.2642E+00
	STD	1.0489E−01	1.1737E−01	2.3937E−01	1.6508E−01	1.3622E−01	2.4492E−01	1.4437E−01	2.3184E−01	1.0799E−01	1.1211E−01	1.3942E−01	4.7826E−01	1.2416E−01
RCSA	AVG	4.2753E+00	4.3099E+00	2.5623E+01	5.0675E+00	4.7054E+00	5.7008E+00	1.8636E+01	8.2537E+00	8.0402E+00	8.3868E+00	9.1086E+00	3.4595E+01	3.4293E+01
	STD	2.3778E−01	2.8296E−01	1.7817E+00	4.2510E−01	3.6311E−01	6.7003E−01	4.3134E+00	7.1708E−01	2.6907E−01	2.9262E−01	7.9508E−01	4.5479E−01	1.4686E−01
HS	AVG	5.0774E−01	5.3201E−01	7.0142E−01	6.0783E−01	4.9574E−01	6.6971E−01	7.7288E−01	6.6754E−01	6.7658E−01	6.5485E−01	6.8114E−01	8.2614E−01	8.2002E−01
	STD	6.2270E−02	1.1182E−01	1.3988E−01	9.9916E−02	3.3266E−02	9.2869E−02	1.7864E−01	9.7695E−02	7.2896E−02	5.5761E−02	5.9059E−02	5.0919E−02	5.1137E−02
COVIDOA	AVG	3.7897E−01	3.9030E−01	5.7401E−01	4.2700E−01	3.9438E−01	4.6957E−01	5.5545E−01	4.6839E−01	4.8532E−01	4.7601E−01	4.8997E−01	6.7880E−01	6.9530E−01
	STD	2.3267E−01	2.3949E−01	4.4476E−01	3.0495E−01	2.3579E−01	3.2913E−01	4.5394E−01	3.3167E−01	3.2510E−01	3.5114E−01	3.4839E−01	5.3105E−01	5.1686E−01
KMA	AVG	2.0081E+00	3.8613E+00	2.7283E+00	4.7386E+00	4.2671E+00	5.3297E+00	1.2981E+00	7.4111E−03	1.5990E−01	5.2440E+00	1.8593E−01	6.4371E+00	6.5126E+00
	STD	1.9152E+00	3.7399E+00	2.6721E+00	4.8408E+00	4.0725E+00	5.5399E+00	3.2927E+00	6.8968E−03	1.6235E−01	5.5873E+00	1.9843E−01	6.5606E+00	6.4194E+00
QIO	AVG	3.9206E−01	3.9783E−01	5.0929E−01	4.5125E−01	3.9753E−01	5.0469E−01	5.5660E−01	5.3142E−01	5.2702E−01	5.0371E−01	5.1538E−01	6.6642E−01	6.2442E−01
	STD	3.9283E−01	4.0970E−01	5.3866E−01	4.9351E−01	3.9485E−01	5.5433E−01	6.3767E−01	6.0837E−01	5.6740E−01	5.5686E−01	5.6861E−01	8.4930E−01	6.5381E−01

5.1.4. Search trajectory analysis

In Figs. 10(a)–10(x), we illustrate HOA's search trajectory analysis of the hikers, taking into consideration unimodal functions (i.e. F1 and F4), multimodal functions (i.e. F8 and F9), and fixed-dimension multimodal functions (i.e. F14 and F23).

In Figs. 10(a)–10(x), we observe that, at the beginning of the HOA hikers' hike, exploration of the search landscape takes precedence over-exploitation. This gives HOA the ability to avoid the local optima trap, especially for multimodal functions. However, the drawback is a longer convergence time. Moreover, as the iteration progresses, exploitation takes precedence to achieve convergence and an optimal solution.

5.1.5. Statistical analysis: Wilcoxon rank sum test, friedman test and dunn test

In Tables 15–22, we examine the statistical significance of HOA's results and other metaheuristics employed in the comparison conducted in this work. In order to assess the statistical significance and performance of the results obtained from benchmarking HOA against other metaheuristics, we employ the Wilcoxon rank sum test, the Friedman test, and the Dunn test. In Tables 15–18, we employ the Wilcoxon rank sum test, which is a non-parametric test, and specifically consider the probability values (i.e. p-values) with the respective benchmark test functions with dimension sizes of 30, 100, and 250.

Table 14
Results of computational time test in seconds (s) with fixed-dimension multimodal benchmark functions.

Alg.	Metric	F14	F15	F16	F17	F18	F19	F20	F21	F22	F23
HOA	AVG	1.4271E−01	3.2391E−02	3.1921E−02	2.9713E−02	2.9164E−02	3.5588E−02	3.6933E−02	3.8760E−02	4.3020E−02	4.7276E−02
	STD	1.1174E−02	3.8473E−03	3.9821E−03	3.0108E−03	3.0471E−03	5.1438E−03	4.6705E−03	5.7568E−03	6.9727E−03	6.7024E−03
TLBO	AVG	1.6514E−01	2.6932E−02	2.7211E−02	2.3458E−02	2.1803E−02	2.8824E−02	3.0289E−02	3.2391E−02	3.8637E−02	4.2101E−02
	STD	1.5218E−02	4.1870E−03	4.4451E−03	4.1345E−03	3.4780E−03	4.5784E−03	4.5891E−03	6.8266E−03	6.7146E−03	6.8436E−03
GA	AVG	7.7487E−02	1.3672E−02	1.3634E−02	1.1780E−02	1.2155E−02	1.4986E−02	1.6026E−02	1.7077E−02	1.8712E−02	2.0766E−02
	STD	8.2511E−03	3.1625E−03	2.8594E−03	2.6201E−03	2.6994E−03	2.6959E−03	2.9287E−03	3.6907E−03	3.2483E−03	3.3309E−03
DE	AVG	8.8359E−02	2.2399E−02	2.4059E−02	2.0910E−02	2.1139E−02	2.3349E−02	2.4748E−02	2.5664E−02	2.7616E−02	2.8414E−02
	STD	1.3954E−02	4.6697E−03	4.9878E−03	5.0272E−03	4.7902E−03	4.9023E−03	4.8809E−03	6.6803E−03	6.1535E−03	6.0529E−03
PSO	AVG	6.8170E−02	4.6173E−03	5.2266E−03	3.3385E−03	3.4771E−03	5.9620E−03	6.5644E−03	7.6833E−03	8.9112E−03	1.0826E−02
	STD	1.0498E−02	1.5120E−03	1.0509E−03	1.0243E−03	1.0417E−03	1.6502E−03	1.6799E−03	2.4602E−03	2.3608E−03	3.0737E−03
ABC	AVG	1.5906E−01	2.1316E−02	2.2306E−02	1.8125E−02	1.7290E−02	2.3742E−02	2.5201E−02	2.8931E−02	3.1304E−02	3.4676E−02
	STD	2.1806E−02	5.4580E−03	4.9349E−03	4.4078E−03	4.4469E−03	5.4680E−03	5.5901E−03	5.4452E−03	6.5335E−03	6.9388E−03
GWO	AVG	6.4058E−02	3.2808E−03	2.2934E−03	1.3818E−03	1.3303E−03	4.2217E−03	4.9045E−03	5.8701E−03	7.8300E−03	9.4372E−03
	STD	9.4332E−03	1.8703E−03	1.3868E−03	1.2766E−03	1.2236E−03	1.7908E−03	1.9770E−03	2.2994E−03	2.5738E−03	3.2084E−03
SCA	AVG	6.8530E−02	6.6328E−03	5.8967E−03	4.3046E−03	3.8769E−03	7.5588E−03	8.6413E−03	9.5580E−03	1.1094E−02	1.2977E−02
	STD	1.1267E−02	2.3359E−03	2.6569E−03	2.3457E−03	1.9406E−03	2.2798E−03	2.6660E−03	3.3750E−03	3.0938E−03	3.6856E−03
BBO	AVG	1.0878E−01	5.0407E−02	3.7334E−02	3.6362E−02	3.6123E−02	4.4703E−02	6.6983E−02	5.4420E−02	5.7260E−02	6.0211E−02
	STD	1.7212E−02	1.1161E−02	9.1318E−03	8.1787E−03	8.5317E−03	1.0380E−02	1.3394E−02	1.0735E−02	1.3539E−02	1.2419E−02
ACO	AVG	1.5347E−01	7.5291E−02	6.0909E−02	5.6535E−02	5.6775E−02	7.0043E−02	9.5282E−02	8.2155E−02	8.2090E−02	8.4110E−02
	STD	2.5581E−02	1.5000E−02	1.2992E−02	1.2565E−02	1.3511E−02	1.4533E−02	2.0469E−02	1.6658E−02	1.8752E−02	1.6399E−02
RCSA	AVG	9.3616E+00	2.5086E+00	2.3893E+00	2.2140E+00	2.1654E+00	2.7181E+00	2.8688E+00	2.8492E+00	3.0059E+00	3.2310E+00
	STD	2.5759E−01	1.6533E−01	1.8749E−01	1.7864E−01	2.0519E−01	2.1683E−01	1.9061E−01	1.6847E−01	1.6246E−01	2.0306E−01
HS	AVG	8.4933E−02	4.2634E−02	3.4140E−02	3.1445E−02	3.4646E−02	4.1056E−02	4.6993E−02	4.3870E−02	4.4085E−02	4.3928E−02
	STD	1.0401E−02	8.1843E−03	6.3012E−03	6.3281E−03	7.4313E−03	9.3433E−03	8.8363E−03	9.5918E−03	9.3546E−03	9.1696E−03
COVIDOA	AVG	3.3288E−01	2.0463E−01	1.9272E−01	1.8530E−01	1.9086E−01	2.1702E−01	2.2014E−01	2.1801E−01	2.2406E−01	2.2748E−01
	STD	7.1394E−02	3.2890E−02	4.5346E−02	2.4293E−02	3.0505E−02	2.4895E−02	3.1016E−02	2.5887E−02	2.8996E−02	2.9305E−02
KMA	AVG	6.0159E−01	6.2628E−01	5.7826E−02	6.6903E−02	3.0467E−01	5.8971E−01	7.3924E−01	6.4280E−01	6.5232E−01	6.7631E−01
	STD	5.8032E−01	9.1522E−02	1.5204E−01	1.5643E−01	2.3019E−01	1.0177E−01	1.0713E−01	9.9667E−02	1.5009E−01	1.2542E−01
QIO	AVG	9.2324E−02	3.4756E−02	2.8653E−02	2.5731E−02	2.4470E−02	3.3261E−02	4.6912E−02	3.7238E−02	3.9823E−02	4.1123E−02
	STD	2.4447E−02	6.3570E−03	7.5688E−03	5.9764E−03	6.0394E−03	9.3900E−03	1.1069E−02	6.8258E−03	9.7169E−03	9.2238E−03

Table 15
Results of rank-sum metric test with unimodal and multimodal benchmark functions having 30 dimensions.

Alg.	F1	F2	F3	F4	F5	F6	F7	F8	F9	F10	F11	F12	F13
HOA	1.0704E−21	1.1783E−21	6.4504E−33	1.1945E−21	9.6472E−46	1.1902E−03	3.2910E−41	5.2459E−27	3.3129E−34	1.0590E−21	3.4822E−40	2.5888E−03	8.9078E−08
TLBO	5.5942E−33	6.4961E−33	1.1729E−21	6.6359E−33	1.2773E−25	2.3568E−46	2.4614E−26	4.1065E−03	8.7458E−22	5.5017E−33	3.4822E−40	9.9951E−36	5.0442E−12
GA	5.9189E−63	7.9259E−63	1.1584E−61	8.9322E−49	8.2626E−63	8.2626E−63	8.2626E−63	8.2624E−39	9.6055E−63	1.6095E−29	5.4769E−64	8.3292E−63	8.2626E−63
DE	5.7381E−06	2.0810E−05	4.8456E−01	6.0732E−01	1.5469E−01	6.8709E−21	4.5266E−02	1.5934E−05	1.8295E−27	4.0213E−06	2.3281E−06	1.9669E−22	3.7671E−30
PSO	1.0778E−04	2.7134E−36	3.8165E−02	5.2361E−07	5.0769E−02	4.5491E−04	1.5287E−27	3.5235E−02	2.5425E−02	2.0054E−09	1.1977E−04	8.2624E−06	1.9296E−26
ABC	1.8576E−43	1.0012E−22	1.7752E−31	6.2650E−33	3.7814E−29	1.8925E−43	3.3668E−46	7.9172E−07	1.6204E−08	2.1744E−15	9.8209E−45	9.8248E−19	9.1262E−27
GWO	2.4605E−01	6.3288E−02	2.4749E−01	6.0716E−01	3.0212E−02	8.5579E−01	4.7715E−12	1.9237E−06	2.8147E−21	5.7293E−63	1.4871E−01	9.5177E−37	1.6892E−08
SCA	2.4906E−03	5.9639E−02	5.6574E−08	1.9407E−20	3.4007E−15	3.2843E−04	9.3180E−02	2.6977E−52	3.9255E−02	1.1909E−15	7.2870E−04	1.1638E−09	1.9448E−38
BBO	2.4771E−01	4.8814E−02	9.9931E−06	2.1295E−06	2.9161E−03	4.7811E−07	3.1819E−05	8.4474E−16	4.5075E−02	1.2825E−02	5.0741E−01	1.5722E−10	4.1830E−22
ACO	1.1129E−26	1.1527E−37	2.1104E−47	1.6209E−59	2.7257E−43	5.6118E−27	4.4654E−22	5.8217E−28	2.9440E−47	3.2336E−37	2.1408E−27	5.7197E−37	8.8681E−05
RCSA	2.3325E−12	3.1556E−09	7.4846E−13	7.5623E−13	1.0792E−26	2.2596E−32	4.0412E−13	7.3215E−34	1.2726E−06	7.7220E−13	5.4552E−13	1.0357E−40	1.9311E−46
HS	2.1541E−13	1.7537E−06	5.1004E−22	9.8164E−09	9.6537E−11	5.0723E−13	1.1326E−05	1.7150E−45	6.7107E−10	3.9133E−01	7.6454E−13	3.2886E−07	3.6930E−02
COVIDOA	3.7465E−28	6.1706E−15	1.7917E−06	1.1773E−01	9.6077E−16	9.0417E−28	1.6469E−01	2.9381E−04	4.4475E−11	8.5028E−04	5.7138E−28	3.6629E−02	3.1472E−02
KMA	1.5635E−54	7.9259E−63	5.7730E−62	1.2337E−62	1.6823E−14	5.3344E−10	1.7047E−54	2.9022E−08	6.3571E−48	1.5202E−54	3.4822E−40	5.7181E−03	2.1926E−04
QIO	1.5635E−54	1.2311E−46	2.1623E−47	8.9938E−47	6.2062E−61	8.2626E−63	6.0237E−38	8.2625E−63	6.3571E−48	1.5202E−54	3.4822E−40	8.2626E−63	8.2626E−63

Table 16
Results of rank-sum metric test with unimodal and multimodal benchmark functions having 100 dimensions.

Alg.	F1	F2	F3	F4	F5	F6	F7	F8	F9	F10	F11	F12	F13
HOA	1.0704E−21	1.1783E−21	6.4732E−33	1.1886E−21	1.9848E−45	4.3597E−13	1.2576E−41	4.4779E−24	1.4352E−29	5.2711E−22	3.4822E−40	1.5322E−02	1.1945E−21
TLBO	5.5942E−33	6.4961E−33	1.1778E−21	6.5847E−33	3.9743E−33	6.6359E−33	1.9207E−25	7.0940E−01	1.8644E−39	4.1227E−32	3.4822E−40	1.4767E−32	2.4945E−01
GA	5.1479E−62	7.9863E−58	3.3552E−61	3.1494E−16	2.2051E−48	5.1166E−62	9.2578E−50	4.8476E−39	2.6023E−50	4.3811E−34	6.8059E−63	2.8044E−47	8.2626E−63
DE	9.8044E−01	2.7713E−02	1.3014E−03	3.2513E−42	6.2278E−01	9.0309E−01	5.8430E−01	1.7606E−09	1.4868E−13	2.1228E−02	9.4009E−01	1.0742E−08	1.7119E−09
PSO	5.4766E−07	3.0356E−32	1.3549E−02	1.6864E−02	1.2041E−02	1.4300E−06	3.0137E−10	2.8239E−08	3.7687E−02	1.4943E−07	2.1321E−06	2.2376E−03	2.6818E−22
ABC	5.5942E−33	3.5162E−20	2.4063E−17	6.8019E−11	6.2249E−31	1.0295E−32	7.1920E−33	5.9934E−04	7.1408E−25	2.0996E−14	1.6542E−33	2.9955E−32	7.3399E−32
GWO	2.7300E−02	2.9569E−06	2.1398E−01	9.5713E−18	7.7142E−02	3.4575E−02	6.5430E−02	1.2982E−11	2.4231E−10	5.7170E−63	2.6272E−02	9.3692E−10	1.5882E−01
SCA	2.5706E−03	2.4228E−01	4.8991E−04	6.4306E−09	1.0992E−21	1.4048E−03	1.0289E−19	5.8918E−56	2.0426E−05	2.7743E−16	5.6620E−04	1.1079E−06	2.3071E−06
BBO	1.7109E−06	1.8386E−01	3.3946E−06	1.7577E−06	1.7599E−06	1.7599E−06	1.7578E−06	2.2267E−19	1.1802E−04	1.3427E−06	1.3988E−06	4.9577E−13	6.6359E−33
ACO	1.5279E−47	3.9719E−51	1.6473E−47	2.2799E−45	8.5445E−61	2.6255E−47	2.8749E−59	5.2707E−32	1.9393E−60	5.2671E−42	1.9430E−48	4.7434E−62	1.2694E−46
RCSA	7.1063E−13	3.9275E−12	7.5021E−13	7.5410E−13	3.0663E−13	1.2694E−46	7.5755E−13	1.0094E−43	5.5158E−12	4.9701E−13	4.5597E−13	7.4187E−46	1.2694E−46
HS	7.2952E−13	1.9746E−06	3.4865E−26	9.3648E−01	7.5734E−11	5.3751E−13	3.1343E−07	2.0564E−35	5.5855E−01	4.2245E−01	1.7328E−12	3.8225E−02	7.4195E−05
COVIDOA	1.0672E−17	2.1475E−14	6.8153E−19	1.4388E−23	2.6552E−08	1.2479E−17	6.6476E−04	4.9787E−02	4.3907E−22	1.1617E−02	1.8084E−18	2.7549E−15	1.2103E−08
KMA	1.5635E−54	7.9259E−63	9.6740E−63	8.1386E−63	9.1987E−22	2.4592E−21	2.1589E−56	4.0753E−05	1.1040E−41	1.5174E−54	3.4822E−40	2.8778E−18	8.7555E−09
QIO	1.5635E−54	1.2311E−46	1.0389E−46	1.2553E−46	8.2626E−63	8.2626E−63	1.4657E−37	8.2626E−63	1.1040E−41	1.5174E−54	3.4822E−40	8.2626E−63	8.2626E−63

In Tables 15–18, we observe that HOA's p-values for all the test functions, irrespective of the number of dimensions, are far lower than 0.05. This clearly shows that the performance of HOA is not a random occurrence. Consequently, the null hypothesis is rejected and the alternative hypothesis is true (i.e. the superior performance of HOA is statistically significant). We observe that, in most instances, HOA's *p*-value is less than the other metaheuristics.

Furthermore, we explore the Friedman test to give a perspicuous ranking of the metaheuristics by leveraging Tables 15–18. The Friedman test allows us to compare more than two populations with a blocking variable without assuming the observations are normal distributions. Therefore, we use the ranks of the observed values to determine the rankings of the metaheuristics. A brief mathematical basis of the Friedman test is described in the appendix of [69]. In the Friedman test, two hypotheses are tested to examine the statistical significance of the results obtained. In this work, the null hypothesis states that there is no statistical difference in the results of the metaheuristics, whereas the alternative hypothesis states that there is a statistical difference in the results obtained from the metaheuristics.

For each benchmark function in Tables 19–22, the performance of the selected metaheuristics are ranked on a scale of 1 to 15, with the best being 1 and worst being 15. In Table 19, we observe that the Friedman statistic, 138.71, is greater than the critical value of 23.68, and also that the *p*-value of 1.2805E-22 is less than the threshold of 0.05; hence, the null hypothesis is rejected. Furthermore, in Table 20, the Friedman statistic, 152.05, is greater than the critical value of 23.68, and also a *p*-value of 2.8E-25 less than 0.05; therefore, the null hypothesis is rejected. Moreover, in Table 21, the critical value of 23.68

Table 17
Results of rank-sum metric test with unimodal and multimodal benchmark functions having with 250 dimensions.

Alg.	F1	F2	F3	F4	F5	F6	F7	F8	F9	F10	F11	F12	F13
HOA	1.0721E−21	1.1778E−21	3.8428E−33	1.1796E−21	9.3506E−45	6.6567E−13	1.6558E−42	4.1420E−20	1.6705E−30	4.9984E−23	3.4822E−40	2.6554E−10	1.5502E−32
TLBO	5.6085E−33	6.4919E−33	1.1778E−21	6.5078E−33	1.2550E−33	1.6555E−32	2.0659E−25	7.4636E−01	1.7405E−41	9.5391E−29	3.4822E−40	1.4678E−23	1.2346E−02
GA	1.4684E−50	6.2522E−48	5.5643E−60	1.7670E−13	6.0387E−49	9.1269E−50	1.1673E−48	1.3034E−41	2.0590E−47	1.8948E−40	5.0459E−51	1.0984E−46	6.6267E−54
DE	5.4316E−01	7.9733E−01	1.7118E−02	3.6180E−29	4.2333E−01	5.1902E−01	3.1468E−01	3.5042E−10	4.1993E−12	3.3701E−02	5.4328E−01	1.9590E−02	6.8377E−01
PSO	2.3645E−06	9.7283E−10	1.0357E−02	1.6165E−02	2.1643E−02	1.0302E−06	8.6002E−03	4.5208E−06	1.5661E−01	1.0442E−03	1.3278E−06	1.1304E−02	2.0296E−20
ABC	5.6085E−33	2.7585E−30	9.9745E−09	1.6603E−04	6.7708E−33	6.6359E−33	6.4664E−33	1.0593E−02	1.4313E−32	8.3254E−14	1.6542E−33	6.8294E−33	6.6359E−33
GWO	1.7094E−02	9.0243E−13	6.7305E−07	1.8285E−47	1.4008E−01	2.0732E−02	1.6954E−01	3.9981E−10	2.5925E−06	5.7871E−63	1.6811E−02	7.2292E−03	2.3983E−06
SCA	4.4938E−02	9.2974E−06	1.9647E−02	1.6669E−16	8.6410E−19	7.9285E−02	1.1532E−18	1.9411E−56	2.6546E−11	3.4063E−16	4.9725E−02	1.4371E−02	4.7521E−02
BBO	1.7116E−06	7.3452E−03	4.2063E−06	1.8927E−06	1.7599E−06	1.7599E−06	1.7599E−06	1.8851E−18	4.5114E−03	4.4540E−07	1.3988E−06	1.8029E−08	6.1576E−20
ACO	1.1776E−58	2.4342E−61	2.1903E−47	1.3786E−28	3.6352E−60	2.9201E−59	1.8063E−60	5.1812E−33	9.2483E−64	1.2531E−38	5.1861E−60	9.7784E−63	6.5239E−55
RCSA	7.1129E−13	2.7916E−07	7.5021E−13	7.5088E−13	6.7860E−13	1.2694E−46	7.5623E−13	4.2062E−46	2.2173E−09	9.9817E−14	4.5597E−13	1.2781E−46	1.2694E−46
HS	1.7025E−12	3.8478E−03	8.7359E−24	1.0000E+00	4.2086E−07	1.4295E−12	1.6002E−07	2.2805E−29	1.5584E−01	4.3012E−01	1.0939E−12	3.2082E−11	4.8653E−07
COVIDOA	1.6246E−21	2.9607E−23	1.7830E−26	4.7768E−27	3.5294E−14	3.3032E−21	6.0881E−13	6.0665E−03	1.5226E−22	7.1348E−05	9.6807E−22	1.4465E−21	5.4321E−13
KMA	1.3027E−54	9.6740E−63	9.6740E−63	1.2118E−62	2.7974E−22	6.7576E−22	1.7124E−56	1.8113E−15	1.7405E−41	1.8483E−54	3.4822E−40	1.2672E−30	2.8286E−14
QIO	1.8926E−54	1.0353E−46	1.9368E−46	8.5949E−47	8.2626E−63	8.2626E−63	1.0815E−36	8.2625E−63	1.7405E−41	1.2720E−54	3.4822E−40	8.2626E−63	8.2626E−63

Table 18
Results of rank-sum metric test with fixed-dimensional benchmark functions.

Alg.	F14	F15	F16	F17	F18	F19	F20	F21	F22	F23
HOA	3.1935E−32	1.4666E−21	8.3859E−11	6.5673E−02	2.2910E−31	4.3644E−03	2.4446E−02	9.6405E−05	2.0852E−01	5.8593E−01
TLBO	1.8550E−47	4.6053E−24	7.0885E−40	1.5191E−39	1.3463E−43	4.3644E−03	4.7663E−26	8.9961E−03	1.0439E−12	7.3395E−19
GA	1.6270E−08	2.3680E−45	5.0369E−51	1.1555E−59	1.0660E−44	4.3644E−03	4.7921E−48	1.6500E−62	2.5134E−61	6.1216E−62
DE	9.8655E−31	1.0200E−03	9.8023E−41	1.5191E−39	7.7987E−45	1.5568E−02	1.5265E−05	2.6634E−26	3.7308E−30	8.6753E−37
PSO	1.5122E−10	4.7684E−01	1.5589E−36	1.5191E−39	6.4463E−31	4.3644E−03	7.9062E−11	8.3115E−01	1.0225E−02	3.7981E−04
ABC	9.0995E−03	2.2962E−06	8.8127E−01	2.0344E−01	9.9616E−11	4.3644E−03	6.7933E−08	3.3041E−04	6.0827E−01	3.8357E−01
GWO	3.4431E−55	7.8052E−06	1.6617E−30	1.8809E−33	1.5857E−33	4.6577E−01	7.9303E−02	2.2530E−03	1.2016E−06	1.0045E−09
SCA	2.2794E−08	2.5069E−04	6.6544E−20	6.5938E−32	8.8220E−05	4.3644E−03	2.6693E−32	1.3507E−35	3.2919E−22	1.0526E−23
BBO	5.2770E−17	3.6255E−09	4.0126E−09	2.8048E−06	8.3437E−02	4.3644E−03	1.6764E−12	3.0515E−07	5.3390E−01	6.4595E−01
ACO	1.5099E−41	1.3740E−01	1.7558E−42	1.5191E−39	1.8153E−38	4.3644E−03	2.2878E−14	3.2907E−33	2.2343E−01	9.8958E−10
RCSA	4.4414E−21	1.0919E−34	7.2081E−10	2.4106E−11	7.9307E−09	4.3644E−03	3.4218E−02	6.1281E−02	4.1396E−02	8.7968E−02
HS	6.5026E−05	2.5763E−08	2.8974E−03	6.2248E−04	1.3435E−03	4.3644E−03	1.8411E−06	9.9454E−11	3.9178E−01	2.2295E−01
COVIDOA	1.6072E−01	8.8994E−26	8.7801E−42	1.1635E−35	2.5707E−31	4.3644E−03	3.4859E−29	7.0755E−01	2.6249E−04	2.1542E−01
KMA	8.6730E−14	3.4862E−15	1.0382E−15	2.7182E−13	3.5292E−01	4.3644E−03	3.0313E−44	2.8463E−01	5.2642E−05	1.4019E−13
QIO	8.7069E−12	5.9934E−50	1.0609E−01	1.6060E−02	3.3804E−02	1.8535E−305	5.7328E−13	5.6840E−29	2.0650E−29	1.3440E−23

Table 19
Results of the Friedman test ranking for the unimodal and multimodal benchmark functions with 30 dimensions.

Alg.	F1	F2	F3	F4	F5	F6	F7	F8	F9	F10	F11	F12	F13	Total
HOA	4	4	3	4	2	7	2	12	3	4	2.5	9	6	62.5
TLBO	3	3	4	3	3	2	4	7	4	3	2.5	2	5	45.5
GA	15	15	15	14	15	15	15	14	15	14	15	15	15	192
DE	6	6	8	8	8	4	7	9	13	6	6	3	4	88
PSO	10	13	9	10	9	9	13	8	9	10	10	10	13	133
ABC	14	12	13	13	13	14	14	5	10	12	14	12	12	158
GWO	8	7	7	7	7	8	11	10	12	15	7	14	11	124
SCA	9	8	11	12	12	10	9	15	8	11	9	11	14	139
BBO	7	9	6	6	6	6	6	4	7	7	8	5	3	80
ACO	12	14	14	15	14	12	12	13	14	13	13	13	9	168
RCSA	5	5	5	5	5	3	5	3	6	5	5	4	2	58
HS	11	10	12	11	10	11	10	2	5	8	11	6	7	114
COVIDOA	13	11	10	9	11	13	8	6	11	9	12	8	8	129
KMA	1.5	1	1	1	4	5	1	11	1.5	1.5	2.5	7	10	48
QIO	1.5	2	2	2	1	1	3	1	1.5	1.5	2.5	1	1	21

is less than the Friedman statistic of 148.61, and the p-value of 1.37E-24 is less than the set threshold of 0.05. To this end, the results obtained in Table 21 are statistically significant. Similarly, the results obtained in Table 22 are statistically significant since the Friedman statistic, 55.49 is greater than the critical value of 23.68; moreover, the p-value of 7.12E-07 is less than the 0.05 set threshold.

Consequently, in Tables 19–21, we see that the performance of HOA improved as the variable dimensional sizes increased for both unimodal and multimodal benchmark functions. In several instances, either HOA outperformed several other metaheuristics. Given the statistical significance revealed by the Friedman test, it becomes essential to conduct a post-hoc analysis utilizing Dunn's test. Dunn's test facilitates pairwise comparisons between groups while accounting for multiple comparisons, thus pinpointing specific groups that exhibit significant differences. Together, the Friedman test and Dunn's test offer a dependable approach for analyzing data with multiple paired groups in non-parametric scenarios.

Tables 23 through 26 provide a comprehensive presentation of the results derived from pairwise Dunn's post-hoc analysis conducted on both unimodal and multimodal benchmark functions across varying dimensions: 30, 100, and 250, as well as fixed-dimensions multimodal benchmark functions. This analysis offers insights into the comparative performance of different optimization algorithms. Upon thorough examination of Tables 23 to 26, a significant observation emerges: the algorithm denoted as HOA exhibits statistically discernible differences when compared to other algorithms such as GA, ABC, ACO, SCA, and COVIDOA. This finding suggests that HOA operates distinctively in the

Table 20
Results of the Friedman test ranking for the unimodal and multimodal benchmark functions with 100 dimensions.

Alg.	F1	F2	F3	F4	F5	F6	F7	F8	F9	F10	F11	F12	F13	Total
HOA	4	4	3	4	2	5	2	12	4	3	2.5	7	4	56.5
TLBO	3	3	4	3	3	3	4	8	3	5	2.5	3	7	51.5
GA	15	15	15	13	14	15	14	14	14	13	15	14	15	186
DE	8	9	9	14	8	8	8	10	11	7	8	6	5	111
PSO	10	12	7	7	9	10	11	5	9	10	10	9	12	121
ABC	13	13	11	12	13	13	13	7	13	12	13	13	13	159
GWO	7	6	8	11	7	7	7	11	10	15	7	11	8	115
SCA	9	8	10	9	12	9	12	15	6	11	9	10	10	130
BBO	6	7	6	6	6	6	6	4	7	6	6	5	3	74
ACO	14	14	14	15	15	14	15	13	15	14	14	15	14	186
RCSA	5	5	5	5	5	2	5	2	5	4	5	2	2	52
HS	11	10	13	8	11	11	10	3	8	8	11	8	9	121
COVIDOA	12	11	12	10	10	12	9	9	12	9	12	12	11	141
KMA	1.5	1	1	1	4	4	1	6	1.5	1.5	2.5	4	6	35
QIO	1.5	2	2	2	1	1	3	1	1.5	1.5	2.5	1	1	21

Table 21
Results of the Friedman test ranking for the unimodal and multimodal benchmark functions with 250 dimensions.

Alg.	F1	F2	F3	F4	F5	F6	F7	F8	F9	F10	F11	F12	F13	Total
HOA	4	4	3	4	2	5	2	12	4	3	2.5	5	3	53.5
TLBO	3	3	4	3	3	3	4	8	2	5	2.5	4	7	51.5
GA	14	14	15	10	14	14	14	14	14	14	14	14	14	179
DE	8	8	9	14	8	8	7	10	11	7	8	7	8	113
PSO	10	10	7	7	9	10	9	6	8	9	10	9	12	116
ABC	13	13	11	9	13	13	13	7	13	12	13	13	13	156
GWO	7	5	10	15	7	7	8	11	10	15	7	10	6	118
SCA	9	6	8	11	12	9	12	15	5	11	9	8	9	124
BBO	6	7	6	6	6	6	6	4	7	6	6	6	4	76
ACO	15	15	14	13	15	15	15	13	15	13	15	15	15	188
RCSA	5	11	5	5	5	2	5	2	6	4	5	2	2	59
HS	11	9	12	8	10	11	10	3	9	8	11	11	10	123
COVIDOA	12	12	13	12	11	12	11	9	12	10	12	12	11	149
KMA	1.5	1	1	1	4	4	1	5	2	2	2.5	3	5	33
QIO	1.5	2	2	2	1	1	3	1	2	1	2.5	1	1	21

Table 22
Results of the Friedman test ranking for the fixed dimensions benchmark functions.

Alg.	F14	F15	F16	F17	F18	F19	F20	F21	F22	F23	Total
HOA	14	2	12	10	13	6.5	11	3	5	7	83.5
TLBO	1.5	3	2.5	2.5	2	6.5	2	9	4	4	37
GA	10	15	15	15	14	6.5	14	15	15	15	134.5
DE	8	8	2.5	2.5	2	15	10	5	3	2	58
PSO	12	12	2.5	2.5	10	6.5	9	11	13	12	90.5
ABC	5	7	8	8	7	6.5	1	10	8	5	65.5
GWO	15	5	14	13	15	14	8	4	10	11	109
SCA	9	6	10	12	6	6.5	13	14	14	14	104.5
BBO	13	11	6	7	12	6.5	5	13	11	10	94.5
ACO	7	10	2.5	2.5	2	6.5	7	2	9	9	57.5
RCSA	1.5	4	5	5	4	6.5	6	7	6	6	51
HS	4	13	9	9	11	6.5	4	12	7	8	83.5
COVIDOA	6	9	13	14	8	6.5	12	6	2	3	79.5
KMA	11	14	11	11	9	6.5	15	8	12	13	110.5
QIO	3	1	7	6	5	13	3	1	1	1	41

context of these benchmark functions and dimensions, highlighting its unique characteristics or efficacy in optimization tasks.

5.2. Composite test benchmark

In this study, we subject HOA to a battery of six composite benchmark test functions, each designed to challenge various aspects of algorithmic performance. These functions include: (i) Hybrid composition function 1, (ii) Rotated hybrid composition function 1, (iii) Rotated hybrid composition function 1 with added noise in fitness, (iv) Rotated hybrid composition function 2, (v) Rotated hybrid composition function 2 with a narrow basin for the global optimum, and (vi) Rotated hybrid composition function 2 with the global optimum situated on the bounds. For a comprehensive understanding of these test functions, refer to the concise descriptions provided in Table 5.

Furthermore, our investigation into the performance of HOA encompasses various facets including test accuracy, search and convergence dynamics, search trajectory, computational time, and a suite of statistical analyses. These analyses entail rigorous examinations utilizing techniques such as the Wilcoxon rank sum test, Friedman test, and Dunn's

Table 23
Results of the Dunn's post-hoc analysis for the unimodal and multimodal benchmark functions with 30 dimensions.

Alg.	HOA	TLBO	GA	DE	PSO	ABC	GWO	SCA	BBO	ACO	RCSA	HS	COVIDOA	KMA	QIO
HOA	1	1	5.3400E−07	1	1.5801E−01	1.7506E−03	5.9521E−01	5.9889E−02	1	2.0530E−04	1	1	2.9037E−01	1	1
TLBO	1	1	4.3197E−09	1	8.9450E−03	4.3810E−05	4.4984E−02	2.7916E−03	1	3.6922E−06	1	2.2530E−01	1.8698E−02	1	1
GA	5.3400E−07	4.3197E−09	1	2.7477E−04	7.9500E−01	1	2.1882E−01	1	4.3412E−05	1	1.4904E−07	4.3530E−02	4.5666E−01	5.8562E−09	7.5987E−13
DE	1	1	2.7477E−04	1	1	1.6577E−01	1	1	1	3.1848E−02	1	1	1	1	2.1628E−01
PSO	1.5801E−01	8.9450E−03	7.9500E−01	1	1	1	1	1	1	1	7.5379E−02	1	1	1.0787E−02	3.3886E−05
ABC	1.7506E−03	4.3810E−05	1	1.6577E−01	1	1	1	1	4.4690E−02	1	6.6714E−04	1	1	5.5496E−05	4.5571E−08
GWO	5.9521E−01	4.4984E−02	2.1882E−01	1	1	1	1	1	1	1	3.0737E−01	1	1	5.3308E−02	2.7013E−04
SCA	5.9889E−02	2.7916E−03	1	1	1	1	1	1	8.1165E−01	1	2.7084E−02	1	1	3.4061E−03	7.7667E−06
BBO	1	1	4.3412E−05	1	1	4.4690E−02	1	8.1165E−01	1	7.3492E−03	1	1	1	1	6.9043E−01
ACO	2.0530E−04	3.6922E−06	1	3.1848E−02	1	1	1	1	7.3492E−03	1	7.1430E−05	1	1	4.7709E−06	2.2813E−09
RCSA	1	1	1.4904E−07	1	7.5379E−02	6.6714E−04	3.0737E−01	2.7084E−02	1	7.1430E−05	1	1	1.4350E−01	1	1
HS	1	2.2530E−01	4.3530E−02	1	1	1	1	1	1	1	1	1	1	2.6191E−01	2.2482E−03
COVIDOA	2.9037E−01	1.8698E−02	4.5666E−01	1	1	1	1	1	1	1	1.4350E−01	1	1	2.2373E−02	8.6958E−05
KMA	1	1	5.8562E−09	1	1.0787E−02	5.5496E−05	5.3308E−02	3.4061E−03	1	4.7709E−06	1	2.6191E−01	2.2373E−02	1	1
QIO	1	1	7.599E−13	2.1628E−01	3.3886E−05	4.5571E−08	2.7013E−04	7.7667E−06	6.9043E−01	2.2813E−09	1	2.2482E−03	8.6958E−05	1	1

Table 24
Results of the Dunn's post-hoc analysis for the unimodal and multimodal benchmark functions with 100 dimensions.

Alg.	HOA	TLBO	GA	DE	PSO	ABC	GWO	SCA	BBO	ACO	RCSA	HS	COVIDOA	KMA	QIO
HOA	1	1	5.3961E−07	1	3.9131E−01	4.0203E−04	8.9965E−01	9.8737E−02	1	5.3961E−07	1	3.8484E−01	1.4847E−02	1	1
TLBO	1	1	1.5395E−07	8.3720E−01	1.9923E−01	1.4635E−04	4.8229E−01	4.6484E−02	1	1.5395E−07	1	1.9573E−01	6.3450E−03	1	1
GA	5.3961E−07	1.5395E−07	1	7.2103E−02	3.4219E−01	1	1.3755E−01	1	4.3412E−05	1	1.3967E−07	3.4801E−01	1	6.8355E−10	6.2710E−12
DE	1	8.3720E−01	7.2103E−02	1	1	1	1	1	1	7.2103E−02	7.9913E−01	1	1	5.4005E−02	4.0857E−03
PSO	3.9131E−01	1.9923E−01	3.4219E−01	1	1	1	1	1	1	3.4219E−01	1.8892E−01	1	1	9.0754E−03	5.2075E−04
ABC	4.0203E−04	1.4635E−04	1	1	1	1	1	1	1.2891E−02	1	1.3526E−04	1	1	1.7256E−06	3.4084E−08
GWO	8.9965E−01	4.8229E−01	1.3755E−01	1	1	1	1	1	1	1.3755E−01	4.5916E−01	1	1	2.7084E−02	1.8351E−03
SCA	9.8737E−02	4.6484E−02	1	1	1	1	1	1	1	1	4.3817E−02	1	1	1.5430E−03	6.8910E−05
BBO	1	1	4.3412E−05	1	1	1.2891E−02	1	1	1	4.3412E−05	1	1	2.6041E−01	1	1
ACO	5.3961E−07	1.5395E−07	1	7.2103E−02	3.4219E−01	1	1.3755E−01	1	4.3412E−05	1	1.3967E−07	3.4801E−01	1	6.8355E−10	6.2710E−12
RCSA	1	1	1.3967E−07	7.9913E−01	1.8892E−01	1.3526E−04	4.5916E−01	4.3817E−02	1	1.3967E−07	1	1.8560E−01	5.9368E−03	1	1
HS	3.8484E−01	1.9573E−01	3.4801E−01	1	1	1	1	1	1	3.4801E−01	1.8560E−01	1	1	8.8805E−03	5.0794E−04
COVIDOA	1.4847E−02	6.3450E−03	1	1	1	1	1	1	2.6041E−01	1	5.9368E−03	1	1	1.4256E−04	4.6781E−06
KMA	1	1	6.8355E−10	5.4005E−02	9.0754E−03	1.7256E−06	2.7084E−02	1.5430E−03	1	6.8355E−10	1	8.8805E−03	1.4256E−04	1	1
QIO	1	1	6.2710E−12	4.0857E−03	5.2075E−04	3.4084E−08	1.8351E−03	6.8910E−05	1	6.2710E−12	1	5.0794E−04	4.6781E−06	1	1

Table 25
Results of the Dunn's post-hoc analysis for the unimodal and multimodal benchmark functions with 250 dimensions.

Alg.	HOA	TLBO	GA	DE	PSO	ABC	GWO	SCA	BBO	ACO	RCSA	HS	COVIDOA	KMA	QIO
HOA	1	1	1.6197E−06	7.9865E−01	5.2853E−01	4.1157E−04	3.9760E−01	1.6171E−01	1	1.3927E−07	1	1.8435E−01	1.8038E−03	1	1
TLBO	1	1	1.0445E−06	6.3743E−01	4.1790E−01	2.8622E−04	3.1241E−01	1.2468E−01	1	8.7176E−08	1	1.4252E−01	1.2833E−03	1	1
GA	1.6197E−06	1.0445E−06	1	2.9515E−01	4.5634E−01	1	6.0442E−01	1	3.3344E−04	1	5.4596E−06	1	1	3.5243E−09	6.6005E−11
DE	7.9865E−01	6.3743E−01	2.9515E−01	1	1	1	1	1	1	7.2034E−02	1	1	1	2.8369E−02	2.7240E−03
PSO	5.2853E−01	4.1790E−01	4.5634E−01	1	1	1	1	1	1	1.1727E−01	1	1	1	1.6591E−02	1.4809E−03
ABC	4.1157E−04	2.8622E−04	1	1	1	1	1	1	3.1179E−02	1	1.1201E−03	1	1	2.4000E−06	7.9851E−08
GWO	3.9760E−01	3.1241E−01	6.0442E−01	1	1	1	1	1	1	1.6075E−01	7.6614E−01	1	1	1.1490E−02	9.7677E−04
SCA	1.6171E−01	1.2468E−01	1	1	1	1	1	1	1	3.9540E−01	3.2872E−01	1	1	3.6423E−03	2.6736E−04
BBO	1	1	3.3344E−04	1	1	3.1179E−02	1	1	1	4.2539E−05	1	1	1.0113E−01	1	1
ACO	1.3927E−07	8.7176E−08	1	7.2034E−02	1.1727E−01	1	1.6075E−01	3.9540E−01	4.2539E−05	1	5.1073E−07	3.4971E−01	1	2.0561E−10	3.0726E−12
RCSA	1	1	5.4596E−06	1	1	1.1201E−03	7.6614E−01	3.2872E−01	1	5.1073E−07	1	3.7192E−01	4.6021E−03	1	1
HS	1.8435E−01	1.4252E−01	1	1	1	1	1	1	1	3.4971E−01	3.7192E−01	1	1	4.3012E−03	3.2234E−04
COVIDOA	1.8038E−03	1.2833E−03	1	1	1	1	1	1	1.0113E−01	1	4.6021E−03	1	1	1.4171E−05	5.6113E−07
KMA	1	1	3.5243E−09	2.8369E−02	1.6591E−02	2.4000E−06	1.1490E−02	3.6423E−03	1	2.0561E−10	1	4.3012E−03	1.4171E−05	1	1
QIO	1	1	6.6005E−11	2.7240E−03	1.4809E−03	7.9851E−08	9.7677E−04	2.6736E−04	1	3.0726E−12	1	3.2234E−04	5.6113E−07	1	1

Table 26
Results of the Dunn's post-hoc analysis for the fixed dimensions benchmark functions.

Alg.	HOA	TLBO	GA	DE	PSO	ABC	GWO	SCA	BBO	ACO	RCSA	HS	COVIDOA	KMA	QIO
HOA	1	1	8.9754E−01	1	1	1	1	1	1	1	1	1	1	1	1
TLBO	1	1	3.297E−05	1	4.3184E−01	1	1.5508E−02	4.3314E−02	2.4248E−01	1	1	1	1	8.8623E−03	1
GA	8.9754E−01	3.2965E−05	1	7.6219E−03	1	5.0586E−02	1	1	1	8.9578E−03	8.2988E−04	1	4.2139E−01	1	1.0149E−04
DE	1	1	7.6219E−03	1	1	1	8.5101E−01	1	1	1	1	1	1	5.6325E−01	1
PSO	1	4.3184E−01	1	1	1	1	1	1	1	1	1	1	1	1	8.3812E−01
ABC	1	1	5.0586E−02	1	1	1	1	1	1	1	1	1	1	1	1
GWO	1	1.5508E−02	1	8.5101E−01	1	1	1	1	1	9.5348E−01	1.7272E−01	1	1	1	3.6306E−02
SCA	1	4.3314E−02	1	1	1	1	1	1	1	1	4.1118E−01	1	1	1	9.6092E−02
BBO	1	2.4248E−01	1	1	1	1	1	1	1	1	1	1	1	1	4.8767E−01
ACO	1	1	8.9578E−03	1	1	1	9.5348E−01	1	1	1	1	1	1	6.3414E−01	1
RCSA	1	1	8.2988E−04	1	1	1	1.7272E−01	4.1118E−01	1	1	1	1	1	1.0729E−01	1
HS	1	1	1	1	1	1	1	1	1	1	1	1	1	1	1
COVIDOA	1	1	4.2139E−01	1	1	1	1	1	1	1	1	1	1	1	1
KMA	1	8.8623E−03	1	5.6325E−01	1	1	1	1	1	6.3414E−01	1.0729E−01	1	1	1	2.1338E−02
QIO	1	1	1.0149E−04	1	8.3812E−01	1	3.6306E−02	9.6092E−02	4.8767E−01	1	1	1	1	2.1338E−02	1

post hoc test to elucidate the algorithm's efficacy in comparison to 11 well-established metaheuristics. This comprehensive evaluation aims to provide a nuanced understanding of HOA's capabilities across diverse problem landscapes, shedding light on its strengths and potential areas for improvement in optimization tasks.

5.2.1. Accuracy test benchmark

In Table 27, HOA's accuracy is compared to other metaheuristics when subjected to the six composite benchmark functions. With a variable dimension of 30, and maximum iterations of 500 for 200 runs, we observe that HOA outperformed some of the metaheuristics, such as GA, GWO, DE, ABC, SCA, BBO, and HS for functions F24, F25, and F26, respectively. For functions F27, and F28, HOA outperformed all other metaheuristics except for RCSA.

5.2.2. Computational time benchmark

In Table 28, we present the results of HOA's computational time benchmark compared to other metaheuristics in tandem with the composite functions. HOA's performance is comparable to other metaheuristics. In solving the composite functions, HOA's average computational running time is 7.43 s, which is fair considering the harsh search landscape of composite functions.

5.2.3. Wilcoxon rank sum test, friedman test, and dunn test

In this subsection, we examine the statistical significance of the results provided by HOA and the compared metaheuristics in Table 29. Similar to the traditional benchmark functions, we employ the Wilcoxon rank sum test in determining the results' statistical significance. In Table 29, we observe that the majority of the metaheuristics

Table 27
Results of accuracy test with composite benchmark functions.

Func.	Metric	HOA	TLBO	GA	DE	PSO	ABC	GWO	SCA	BBO	ACO	RCSA	HS
24	AVG.	5.20E+01	8.59E+00	1.51E+02	4.65E+01	3.91E+00	7.93E+01	3.90E+02	7.66E+01	3.31E+01	3.05E+00	5.35E−02	2.41E+01
	STD.	2.92E+01	6.93E+00	8.61E+01	2.48E+01	3.34E+00	4.50E+01	3.45E+02	4.62E+01	2.22E+01	2.48E+00	3.98E−02	1.52E+01
25	AVG.	1.10E+02	1.90E+01	3.56E+02	1.22E+02	1.83E+01	3.54E+02	1.52E+02	2.47E+02	1.31E+02	1.46E+01	1.98E−01	1.21E+02
	STD.	6.62E+01	1.09E+01	1.71E+02	1.08E+02	2.79E+01	2.01E+02	9.14E+01	1.01E+02	6.19E+01	1.37E+01	7.45E−02	7.65E+01
26	AVG.	2.21E+02	1.51E+01	1.55E+02	6.15E+01	8.75E+00	2.48E+02	1.44E+03	1.34E+02	6.59E+01	8.41E+00	9.98E−02	6.85E+01
	STD.	1.10E+02	1.51E+01	9.83E+01	3.42E+01	6.10E+00	1.70E+02	7.68E+02	8.09E+01	3.20E+01	6.80E+00	5.46E−02	4.43E+01
27	AVG.	5.85E+02	5.86E+02	8.01E+02	7.30E+02	6.23E+02	7.84E+02	1.06E+03	7.54E+02	6.09E+02	7.04E+02	3.28E+02	6.76E+02
	STD.	1.33E+01	1.97E+01	4.32E+01	3.66E+01	2.75E+01	3.97E+01	1.15E+02	5.52E+01	2.70E+01	4.80E+01	2.86E+01	3.15E+01
28	AVG.	6.40E+02	6.35E+02	8.64E+02	7.91E+02	6.78E+02	8.43E+02	1.18E+03	8.41E+02	6.56E+02	7.93E+02	3.38E+02	7.38E+02
	STD.	1.77E+01	1.93E+01	5.79E+01	4.20E+01	4.00E+01	4.77E+01	1.24E+02	5.31E+01	3.50E+01	4.84E+01	4.78E+01	3.48E+01
29	AVG.	6.45E+02	6.35E+02	8.45E+02	7.80E+02	6.54E+02	8.35E+02	1.24E+03	8.16E+02	6.71E+02	7.36E+02	3.25E+02	7.17E+02
	STD.	2.02E+01	1.93E+01	5.14E+01	3.76E+01	3.91E+01	5.51E+01	1.53E+02	4.95E+01	2.42E+01	4.91E+01	4.22E+01	3.05E+01

Table 28
Results of computational time test in seconds (s) with composite benchmark functions.

Func.	Metric	HOA	TLBO	GA	DE	PSO	ABC	GWO	SCA	BBO	ACO	RCSA	HS
24	AVG	6.99E+00	6.83E+00	3.44E+00	3.44E+00	3.44E+00	6.92E+00	3.37E+00	3.37E+00	3.53E+00	6.95E+00	3.40E+02	3.52E+00
	STD	6.07E−01	5.28E−01	2.69E−01	2.69E−01	2.75E−01	5.57E−01	2.67E−01	2.65E−01	2.76E−01	5.43E−01	2.32E+01	2.80E−01
25	AVG	6.90E+00	6.64E+00	3.33E+00	3.34E+00	3.34E+00	6.72E+00	3.27E+00	3.27E+00	3.41E+00	6.74E+00	3.29E+02	3.41E+00
	STD	1.04E+00	4.11E−01	1.94E−01	1.98E−01	1.93E−01	3.97E−01	1.99E−01	1.97E−01	2.02E−01	4.28E−01	1.46E+01	2.05E−01
26	AVG	8.20E+00	7.74E+00	3.91E+00	3.90E+00	3.90E+00	7.90E+00	3.83E+00	3.84E+00	4.01E+00	7.89E+00	3.84E+02	4.00E+00
	STD	1.52E+00	2.32E−01	1.24E−01	1.14E−01	1.21E−01	2.21E−01	1.12E−01	1.12E−01	1.27E−01	2.37E−01	1.01E+01	1.72E−01
27	AVG	7.71E+00	7.55E+00	3.80E+00	3.81E+00	3.80E+00	7.65E+00	3.72E+00	3.72E+00	3.88E+00	7.67E+00	3.78E+02	3.90E+00
	STD	2.36E−01	2.73E−01	1.37E−01	1.38E−01	1.39E−01	2.84E−01	1.35E−01	1.34E−01	1.39E−01	2.14E−01	7.75E+00	1.15E−01
28	AVG	7.39E+00	7.24E+00	3.64E+00	3.65E+00	3.64E+00	7.32E+00	3.56E+00	3.58E+00	3.73E+00	7.35E+00	3.58E+02	3.73E+00
	STD	5.53E−01	5.28E−01	2.68E−01	2.68E−01	2.65E−01	5.27E−01	2.57E−01	2.70E−01	2.77E−01	5.37E−01	2.51E+01	2.73E−01
29	AVG	7.39E+00	7.25E+00	3.64E+00	3.65E+00	3.64E+00	7.30E+00	3.54E+00	3.55E+00	3.70E+00	7.31E+00	3.58E+02	3.71E+00
	STD	5.58E−01	5.46E−01	2.74E−01	2.82E−01	2.89E−01	5.81E−01	2.73E−01	2.77E−01	2.88E−01	5.67E−01	2.69E+01	2.76E−01

Table 29
Results of rank-sum metric test with composite benchmark functions.

Func.	HOA	TLBO	GA	DE	PSO	ABC	GWO	SCA	BBO	ACO	RC_SA	HS
24	1.14E−16	3.35E−06	1.42E−13	8.29E−10	1.18E−09	4.72E−05	3.68E−17	1.42E−04	1.30E−07	1.17E−10	2.50E−09	4.09E−06
25	4.75E−12	7.09E−11	8.09E−19	4.93E−08	9.68E−09	6.20E−11	1.73E−02	3.80E−08	1.42E−06	2.99E−07	3.88E−08	6.02E−05
26	2.65E−17	5.43E−09	1.93E−03	8.14E−09	3.41E−09	7.99E−07	8.09E−19	2.73E−03	4.30E−09	1.81E−07	3.08E−08	4.57E−05
27	6.57E−10	3.88E−08	1.58E−18	7.17E−09	1.79E−03	9.08E−08	1.37E−19	7.76E−05	1.61E−07	1.93E−12	3.64E−08	5.91E−04
28	1.75E−11	1.56E−06	4.62E−19	2.51E−08	1.23E−03	9.91E−07	1.26E−19	2.96E−06	2.28E−07	4.10E−14	3.72E−12	5.46E−04
29	3.42E−07	2.06E−09	6.64E−19	3.15E−09	7.05E−06	1.09E−07	1.56E−19	3.70E−06	1.09E−07	4.18E−19	9.15E−12	3.82E−04

Table 30
Results of the Friedman test ranking for the composite functions.

Func.	HOA	TLBO	GA	DE	PSO	ABC	GWO	SCA	BBO	ACO	RCSA	HS
F24	2	9	3	5	6	11	1	12	8	4	7	10
F25	2	4	1	8	5	3	12	6	10	9	7	11
F26	2	5	11	6	3	9	1	12	4	8	7	10
F27	4	7	2	5	12	8	1	10	9	3	6	11
F28	5	9	2	6	12	8	1	10	7	3	4	11
F29	9	5	3	6	11	7.5	1	10	7.5	2	4	12
	24	39	22	36	49	46.5	17	60	45.5	29	35	65

have a *p*-value of less than 5% and therefore reject the null hypothesis. In line with Friedman's test conducted on unimodal, multimodal, and fixed-dimensional benchmark functions as depicted in Tables 19 to 22, we offer Friedman's test results for the composite functions, showcased in Table 30. In Table 30, it becomes evident that the GWO, GA, and HOA demonstrated exceptional performance. As a consequence, the outcomes produced by HOA and other metaheuristics exhibit statistical significance, warranting further investigation through Dunn's post-hoc analysis. Within Table 31, we present the outcomes of pair-wise comparisons conducted via Dunn's post-hoc test. Notably, the analysis reveals a statistically significant distinction between HOA and HS.

6. Engineering design problems

Unlike the traditional and composite benchmark functions discussed in the preceding sections, engineering design problems (EDPs) are generally associated with constraints-based optimization. EDPs are known to have several equality and inequality constraints, making them challenging to solve. However, recently, metaheuristics have been employed to solve EDPs owing to the reduction in computational cost, accuracy, and versatility. In this work, we employ three popular EDPs, namely: (i) I-beam EDP [100], (ii) Tension/Compression Spring

Table 31
Results of the Dunn's post-hoc analysis for the respective composite benchmark functions.

Alg.	HOA	TLBO	GA	DE	PSO	ABC	GWO	SCA	BBO	ACO	RCSA	HS
HOA	1	1	1	1	1	1	1	0.18487	1	1	1	0.043849
TLBO	1	1	1	1	1	1	1	1	1	1	1	1
GA	1	1	1	1	1	1	1	0.105998	1	1	1	0.023568
DE	1	1	1	1	1	1	1	1	1	1	1	1
PSO	1	1	1	1	1	1	0.520832	1	1	1	1	1
ABC	1	1	1	1	1	1	0.927135	1	1	1	1	1
GWO	1	1	1	1	0.520832	0.927135	1	0.023568	1	1	1	0.004453
SCA	0.18487	1	0.105998	1	1	1	0.023568	1	1	0.67755	1	1
BBO	1	1	1	1	1	1	1	1	1	1	1	1
ACO	1	1	1	1	1	1	1	0.67755	1	1	1	0.189099
RCSA	1	1	1	1	1	1	1	1	1	1	1	0.793686
HS	0.043849	1	0.023568	1	1	1	0.004453	1	1	0.189099	0.793686	1

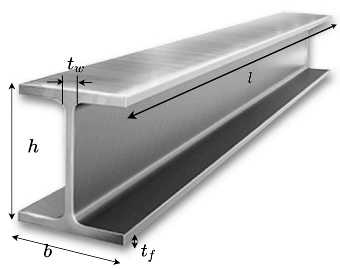

Fig. 5. Structure and parameters of the I-beam.

Fig. 6. Structure and parameters of tension or compression spring EDP.

EDP [100], and (iii) Gear Train EDP. Moreover, similar to the traditional and composite benchmark tests, HOA is compared to the same 11 metaheuristics.

6.1. I-beam EDP

The structural representation of the I-beam is illustrated in Fig. 5. This design problem entails the minimization of the vertical deflection, in which the mathematical formulation is given by [100]:

$$\min_{b,\ h,\ t_w,\ t_f} \quad \frac{5000}{\frac{t_w(h-2t_f)^3}{12}+\frac{bt_f^3}{6}+2bt_f\left(\frac{h-t_f}{2}\right)^2} \tag{6a}$$

subject to :

$$2bt_w \ + \ t_w(h-2t_f) \leq 0 \tag{6b}$$
$$10 \leq \ b \ \leq 50 \tag{6c}$$
$$10 \leq \ h \ \leq 80 \tag{6d}$$
$$0.9 \leq \ t_w \ \leq 5 \tag{6e}$$
$$0.9 \leq \ t_f \ \leq 5 \tag{6f}$$

where b, h, t_w, and t_f denote the width, length, thickness of the vertical bar and thickness of the horizontal bar. Table 32 depicts the results of HOA and other metaheuristics. Here, HOA outperformed certain other metaheuristics such as GA, GWO, BBO, and RCSA with competitive results.

6.2. Tension/compression spring EDP

Unlike the I-beam EDP, which has a single constraint, the tension/compression spring EDP has four constraints embedded with the objective of minimizing the fabrication cost. The decision variables, in this case, are wire diameter, d, the number of active coils denoted as N, and the mean coil diameter, D [100], as illustrated in Fig. 6. The tension/compression spring EDP optimization is given by:

$$\min_{d,\ D,\ N} \quad (N+2)Dd^2 \tag{7a}$$

subject to :

$$1-\frac{D^3N}{71785d^4} \leq 0 \tag{7b}$$
$$\frac{4D^2-dD}{12566(Dd^3-d^4)}+\frac{1}{5108d^2} \leq 0 \tag{7c}$$
$$1-\frac{140.45d}{D^2N} \leq 0 \tag{7d}$$
$$\frac{d+D}{1.5}-1 \ \leq 0 \tag{7e}$$
$$0.05 \leq \ d \ \leq 2.0; \quad 0.15 \leq \ D \ \leq 1.3 \tag{7f}$$
$$2.0 \leq \ N \ \leq 15.0 \tag{7g}$$

Table 33 shows the comparison of HOA to other metaheuristics for the tension/compression spring EDP. In Table 33, we see that HOA outperformed GA, PSO, GWO, BBO, and HS.

6.3. Gear train EDP

The gear train is a mechanical system comprising gears mounted such that the gears' teeth engage each other as illustrated in Fig. 7, thereby resulting in a smooth rotation. Unlike the I-beam and tension/compression spring EDPs, the gear train EDP is a discrete optimization problem ensuring the number of gear teeth for each gear is optimal. The gear train EDP is given by:

$$\min_{n_A,n_B,n_C,n_D} \quad \left(\frac{1}{6.931}-\frac{n_Cn_B}{n_An_D}\right)^2 \tag{8a}$$

subject to :

$$12 \leq n_A,\ n_B,\ n_C,\ n_D \leq 600 \tag{8b}$$

Table 34 depicts HOA's and other metaheuristics' results when employed to find and solve the gear train EDP. We observed that HOA's performance was fair in comparison with the other metaheuristics. We see that the HOA outperformed GA, TLBO, ABC, GWO, SCA, ACO, and HS.

Table 32
Results of the I-beam design problem.

Metah.	Optimal values of variables				Opt. Vert. defl.
	b	h	tw	tf	
HOA	5.0000E+01	8.0000E+01	5.0000E+00	5.0000E+00	7.0791E−03
TLBO	5.0000E+01	8.0000E+01	5.0000E+00	5.0000E+00	7.0791E−03
GA	3.9989E+01	7.2962E+01	3.2185E+00	3.7202E+00	1.5148E−02
DE	5.0000E+01	8.0000E+01	5.0000E+00	5.0000E+00	7.0791E−03
PSO	5.0000E+01	8.0000E+01	5.0000E+00	5.0000E+00	7.0791E−03
ABC	5.0000E+01	8.0000E+01	5.0000E+00	5.0000E+00	7.0791E−03
GWO	4.9919E+01	7.9806E+01	4.9893E+00	4.9878E+00	7.1735E−03
SCA	5.0000E+01	8.0000E+01	5.0000E+00	5.0000E+00	7.0791E−03
BBO	4.9799E+01	7.9855E+01	5.0000E+00	5.0000E+00	7.1299E−03
ACO	5.0000E+01	8.0000E+01	5.0000E+00	5.0000E+00	7.0791E−03
RCSA	4.0302E+01	6.9916E+01	6.1346E+00	5.8884E+00	1.4499E−02
HS	5.0000E+01	8.0000E+01	5.0000E+00	5.0000E+00	7.0791E−03

Table 33
Results of the tension/compression spring design problem.

Metah.	Optimal values of variables			Opt. Weight
	d	D	N	
HOA	5.7123E−02	4.9536E−01	3.7241E+00	1.8118E−02
TLBO	5.0003E−02	5.9524E−01	2.2228E+00	6.2930E−03
GA	5.2602E−02	4.8953E−01	5.7843E+00	1.5547E−01
DE	5.3189E−02	5.4756E−01	4.9932E+00	1.0196E−02
PSO	6.1456E−02	7.3788E−01	5.4838E+00	7.5548E−02
ABC	5.0059E−02	5.4907E−01	2.9406E+00	7.6580E−03
GWO	6.8661E−02	4.4903E−01	5.9846E+00	7.8942E−02
SCA	5.0558E−02	5.4938E−01	3.1659E+00	9.6797E−03
BBO	7.6217E−02	6.1319E−01	6.5711E+00	3.6964E−02
ACO	5.0143E−02	5.9851E−01	2.1385E+00	6.3206E−03
RCSA	5.5127E−02	7.5238E−01	8.9418E−01	1.0690E−02
HS	7.1785E−02	6.5914E−01	6.2798E+00	2.8963E−02

Table 34
Results of the gear train design problem.

Metah.	Opt. values of Var.				f
	n_A	n_B	n_C	n_D	
HOA	38	14	15	39	1.77E−14
TLBO	44	16	17	43	2.18E−12
GA	41	16	14	39	2.60E−05
DE	50	21	19	52	2.21E−15
PSO	56	23	27	58	0
ABC	53	21	21	52	2.23E−11
GWO	55	22	23	55	9.30E−07
SCA	50	18	19	45	2.94E−09
BBO	50	19	20	51	4.56E−27
ACO	51	22	19	53	3.75E−11
RCSA	48	21	20	51	7.13E−22
HS	49	20	19	51	4.80E−13

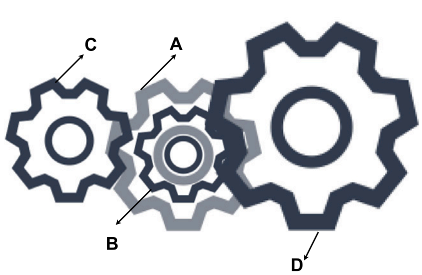

Fig. 7. Structure of the gear train EDP.

7. NP-hard problems

In this section, we focus on HOA's capability to solve NP-Hard problems. In a bid to find exact solutions, NP-Hard problems become computationally intractable. Computationally intractable problems are problems that cannot be solved in a reasonable time that is, polynomial time on a nondeterministic machine. Simply put, as the problem grows increasingly complex, the computational runtime unreasonable. An NP-Hard problem can be polynomial-time reduced to a problem that is tractable and its solution is the same as the NP-Hard problem. For NP-Hard problems, there are no efficient algorithms that can solve them in polynomial time [101]. To this end, most combinatorial problems are NP-Hard, and generally expressed as [102,103]:

$$\sum_{e\in I^*} G(e) = \max\left\{\sum_{e\in I} G(e) \mid I \in \mathcal{J}\right\}, \tag{9}$$

Table 35
HOA's accuracy performance evaluation with varying agent size for six TSPs respectively.

TSP	Accuracy	HOA agent size						
		30	100	250	500	750	1000	5000
5-City	Best	19	19	19	19	19	19	19
	Worst	19	19	19	19	19	19	19
	Mode	19	19	19	19	19	19	19
	Average	19	19	19	19	19	19	19
	Std.	0	0	0	0	0	0	0
13-City	Best	7293	7293	7293	7293	7293	7293	7293
	Worst	8905	8504	8228	8448	8146	8020	7704
	Mode	7293	7293	7293	7293	7293	7293	7293
	Average	7833.750	7598.546	7506.410	7448.416	7436.446	7401.102	7343.012
	Std.	379.938	272.263	215.869	186.242	178.931	152.652	111.755
gr17	Best	2085	2085	2085	2085	2085	2085	2085
	Worst	3016	2758	2648	2564	2584	2547	2412
	Mode	2316	2181	2085	2085	2085	2085	2085
	Average	2397.934	2282.952	2238.710	2205.978	2187.114	2180.486	2139.836
	Std.	164.320	111.891	98.038	85.603	76.902	72.138	52.211
fri26	Best	1031	1031	1031	1031	1031	1031	971
	Worst	1138	1100	1100	1100	1100	1100	1100
	Mode	1100	1100	1100	1100	1100	1100	1031
	Average	1099.984	1097.436	1093.504	1090.426	1083.072	1082.412	1045.018
	Std.	11.143	12.915	19.767	23.410	29.285	29.498	27.436
dantzig42	Best	699	699	699	699	699	699	699
	Worst	699	699	699	699	699	699	699
	Mode	699	699	699	699	699	699	699
	Average	699	699	699	699	699	699	699
	Std.	0	0	0	0	0	0	0
att48	Best	67 392	60 261	56 010	51 166	50 039	49 360	47391
	Worst	117 935	114 169	102 390	105 936	99 534	97 312	97477
	Mode	81 169	78 122	71 008	75 334	67 987	63 298	60795
	Average	92 999.128	84 383.374	79 201.280	75 348.648	73 306.304	71 944.170	65 610.928
	Std.	9923.785	8748.598	8614.018	8753.957	8213.681	8426.278	7633.232

where F is a finite set and $\mathcal{J}$ is a set of subsets of F and is otherwise called a set of feasible solutions. Moreover, $G : F \rightarrow \mathbb{R}$ is a linear objective function. The obtained feasible solution(s) I^*, is such that $I^* \in \mathcal{J}$. Widely known examples of NP-hard problems are the Traveling Salesman's Problem (TSP) [104,105], protein folding problem [106,107], the knapsack problem [108], the satisfiability problem [109,110], and the subset sum problem [111]. In this work, our focus lies in examining the performance of HOA in solving TSP, and knapsack problems.

7.1. Traveling Salesman's problem

The TSP entails finding the shortest route given a set of cities in such a manner that (i) each city is visited once and (ii) the starting city is also the ending city after visiting all the cities [112]. The objective of the TSP is to keep the traveling cost or distance to a minimum. Hence, as the number of cities grows, the focus of TSP is to find the cheapest or approximate solution, rather than the optimal solution. The TSP has been applied to problems related to logistics (i.e. vehicle routing), industry, and manufacturing (i.e. robotic machining). The integer linear programming optimization expression for TSP is given by [112,113]:

$$\min_{x_{ab}} \sum_{a=1}^{m} \sum_{b\neq a,\ b=1}^{m} c_{ab}\, x_{ab} \tag{10a}$$

subject to:

$$\sum_{a=1,\ a\neq b}^{m} x_{ab} = 1, \tag{10b}$$

$$\sum_{b=1,\ b\neq a}^{m} x_{ab} = 1, \tag{10c}$$

$$\sum_{a\in Q} \sum_{b\neq a,\ b\in Q} x_{ab} \leq |Q| - 1,\ \ \forall Q \subsetneq \{1,\dots,m\}, |Q| \geq 2 \tag{10d}$$

$$x_{ab} \in \{0,1\}, \tag{10e}$$

where x_{ab} denotes the decision variable of using the route city a to city b. Additionally, c_{ab} represents the distance of city b from city a; and it is assumed that $c_{ab} > 0$. The objective function in (11a) is to minimize the total tour distance, besides constraints (10d) ensures that the elimination of inclusion of sub-tours in the solutions provided by solving the optimization problem. Additionally, constraint (11b) ensures that each city in the list is arrived at from exactly only one city; while constraint (10c) guarantees that each city is departed from and to exactly only one other city. In this work, we examine the performance of HOA in solving six TSP problems in the TSP library [114,115], namely: (i) a simple 5-city problem with an optimal cost of 19; (ii) a Google OR 13-city problem based on 13 cities in the USA with an optimal cost of 7293; (iii) gr17, a 17-city problem with an optimal solution of 2085 [114]; (iv) fri26, a set of 26 cities with an optimal cost of 937 [114]; (iv) dantzig42, a 42-city problem with an optimal cost of 699 [114]; and (vi) att48, a 48-city problem based on 48 capitals of the USA with an optimal cost of 10628 [114]. In Tables 35 and 36, we present our findings with regard to HOA's performance evaluation in solving the respective TSP problems. In this research, we employ extensively the Monte Carlo simulation technique and consider sensitivity analysis by varying the agent sizes in the range of 30 and 5000 to reach our results. In Table 35, we observe that HOA's output has four optimal results and two near-optimal results.

7.2. Knapsack problems

The knapsack problem primarily involves the collection of items, goods, or entities with unique weights and values in such a manner that the largest value is considered while having a minimum reasonable

Table 36
HOA's computational run time (in seconds) performance evaluation with varying agent size for six TSPs respectively.

TSP	Run time	HOA agent size						
		30	100	250	500	750	1000	5000
5-City	Mean	0.1905	0.6518	1.2193	2.0745	2.8811	3.6913	17.1153
	Std.	0.0344	0.1160	0.0635	0.0491	0.0668	0.0804	1.1139
	Mode	0.1557	0.5852	1.1262	2.0149	2.8722	3.6807	17.1481
	Best	0.1557	0.5758	1.1262	2.0149	2.8320	3.6088	16.4415
	Worst	0.4146	1.2930	1.5696	2.5583	3.5859	4.8075	40.1289
13-City	mean	0.2099	0.7703	1.4089	2.2730	3.1307	4.0386	21.2374
	std	0.0140	0.1504	0.1962	0.1730	0.1355	0.3512	5.0454
	mode	0.2064	0.6624	1.2822	2.1871	3.0588	3.9141	17.6401
	Best	0.1915	0.6473	1.2822	2.1871	3.0588	3.9141	17.6401
	Worst	0.3513	1.5077	3.2023	4.1148	4.8321	8.6642	33.5525
	Mean	0.2297	0.7186	1.6728	2.6353	3.7105	4.5462	19.6205
gr17	std	0.0182	0.0799	0.2247	0.1844	0.4062	0.4723	1.4617
	Mode	0.2250	0.6700	1.1981	2.4480	3.4307	4.2003	18.2715
	Best	0.1721	0.6700	1.1981	2.4480	3.4307	4.2003	18.2715
	Worst	0.3675	1.2870	2.9526	3.8776	7.4468	8.1293	28.4618
fri26	Mean	0.2516	0.7832	1.8116	2.8666	3.9092	5.5417	23.9518
	Std	0.0424	0.1186	0.2942	0.3750	0.6982	0.9003	84.1212
	Mode	0.2375	0.6840	1.5398	2.5215	3.5513	4.4914	18.8635
	Best	0.1808	0.6840	1.5398	2.5215	3.5513	4.4914	18.8635
	Worst	0.6352	1.6995	3.5295	4.9782	8.8726	14.0611	190.7888
dantzig42	mean	0.2758	0.7600	1.5211	2.6200	3.6500	4.7001	21.3050
	std	0.0443	0.0505	0.0552	0.1296	0.0793	0.1122	0.2822
	mode	0.2420	0.7440	1.4979	2.5751	3.6164	4.6568	21.0445
	Best	0.2176	0.7120	1.4907	2.5583	3.5943	4.6308	21.0445
	Worst	0.4925	1.1750	2.1139	3.7332	4.4554	6.1817	24.3237
att48	mean	0.3163	1.1626	2.3289	3.5416	5.0062	6.3366	26.3659
	std	0.0535	0.1916	0.3189	0.3287	0.6850	0.9735	2.7436
	mode	0.1961	0.9049	2.2299	3.2690	4.3094	5.3320	23.2470
	Best	0.1961	0.9049	1.9882	3.269	4.3094	5.3320	23.2470
	Worst	0.6272	1.8079	4.0736	5.7165	8.9296	12.3452	55.5110

weight subject to a stated minimum weight constraint. Herein, we examine two types of knapsack problems: (i) 0–1 knapsack problems [116], and (ii) bounded knapsack problems [117], respectively, and mathematically denoted as:

$$\max_{x_i} \quad \sum_{i=1}^{y} x_i \; k_i \tag{11a}$$

subject to:

$$\sum_{i=1}^{y} x_i \; j_i \; \leq J, \tag{11b}$$

$$x_i \in \{0, 1\}, \tag{11c}$$

and,

$$\max_{x_i} \quad \sum_{i=1}^{y} x_i \; k_i \tag{12a}$$

subject to:

$$\sum_{i=1}^{y} \; x_i \; j_i \leq J, \tag{12b}$$

$$x_i \in \{0, 1, 2, 3, \dots, b\}, \tag{12c}$$

where we have the total number of items in a collection given as y, and each item's unique value and weight are denoted by k_i and j_i, respectively. Moreover, the maximum weight constraint of the knapsack bag is indicated by J, and, moreover, in (11a)–(12b), the index i denotes the item number.

In Table 37–40, HOA's performance is examined in terms of accuracy and computational time for the 0–1 and bounded knapsack problems for varying dimensions ranging from 30 to 1000, and comparisons carried out with an exact solution; in this case, dynamic programming (DP). In Table 37, emphasis is placed on accuracy and the computational cost of achieving this for a 0-1 knapsack problem. We observe that, for all the dimensions, HOA's performance in terms of value and weight accuracy is the same as that of DP. Additionally, in terms of computational cost, we see that the HOA's performance outshines that of DP as the dimension of the problem increases in Table 37 and Fig. 8. For clarity and details, the best, worst, and average performances in terms of accuracy and computational cost of HOA for the examined dimensions are shown in Tables 38 and 39. We observe

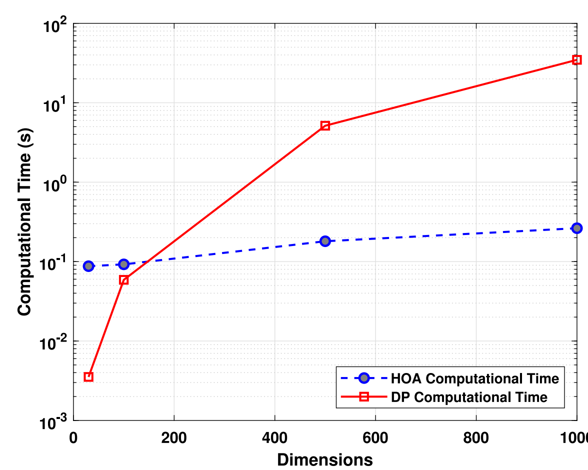

Fig. 8. Computational running time of HOA and DP in solving a 0–1 knapsack problem for varying dimensions of 30, 100, 500, and 1000.

Table 37
Comparing HOA and DP optimized value, weight, and computational run time (in seconds) performances for a 0-1 knapsack problem.

Dim	v_{HOA}	v_{DP}	W_{HOA}	W_{DP}	t_{HOA}	t_{DP}
30	18 946	18 946	1004	1004	0.087541	0.0035311
100	51 929	51 929	3422	3422	0.092304	0.058952
500	255 760	255 760	17 258	17 258	0.18038	5.1359
1000	496 860	496 860	34 801	34 801	0.26318	34.699

Table 38
Comparing best, worst, average, standard deviation, and standard error of HOA best cost value for the various dimensions in a 0-1 knapsack problem.

Dim	Best	Worst	Avg.	Std.	Err.
30	18 946	13 760	18 625	785.24	1.0706
100	51 929	41 751	51 476	1254.8	2.823
500	255 760	192 370	254 150	5301.2	6.8673
1000	496 860	433 670	494 440	8393	10.915

Table 39
Comparing best, worst, average, and standard deviation of the computational run-time performance in seconds of HOA in a 0-1 knapsack problem.

Dim	Best	Worst	Avg.	Std.
30	0.087541	0.18382	0.11094	0.0090905
100	0.092304	0.16367	0.10264	0.0070589
500	0.18038	0.45248	0.20702	0.014264
1000	0.26318	0.80834	0.29919	0.032561

Table 40
Comparing HOA and DP optimized values and weights on a bounded knapsack problem with i =1, 2, 3.

Dim	v_{DP}			v_{HOA}			W_{DP}			W_{HOA}		
	$i=1$	$i=2$	$i=3$	$i=1$	$i=2$	$i=3$	$i=1$	$i=2$	$i=3$	$i=1$	$i=2$	$i=3$
30	18 946	16 827	14 931	18 946	21 132	21 347	1004	1191	1129	1004	1367.9	1286.8
100	51 929	49 661	49 562	51 929	58 512	58 680	3422	3714	3530	3422	4001.5	3806.6
500	255 760	257 610	252 080	255 760	278 190	275 790	17 258	17 419	17 447	17 258	18 057	18 378
1000	496 860	524 770	511 430	496 860	556 900	542 740	34 801	34 571	34 958	34 801	36 041	36 595

that HOA's computational time for all the dimensions examined is less than 1 second.

8. Conclusion

The Hiking Optimizer Algorithm (HOA) proposed in this paper is a revolutionary metaheuristic algorithm. It draws inspiration from hiking patterns, which vary greatly depending on the terrain and hike leader. HOA was tested utilizing 29 commonly used benchmark test functions, including unimodal, multimodal, fixed-multimodal, and composite functions. Furthermore, we assessed HOA's performance on real-world engineering design problems (EDP). We also illustrated HOA's ability to solve NP-hard issues. All performance data was generated using a complete Monte Carlo simulation environment, which includes all benchmark test functions and EDPs. The evaluation comprised assessments of computational running time, accuracy, Wilcoxon rank sum, Friedman ranking test, and Dunn's post-hoc analysis. HOA underwent thorough scrutiny, being meticulously compared against 14 distinct metaheuristics.

We demonstrated the search path of HOA for a few benchmark test functions in Figs. 10(a)–10(x), demonstrating how hikers explore and exploit the search space environment. We showed that HOA's p-values in Tables 15–18 are significantly lower than 0.05, indicative of its superior performance, rejecting the null hypothesis, and proving its statistical significance. According to Friedman's ranking test, HOA outperformed the other 11 metaheuristics in various cases, as demonstrated in Tables 19–22. The results show that HOA has statistical significance, as the Friedman statistics for unimodal, multimodal, and fixed benchmark functions were 30, 100, 250, and fixed dimensions were 138.71, 152.05, 148.61, and 55.49, respectively, all of which are greater than the critical value of 23.68. Similarly, their p-values were less than the 0.05 cutoff. Table 27 shows that HOA outperforms several metaheuristics when dealing with the complexities of composite functions, with the exception of RCSA for functions F27 and F28. Furthermore, we demonstrated in Table 28 that HOA is equivalent to other metaheuristics in terms of efficacy because its average computational execution time for solving composite functions is 7.43 s, which is fair given the functions' rigorous and rough search landscape.

HOA also provided optimal and near-optimal results when applied to real-world EDPs. Furthermore, HOA's performance in solving TSPs like 5, 13, 17, 26, 42, and 48 was commendable, with optimal results in the majority of situations. HOA was able to deal with high-dimensional problems and come up with an optimal or near-optimal solution. Its computational running time is even better than that of the dynamic programming method when solving the 0–1 knapsack problems with dimensionalities of 200 or more, as shown in Fig. 8. We observe that HOA is effective in solving high-dimensional optimization problems, outperforms several renowned metaheuristics, and may be applied to a wide range of applications (see Fig. 9).

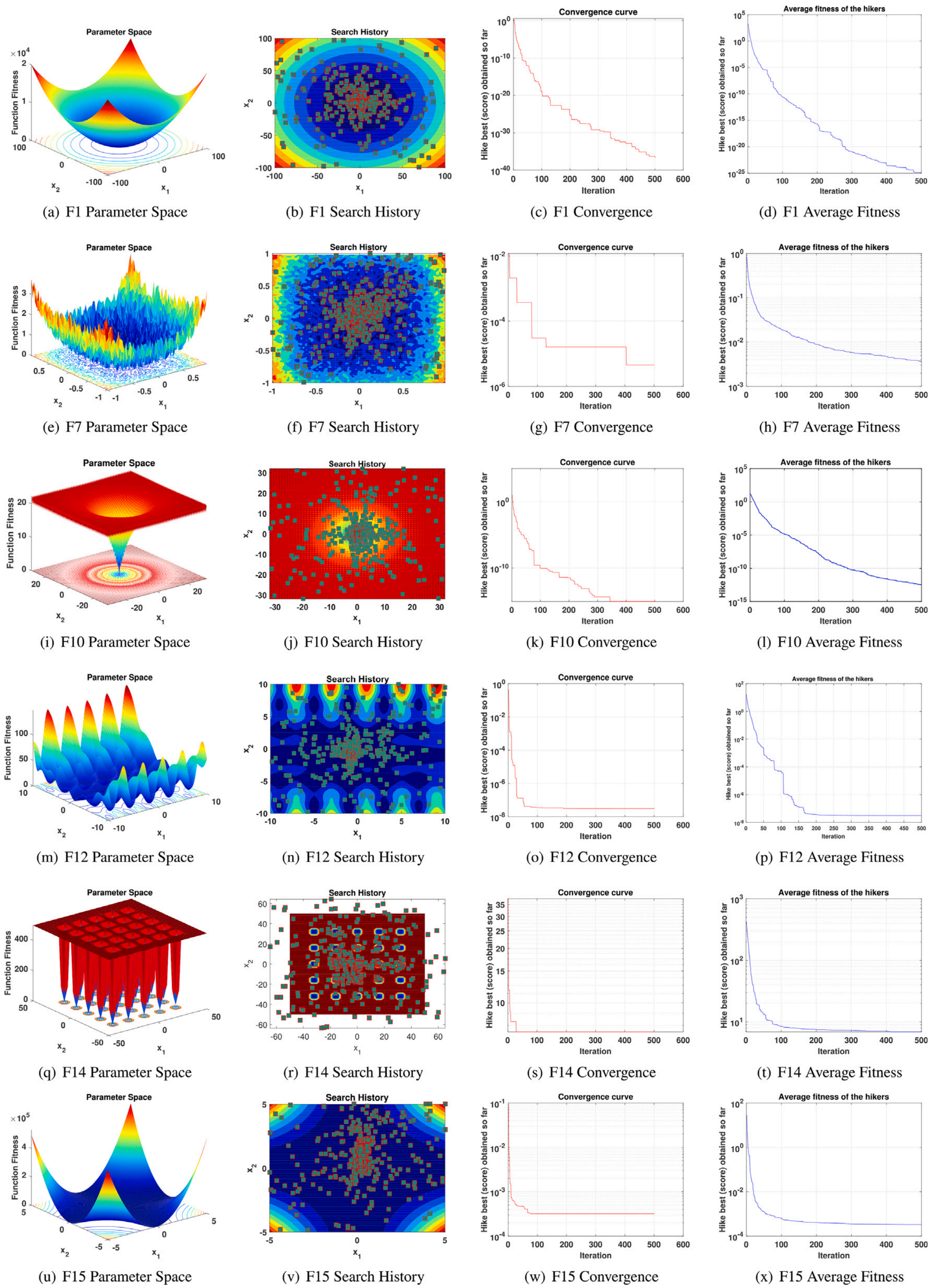

(a) F1 Parameter Space (b) F1 Search History (c) F1 Convergence (d) F1 Average Fitness

(e) F7 Parameter Space (f) F7 Search History (g) F7 Convergence (h) F7 Average Fitness

(i) F10 Parameter Space (j) F10 Search History (k) F10 Convergence (l) F10 Average Fitness

(m) F12 Parameter Space (n) F12 Search History (o) F12 Convergence (p) F12 Average Fitness

(q) F14 Parameter Space (r) F14 Search History (s) F14 Convergence (t) F14 Average Fitness

(u) F15 Parameter Space (v) F15 Search History (w) F15 Convergence (x) F15 Average Fitness

Fig. 9. Illustration of the parameter space, HOA's search, convergence, and fitness average analysis for some functions.

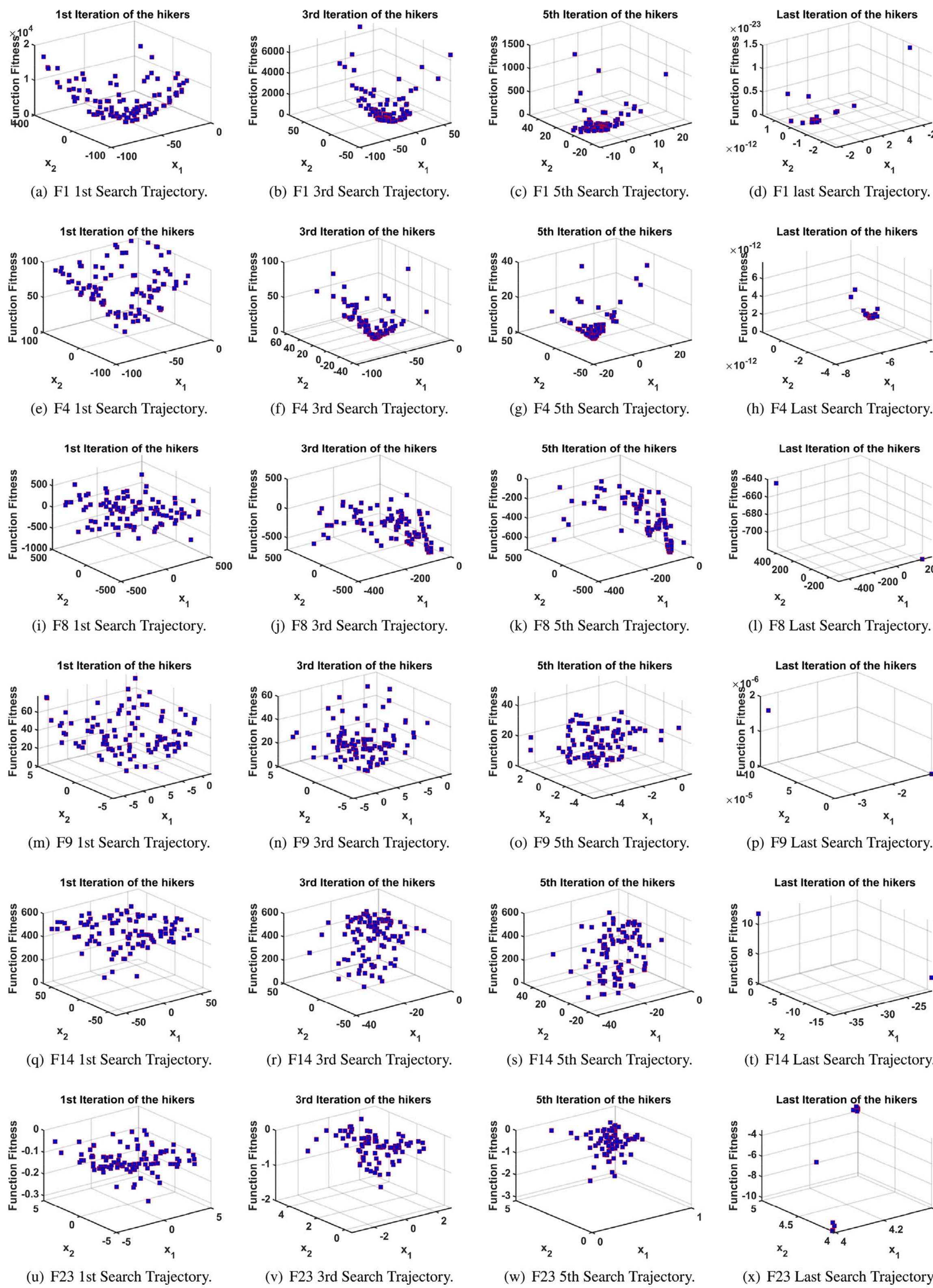

(a) F1 1st Search Trajectory. (b) F1 3rd Search Trajectory. (c) F1 5th Search Trajectory. (d) F1 last Search Trajectory.

(e) F4 1st Search Trajectory. (f) F4 3rd Search Trajectory. (g) F4 5th Search Trajectory. (h) F4 Last Search Trajectory.

(i) F8 1st Search Trajectory. (j) F8 3rd Search Trajectory. (k) F8 5th Search Trajectory. (l) F8 Last Search Trajectory.

(m) F9 1st Search Trajectory. (n) F9 3rd Search Trajectory. (o) F9 5th Search Trajectory. (p) F9 Last Search Trajectory.

(q) F14 1st Search Trajectory. (r) F14 3rd Search Trajectory. (s) F14 5th Search Trajectory. (t) F14 Last Search Trajectory.

(u) F23 1st Search Trajectory. (v) F23 3rd Search Trajectory. (w) F23 5th Search Trajectory. (x) F23 Last Search Trajectory.

Fig. 10. Illustration of the parameter space, HOA's search, convergence, and fitness average analysis for some unimodal, multimodal, and fixed-dimension multimodal functions.

CRediT authorship contribution statement

Sunday O. Oladejo: Writing – review & editing, Writing – original draft, Visualization, Supervision, Software, Methodology, Investigation, Formal analysis, Conceptualization. **Stephen O. Ekwe:** Writing – review & editing, Writing – original draft, Visualization, Supervision, Software, Methodology. **Seyedali Mirjalili:** Writing – original draft, Visualization, Supervision, Methodology.

Declaration of competing interest

The authors declare that they have no known competing financial interests or personal relationships that could have appeared to influence the work reported in this paper.

Data availability

Data will be made available on request.

References

[1] I.D. Wolf, T. Wohlfart, Walking, hiking and running in parks: A multidisciplinary assessment of health and well-being benefits, Landsc. Urban Plan. 130 (2014) 89–103.
[2] D. Mitten, J.R. Overholt, F.I. Haynes, C.C. D'Amore, J.C. Ady, Hiking: A low-cost, accessible intervention to promote health benefits, Am. J. Lifestyle Med. 12 (4) (2018) 302–310.
[3] N. Davies, Who walks, where and why? Practitioners' observations and perspectives on recreational walkers at UK tourist destinations, Ann. Leis. Res. 21 (5) (2018) 553–574.
[4] S. Rybråten, M. Skår, H. Nordh, The phenomenon of walking: Diverse and dynamic, Landsc. Res. 44 (1) (2019) 62–74.
[5] J. Minick, The best short hikes in the great smoky mountains and the best overnight hikes in the great smoky mountains, 1997.
[6] Z. Anderson, C. Lusk, M.D. Jones, Towards understanding hikers' technology preferences, in: Proceedings of the 2017 ACM International Joint Conference on Pervasive and Ubiquitous Computing and Proceedings of the 2017 ACM International Symposium on Wearable Computers, 2017, pp. 1–4.
[7] B.F. Bichler, M. Peters, Soft adventure motivation: An exploratory study of hiking tourism, Tourism Review.
[8] R. Manning, J. Taylor, Preparing for a day hike at Grand Canyon: What information is useful?, in: Wilderness Science in a Time of Change Conference: Wilderness Visitors, Experiences, and Visitor Management, vol. 4, US Department of Agriculture, Forest Service, Rocky Mountain Research Station, 2000, p. 221.
[9] R.C. Lucas, R.P. Rinehart, The neglected hiker, Backpacker Mag. 4 (1).
[10] D. Duran, V. Sacristán, R.I. Silveira, Map construction algorithms: A local evaluation through hiking data, GeoInformatica 24 (3) (2020) 633–681.
[11] S. Mirjalili, S.M. Mirjalili, A. Lewis, Grey wolf optimizer, Adv. Eng. Softw. 69 (2014) 46–61.
[12] S. Mirjalili, A. Lewis, The whale optimization algorithm, Adv. Eng. Softw. 95 (2016) 51–67.
[13] S. Mirjalili, A.H. Gandomi, S.Z. Mirjalili, S. Saremi, H. Faris, S.M. Mirjalili, Salp swarm algorithm: A bio-inspired optimizer for engineering design problems, Adv. Eng. Softw. 114 (2017) 163–191.
[14] E.-G. Talbi, Metaheuristics: From Design To Implementation, vol. 74, John Wiley & Sons, 2009.
[15] S.O. Oladejo, O.E. Falowo, Latency-aware dynamic resource allocation scheme for multi-tier 5 g network: A network slicing-multitenancy scenario, IEEE Access 8 (2020) 74834–74852, http://dx.doi.org/10.1109/ACCESS.2020.2988710.
[16] S.O. Oladejo, O.E. Falowo, Latency-aware dynamic resource allocation scheme for 5 g heterogeneous network: A network slicing-multitenancy scenario, in: 2019 International Conference on Wireless and Mobile Computing, Networking and Communications, WiMob, 2019, pp. 1–7, http://dx.doi.org/10.1109/WiMOB.2019.8923397.
[17] S.O. Oladejo, O.E. Falowo, Profit-aware resource allocation for 5 g sliced networks, in: 2018 European Conference on Networks and Communications, EuCNC, 2018, pp. 43–47, http://dx.doi.org/10.1109/EuCNC.2018.8442661.
[18] S.O. Ekwe, S.O. Oladejo, L.A. Akinyemi, N. Ventura, A socially-inspired energy-efficient resource allocation algorithm for future wireless network, in: 2020 16th International Computer Engineering Conference, ICENCO, 2020, pp. 168–173, http://dx.doi.org/10.1109/ICENCO49778.2020.9357387.
[19] S.O. Ekwe, L.A. Akinyemi, S.O. Oladejo, N. Ventura, Social-aware joint uplink and downlink resource allocation scheme using genetic algorithm, in: 2021 IEEE AFRICON, IEEE, 2021, pp. 1–6.
[20] S.O. Oladejo, S.O. Ekwe, L.A. Akinyemi, Multi-tier multi-domain network slicing: A resource allocation perspective, in: 2021 IEEE AFRICON, IEEE, 2021, pp. 1–6.
[21] S.O. Oladejo, S.O. Ekwe, L.A. Akinyemi, Multi-tier multi-tenant network slicing: A multi-domain games approach, ITU J. Future Evol. Technol. 2 (6) http://dx.doi.org/10.52953/DXZQ6155.
[22] S.O. Oladejo, Efficient Radio Resource Management for the Fifth Generation Slice Networks (Doctoral dissertation), University of Cape Town, South Africa, 2021, URL https://open.uct.ac.za/handle/11427/35992.
[23] S.O. Oladejo, S.O. Ekwe, L.A. Akinyemi, S. Mirjalili, A. Ajibare, Tuning SVMs' Hyperparameters using the Whale Optimization Algorithm, in: S. Mirjalili (Ed.), Handbook of Whale Optimization Algorithm, Academic Press, London, United Kingdom, 2023.
[24] M.H. Davis, I. Karatzas, A deterministic approach to optimal stopping, in: F.P. Kelly (Ed.), Probability, Statistics and Optimisation, John Wiley & Sons Ltd, New York Chichester, 1994, pp. 455–466.
[25] M. Birattari, L. Paquete, T. Stützle, K. Varrentrapp, Classification of metaheuristics and design of experiments for the analysis of components, Teknik Rapor, AIDA-01-05.
[26] H. Stegherr, M. Heider, J. Hähner, Classifying metaheuristics: Towards a unified multi-level classification system, Nat. Comput. (2020) 1–17.
[27] N. Abd-Alsabour, S. Ramakrishnan, Hybrid metaheuristics for classification problems, Pattern Recognit. Anal. Appl. 10 (2016) 65253.
[28] I. Boussaïd, J. Lepagnot, P. Siarry, A survey on optimization metaheuristics, Inform. Sci. 237 (2013) 82–117, Prediction, Control and Diagnosis using Advanced Neural Computations.
[29] F. Glover, Future paths for integer programming and links to artificial intelligence, Comput. Oper. Res. 13 (5) (1986) 533–549.
[30] S. Samsuddin, M.S. Othman, L.M. Yusuf, A review of single and population-based metaheuristic algorithms solving multi depot vehicle routing problem, Int. J. Softw. Eng. Comput. Syst. 4 (2) (2018) 80–93.
[31] F. Glover, M. Laguna, Tabu search, in: Handbook of Combinatorial Optimization, Springer, 1998, pp. 2093–2229.
[32] S. Kirkpatrick, C.D. Gelatt Jr., M.P. Vecchi, Optimization by simulated annealing, in: Readings in Computer Vision, Elsevier, 1987, pp. 606–615.
[33] T.A. Feo, M.G. Resende, A probabilistic heuristic for a computationally difficult set covering problem, Oper. Res. Lett. 8 (2) (1989) 67–71.
[34] H.R. Lourenço, O.C. Martin, T. Stützle, Iterated local search, in: Handbook of Metaheuristics, Springer, 2003, pp. 320–353.
[35] E. Aarts, E.H. Aarts, J.K. Lenstra, Local Search in Combinatorial Optimization, Princeton University Press, 2003.
[36] J. Kennedy, R. Eberhart, Particle swarm optimization, in: Proceedings of ICNN'95-International Conference on Neural Networks, vol. 4, IEEE, 1995, pp. 1942–1948.
[37] M. Dorigo, Optimization, Learning and Natural Algorithms (Ph.D. thesis), Politecnico di Milano.
[38] J.H. Holland, et al., Adaptation in Natural and Artificial Systems: An Introductory Analysis with Applications To Biology, Control, and Artificial Intelligence, MIT Press, 1992.
[39] J.H. Holland, Genetic algorithms, Sci. Am. 267 (1) (1992) 66–73.
[40] R. Storn, K. Price, Differential evolution–a simple and efficient heuristic for global optimization over continuous spaces, J. Global Optim. 11 (4) (1997) 341–359.
[41] D. Karaboga, An Idea Based on Honey Bee Swarm for Numerical Optimization, Tech. Rep. Technical Report-Tr06, Erciyes University, Engineering Faculty, 2005.
[42] D. Karaboga, B. Basturk, A powerful and efficient algorithm for numerical function optimization: Artificial Bee Colony (abc) algorithm, J. Global Optim. 39 (3) (2007) 459–471.
[43] A.A. Heidari, S. Mirjalili, H. Faris, I. Aljarah, M. Mafarja, H. Chen, Harris hawks optimization: Algorithm and applications, Future Gener. Comput. Syst. 97 (2019) 849–872.
[44] X.-S. Yang, Nature-Inspired Metaheuristic Algorithms, Luniver Press, 2010.
[45] D. Simon, Biogeography-based optimization, IEEE Trans. Evol. Comput. 12 (6) (2008) 702–713.
[46] N. Hansen, The CMA evolution strategy: A comparing review, Towards A New Evol. Comput. (2006) 75–102.
[47] I. Rechenberg, Evolution strategy: Nature's way of optimization, in: Optimization: Methods and Applications, Possibilities and Limitations, Springer, 1989, pp. 106–126.
[48] J.R. Koza, Genetic programming as a means for programming computers by natural selection, Stat. Comput. 4 (2) (1994) 87–112.
[49] D.B. Fogel, System Identification Through Simulated Evolution: A Machine Learning Approach To Modeling, Ginn Press, 1991.
[50] H. Talbi, A. Draa, A new real-coded quantum-inspired evolutionary algorithm for continuous optimization, Appl. Soft Comput. 61 (2017) 765–791.
[51] S. Saremi, S. Mirjalili, A. Lewis, Grasshopper optimisation algorithm: Theory and application, Adv. Eng. Softw. 105 (2017) 30–47.
[52] X.-S. Yang, S. Deb, Cuckoo search via Lévy flights, in: 2009 World Congress on Nature & Biologically Inspired Computing, NaBIC, IEEE, 2009, pp. 210–214.

[53] S. Mirjalili, The ant lion optimizer, Adv. Eng. Softw. 83 (2015) 80–98.
[54] X.-S. Yang, Firefly algorithm, stochastic test functions and design optimisation, Int. J. Bio-inspired Comput. 2 (2) (2010) 78–84.
[55] X.-S. Yang, A.H. Gandomi, Bat algorithm: A novel approach for global engineering optimization, Eng. Comput.
[56] A. Kaveh, N. Farhoudi, A new optimization method: Dolphin echolocation, Adv. Eng. Softw. 59 (2013) 53–70.
[57] A.P. Engelbrecht, Computational Intelligence: An Introduction, John Wiley & Sons, 2007.
[58] A.P. Engelbrecht, Fundamentals of Computational Swarm Intelligence, John Wiley & Sons, Inc., 2006.
[59] F. Zitouni, S. Harous, R. Maamri, The solar system algorithm: A novel metaheuristic method for global optimization, IEEE Access 9 (2020) 4542–4565.
[60] S. Mirjalili, SCA: A sine cosine algorithm for solving optimization problems, Knowl.-Based Syst. 96 (2016) 120–133.
[61] R.A. Formato, Central force optimization, Prog. Electromagn. Res. 77 (1) (2007) 425–491.
[62] O.K. Erol, I. Eksin, A new optimization method: Big bang–big crunch, Adv. Eng. Softw. 37 (2) (2006) 106–111.
[63] E. Rashedi, H. Nezamabadi-Pour, S. Saryazdi, GSA: A gravitational search algorithm, Inform. Sci. 179 (13) (2009) 2232–2248.
[64] Y. Tan, Y. Zhu, Fireworks algorithm for optimization, in: Y. Tan, Y. Shi, K.C. Tan (Eds.), Advances in Swarm Intelligence, Springer Berlin Heidelberg, Berlin, Heidelberg, 2010, pp. 355–364.
[65] Z.W. Geem, J.H. Kim, G.V. Loganathan, A new heuristic optimization algorithm: harmony search, Simulation 76 (2) (2001) 60–68.
[66] R.V. Rao, V.J. Savsani, D. Vakharia, Teaching–learning-based optimization: A novel method for constrained mechanical design optimization problems, Comput. Aided Des. 43 (3) (2011) 303–315.
[67] S. He, Q. Wu, J. Saunders, A novel group search optimizer inspired by animal behavioural ecology, in: 2006 IEEE International Conference on Evolutionary Computation, IEEE, 2006, pp. 1272–1278.
[68] S. Talatahari, H. Bayzidi, M. Saraee, Social network search for global optimization, IEEE Access 9 (2021) 92815–92863.
[69] S.O. Oladejo, S.O. Ekwe, L.A. Akinyemi, S. Mirjalili, The deep sleep optimizer: A human-based metaheuristic approach, IEEE Access 11 (2023) 83639–83665, http://dx.doi.org/10.1109/ACCESS.2023.3298105.
[70] D.H. Wolpert, W.G. Macready, No free lunch theorems for optimization, IEEE Trans. Evol. Comput. 1 (1) (1997) 67–82.
[71] S. Suyanto, A.A. Ariyanto, A.F. Ariyanto, Komodo mlipir algorithm, Appl. Soft Comput. 114 (2022) 108043.
[72] Q. Liu, X. Zhang, Improved adaptive komodo mlipir algorithm, IEEE Access 10 (2022) 67883–67897.
[73] L. Li, M. Zhao, A novel komodo mlipir algorithm and its application in pm2. 5 detection, Atmosphere 13 (12) (2022) 2051.
[74] M. Noroozi, H. Mohammadi, E. Efatinasab, A. Lashgari, M. Eslami, B. Khan, Golden search optimization algorithm, IEEE Access 10 (2022) 37515–37532.
[75] A. Mohammadi-Balani, M.D. Nayeri, A. Azar, M. Taghizadeh-Yazdi, Golden eagle optimizer: A nature-inspired metaheuristic algorithm, Comput. Ind. Eng. 152 (2021) 107050.
[76] A.M. Khalid, K.M. Hosny, S. Mirjalili, COVIDOA: a novel evolutionary optimization algorithm based on coronavirus disease replication lifecycle, Neural Comput. Appl. 34 (24) (2022) 22465–22492.
[77] D.S. Khafaga, E.A. Aldakheel, A.M. Khalid, H.M. Hamza, K.M. Hosny, Compression of bio-signals using block-based haar wavelet transform and COVIDOA for iomt systems, Bioengineering 10 (4) (2023) 406.
[78] J. Poongavanan, J. Xavier, M. Dunaiski, H. Tegally, S.O. Oladejo, O. Ayorinde, E. Wilkinson, C. Baxter, T.d. Oliveira, Managing and assembling population-scale data streams, tools and workflows to plan for future pandemics within the inform-Africa consortium, S. Afr. J. Sci. 119 (5–6) (2023) 1–4.
[79] S.O. Oladejo, L.R. Watson, B.W. Watson, K. Rajaratnam, M.J. Kotze, D.B. Kell, E. Pretorius, Data sharing: A long covid perspective, challenges, and road map for the future, S. Afr. J. Sci. 119 (5–6) (2023) 1–8.
[80] E. Pretorius, C. Venter, G.J. Laubscher, M.J. Kotze, S.O. Oladejo, L.R. Watson, K. Rajaratnam, B.W. Watson, D.B. Kell, Prevalence of symptoms, comorbidities, fibrin amyloid microclots and platelet pathology in individuals with long covid/post-acute sequelae of covid-19 (pasc), Cardiovasc. Diabetol. 21 (1) (2022) 148.
[81] W. Zhao, L. Wang, Z. Zhang, S. Mirjalili, N. Khodadadi, Q. Ge, Quadratic interpolation optimization (QIO): A new optimization algorithm based on generalized quadratic interpolation and its applications to real-world engineering problems, Comput. Methods Appl. Mech. Engrg. 417 (2023) 116446.
[82] J.O. Agushaka, A.E. Ezugwu, L. Abualigah, Gazelle optimization algorithm: a novel nature-inspired metaheuristic optimizer, Neural Comput. Appl. 35 (5) (2023) 4099–4131.
[83] M. Dehghani, Z. Montazeri, E. Trojovská, P. Trojovskỳ, Coati optimization algorithm: A new bio-inspired metaheuristic algorithm for solving optimization problems, Knowl.-Based Syst. 259 (2023) 110011.
[84] H. Jia, H. Rao, C. Wen, S. Mirjalili, Crayfish optimization algorithm, Artif. Intell. Rev. 56 (Suppl 2) (2023) 1919–1979.
[85] F. Zitouni, S. Harous, A. Belkeram, L.E.B. Hammou, The archerfish hunting optimizer: A novel metaheuristic algorithm for global optimization, Arab. J. Sci. Eng. 47 (2) (2022) 2513–2553.
[86] K. Kołodziejczyk, Networks of hiking tourist trails in the krkonoše (Czech Republic) and peneda-gerês (Portugal) national parks—comparative analysis, J. Mountain Sci. 16 (4) (2019) 725–743.
[87] A.H. Bent, The unexplored mountains of North America, Geogr. Rev. 7 (6) (1919) 403–412.
[88] F. Faccini, A. Roccati, M. Firpo, Geo-hiking map of Mt. Penna and Mt. Aiona area (Aveto Natural Park, Italy), J. Maps 8 (3) (2012) 293–303.
[89] R.B. Huey, X. Eguskitza, Limits to human performance: Elevated risks on high mountains, J. Exp. Biol. 204 (18) (2001) 3115–3119.
[90] M.F. Goodchild, Beyond Tobler's hiking function, Geogr. Anal. 52 (4) (2020) 558–569.
[91] W.R. Tobler, Non-isotropic geographic modeling, in: J. Doe (Ed.), Three Presentations on Geographical Analysis and Modeling, National Center for Geographic Information and Analysis, Santa Barbara, CA, 1993, pp. 30–40, URL https://escholarship.org/uc/item/05r820mz.
[92] M. Sarhani, S. Voß, R. Jovanovic, Initialization of metaheuristics: comprehensive review, critical analysis, and research directions, Int. Trans. Oper. Res. 30 (6) (2023) 3361–3397.
[93] J.O. Agushaka, A.E. Ezugwu, Initialisation approaches for population-based metaheuristic algorithms: a comprehensive review, Appl. Sci. 12 (2) (2022) 896.
[94] J.O. Agushaka, A.E. Ezugwu, L. Abualigah, S.K. Alharbi, H.A.E.-W. Khalifa, Efficient initialization methods for population-based metaheuristic algorithms: A comparative study, Arch. Comput. Methods Eng. 30 (3) (2023) 1727–1787.
[95] M. Molga, C. Smutnicki, Test functions for optimization needs, 101, 2005, p. 48.
[96] K. Hussain, M.N.M. Salleh, S. Cheng, R. Naseem, Common benchmark functions for metaheuristic evaluation: A review, JOIV: Int. J. Inf. Vis. 1 (4–2) (2017) 218–223.
[97] M. Jamil, X.-S. Yang, A literature survey of benchmark functions for global optimisation problems, Int. J. Math. Model. Numer. Optim. 4 (2) (2013) 150–194.
[98] J.G. Digalakis, K.G. Margaritis, On benchmarking functions for genetic algorithms, Int. J. Comput. Math. 77 (4) (2001) 481–506.
[99] The Mathworks, Inc., Natick, Massachusetts, MATLAB version 9.10.0.1613233 (R2021a), 2021.
[100] S. Mirjalili, Evolutionary Algorithms and Neural Networks, in: Studies in Computational Intelligence, vol. 780.
[101] M.R. Garey, A guide to the theory of NP-completeness, Comput. Intractability.
[102] B.H. Korte, Modern Applied Mathematics: Optimization and Operations Research: Collection of State-of-the-Art Surveys Based on Lectures Presented At the Summer School 'Optimization and Operations Research', Held at the University of Bonn, September (1979) 14-22, North Holland, 1982.
[103] D.T. Hoang, Metaheuristics for Np-Hard Combinatorial Optimization Problems (Ph.D. thesis), National University of Singapore, 2008.
[104] P. Larranaga, C.M.H. Kuijpers, R.H. Murga, I. Inza, S. Dizdarevic, Genetic algorithms for the travelling salesman problem: A review of representations and operators, Artif. Intell. Rev. 13 (2) (1999) 129–170.
[105] E.L. Lawler, J.K. Lenstra, A.H. Rinnooy Kan, D.B. Shmoys, Erratum: The traveling salesman problem: A guided tour of combinatorial optimization, J. Oper. Res. Soc. 37 (6) (1986) 655.
[106] B. Bošković, J. Brest, Protein folding optimization using differential evolution extended with local search and component reinitialization, Inform. Sci. 454 (2018) 178–199.
[107] F. Campeotto, A. Dal Palu, A. Dovier, F. Fioretto, E. Pontelli, A constraint solver for flexible protein model, J. Artificial Intelligence Res. 48 (2013) 953–1000.
[108] S. Martello, P. Toth, Knapsack Problems: Algorithms and Computer Implementations, John Wiley & Sons, Inc., 1990.
[109] B. Selman, D.G. Mitchell, H.J. Levesque, Generating hard satisfiability problems, Artificial Intelligence 81 (1–2) (1996) 17–29.
[110] T.J. Schaefer, The complexity of satisfiability problems, in: Proceedings of the Tenth Annual ACM Symposium on Theory of Computing, 1978, pp. 216–226.
[111] T.H. Cormen, C.E. Leiserson, R.L. Rivest, C. Stein, Introduction To Algorithms, MIT Press, 2022.
[112] G. Dantzig, R. Fulkerson, S. Johnson, Solution of a large-scale traveling-salesman problem, J. Oper. Res. Soc. Amer. 2 (4) (1954) 393–410.
[113] M. Velednitsky, Short combinatorial proof that the DFJ polytope is contained in the MTZ polytope for the asymmetric traveling salesman problem, Oper. Res. Lett. 45 (4) (2017) 323–324.
[114] G. Reinelt, TSPLIB—A traveling salesman problem library, ORSA J. Comput. 3 (4) (1991) 376–384.

[115] W.J. Cook, D.L. Applegate, R.E. Bixby, V. Chvatal, The Traveling Salesman Problem: A Computational Study, Princeton University Press, New Jersey, USA, 2011.
[116] M. Abdel-Basset, D. El-Shahat, A.K. Sangaiah, A modified nature inspired meta-heuristic whale optimization algorithm for solving 0–1 knapsack problem, Int. J. Mach. Learn. Cybern. 10 (2019) 495–514.
[117] H. Kellerer, U. Pferschy, D. Pisinger, The Bounded Knapsack Problem, Springer Berlin Heidelberg, Berlin, Heidelberg, 2004, pp. 185–209, http://dx.doi.org/10.1007/978-3-540-24777-7_7.

Sunday O. Oladejo is currently a lecturer at the School for Data Science and Computational Thinking, Stellenbosch University, Stellenbosch, South Africa. He obtained a B.Eng in electrical and electronic engineering at the Federal University of Technology Akure, Nigeria, an M.Eng in communication engineering at the Federal University of Technology, Minna, Nigeria, a Master of Business Administration in strategic and project management at the Ecole Supérieure de Gestion, Paris, France, and Ph.D. in electrical and electronic engineering from the University of Cape Town, South Africa. From 2007 to 2017, he was Senior Core Network Engineer with Glo-Mobile, Nigeria. His research interests include artificial intelligence, metaheuristics, machine learning, optimization, computational thinking, data science, and analytics.

Stephen O. Ekwe is currently a lecturer in the Department of Electrical, Electronic, and Computer Engineering at Cape Peninsula University of Technology in South Africa. He holds a bachelor's degree in electrical and electronic engineering from Cross River University of Technology in Calabar, Nigeria, and a master's degree in personal mobile and satellite communication from the University of Bradford in West Yorkshire, England. He is also a doctoral student pursuing a Ph.D. in electrical engineering at the University of Cape Town in South Africa. His research interests include radio resource management in wireless networks, socially aware device-to-device communication, network optimization, meta-heuristics, and artificial intelligence.

Seyedali Mirjalili is currently a Professor of AI at Torrens University Center for Artificial Intelligence Research and Optimization and is internationally recognized for his advances in nature-inspired AI techniques. He is the author of more than 500 publications. With over 100,000 citations and an H-index of 110, he is one of the most influential AI researchers in the world. By Google Scholar metrics, he is globally the most cited researcher in optimization using AI techniques, which is his main area of expertise. He has been a keynote speaker of several international conferences. He is serving as an Associate Editor for top AI journals, including Neurocomputing, Applied Soft Computing, Advances in Engineering Software, Engineering Applications of Artificial Intelligence, and Applied Intelligence.